

Astro/Phys 224

Spring 2014

Origin and Evolution of the Universe

Week 4B

Cosmic Microwave Background

Joel Primack

University of California, Santa Cruz

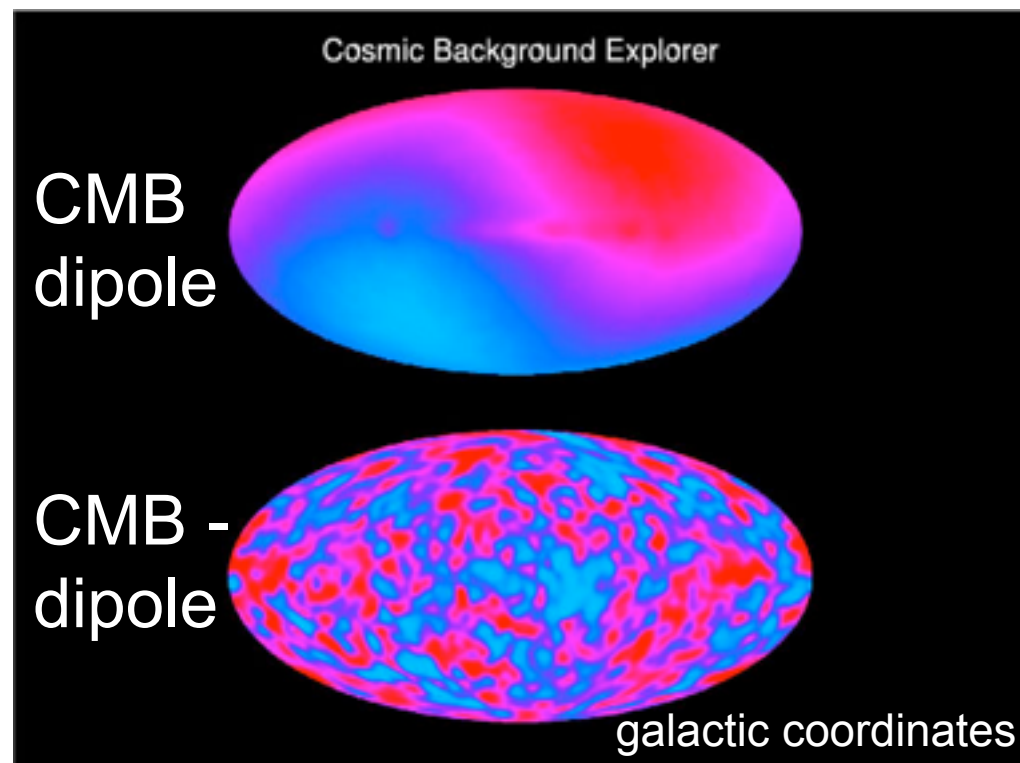
Cosmic Microwave Background

Early History

Although Penzias and Wilson discovered the CMB in 1965, Weinberg (p. 104) points out that Adams and McKellar had shown that the rotational spectra of cyanogen (CN) molecules observed in 1941 suggested that the background temperature is about 3K.

The COBE FIRAS measurements showed that the spectrum is that of thermal radiation with $T = 2.73\text{K}$. John Mather, the FIRAS PI, shared the 2006 Nobel Prize with George Smoot, the COBE/DMR PI.

The earth's motion (including that of the sun and the Milky Way) produces a CMB dipole anisotropy.



The CMB dipole anisotropy was discovered by Paul Henry (1971) and Edward Conklin (1972), and confirmed by Conklin and Wilkinson (1977) and Smoot, Gorenstein, and Muller (1977) -- see <http://www.astro.ucla.edu/~wright/CMB-dipole-history.html>

The upper panel of the figure shows the CMB dipole anisotropy in the COBE data. It is usually subtracted when the temperature anisotropy map is displayed (lower panel).

CMB Temperature Anisotropy

Sachs & Wolfe (1967, ApJ, 147, 73) showed that on large angular scales the temperature anisotropy is $\Delta T/T = \varphi/3c^2$. White & Hu give a pedagogical derivation in <http://background.uchicago.edu/~whu/Papers/sw.pdf>

PERTURBATIONS OF A COSMOLOGICAL MODEL AND ANGULAR VARIATIONS OF THE MICROWAVE BACKGROUND

R. K. SACHS AND A. M. WOLFE

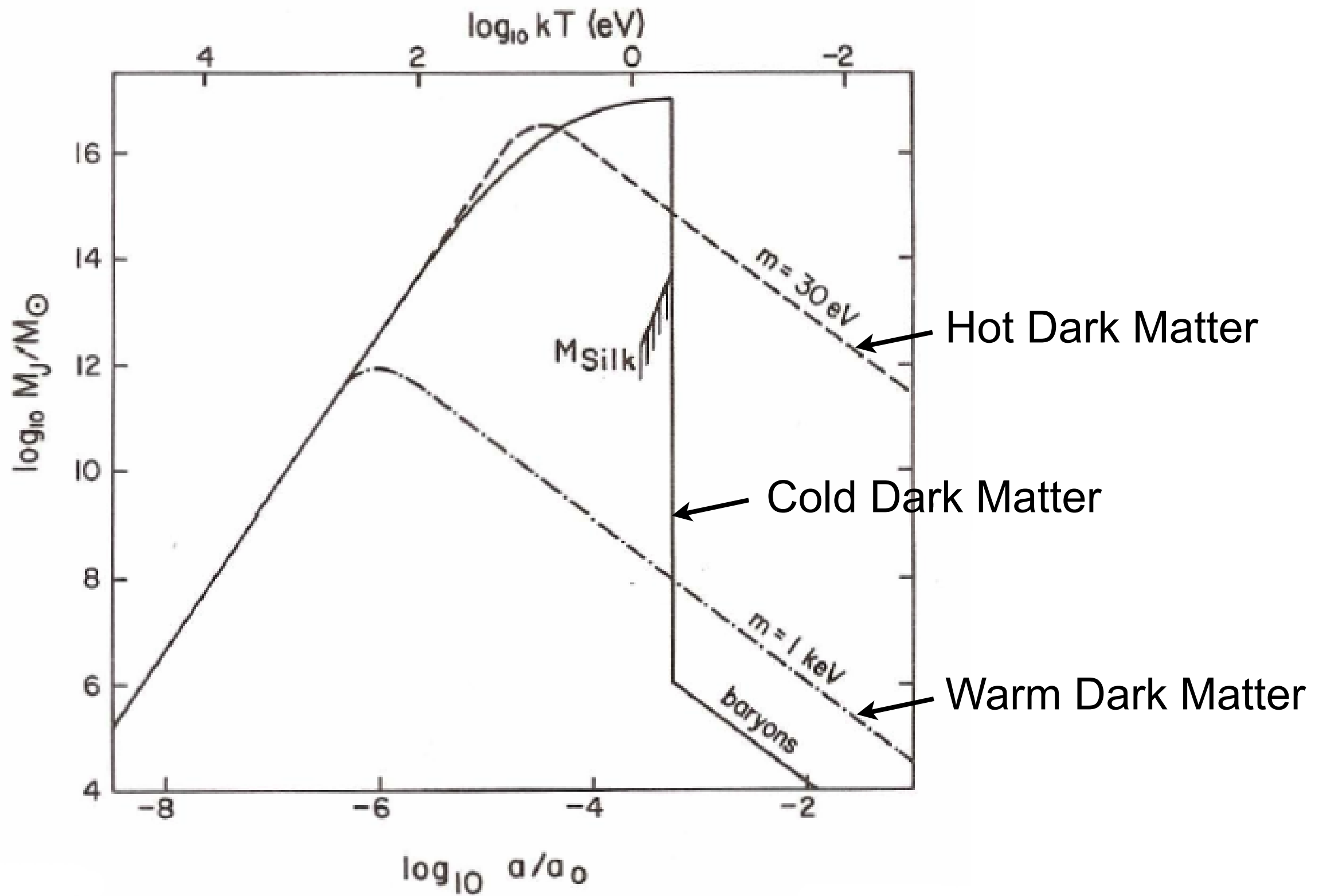
Relativity Center, The University of Texas, Austin, Texas

Received May 13, 1966

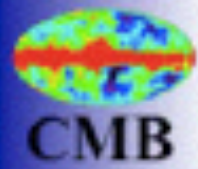
ABSTRACT

We consider general-relativistic, spatially homogeneous, and isotropic $k = 0$ cosmological models with either pressure zero or pressure one-third the energy density. The equations for general linearized perturbations away from these models are explicitly integrated to obtain density fluctuations, rotational perturbations, and gravitational waves. The equations for light rays in the perturbed models are integrated. The models are used to estimate the anisotropy of the microwave radiation, assuming this radiation is cosmological. It is estimated that density fluctuations now of order 10 per cent with characteristic lengths now of order 1000 Mpc would cause anisotropies of order 1 per cent in the observed microwave temperature due to the gravitational redshift and other general-relativistic effects. The $\dot{p} = 0$ models are compared in detail with corresponding Newtonian models. The perturbed Newtonian models do not contain gravitational waves, but the density perturbations and rotational perturbations are surprisingly similar.

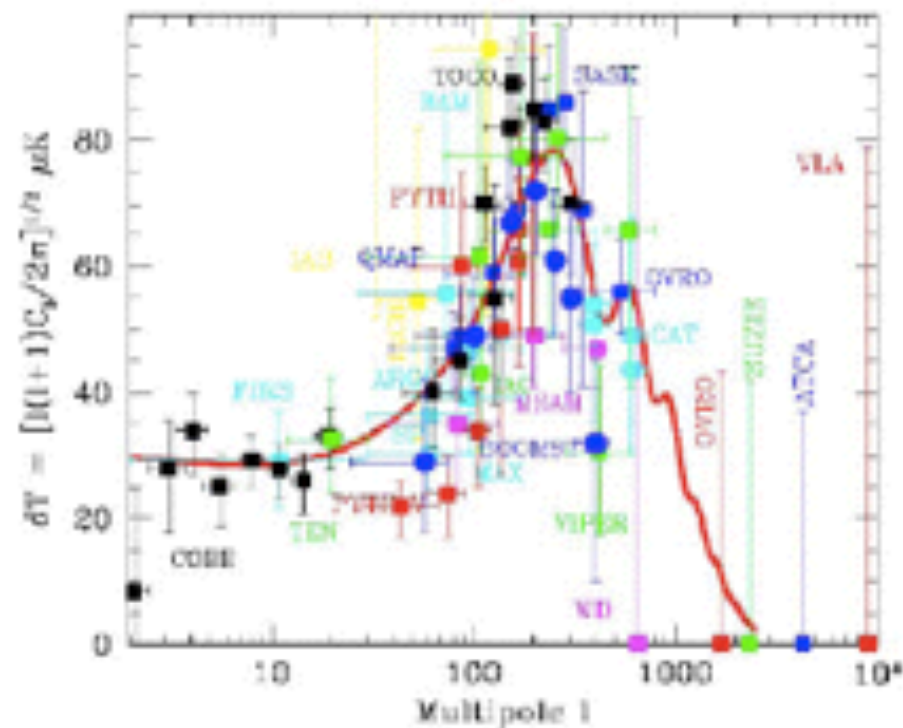
This was first convincingly seen by the COBE DMR experiment, reported by George Smoot on April 27, 1992. Their result $\Delta T/T = 10^{-5}$ had been predicted by the CDM model (Blumenthal, Faber, Primack, & Rees 1984). The search then began for smaller-angular-scale CMB anisotropies.



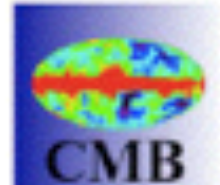
Jeans-type analysis for HDM, WDM, and CDM



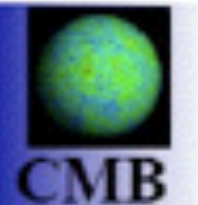
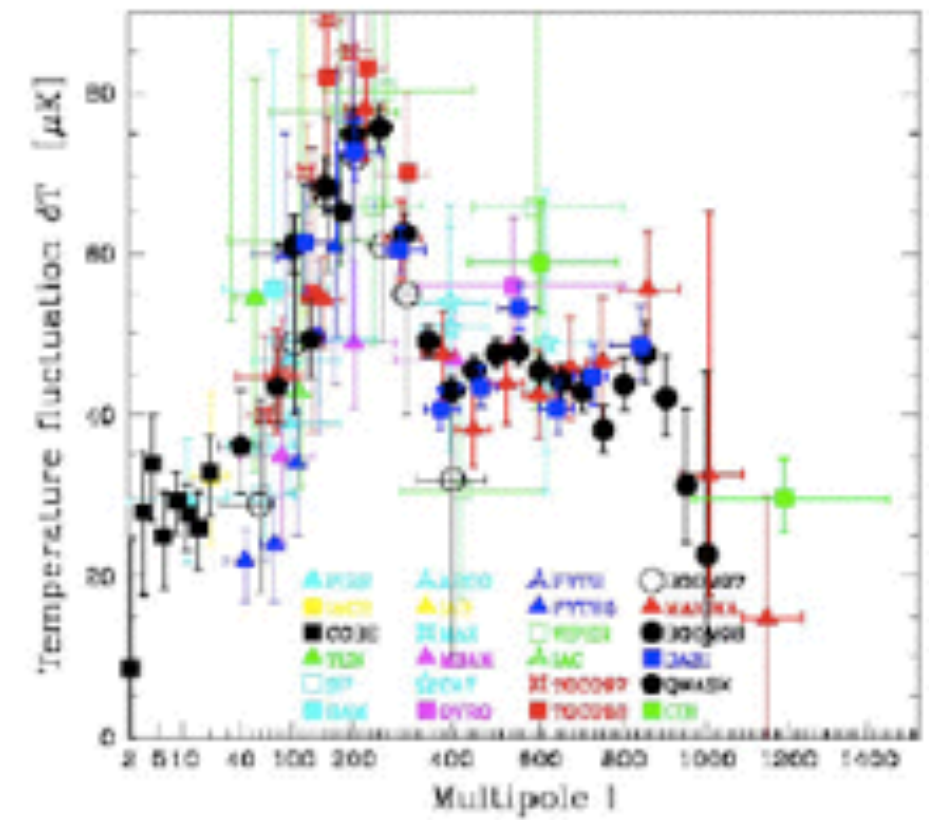
Shown at DM2000:



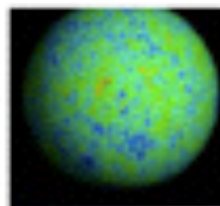
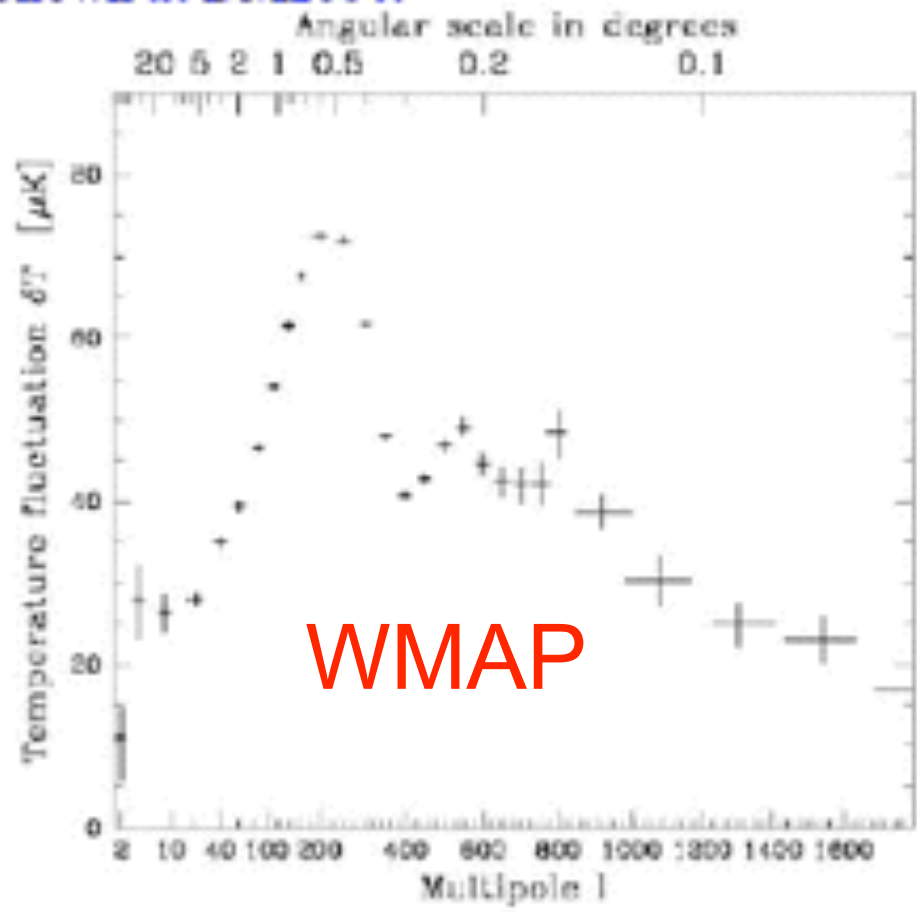
Max Tegmark



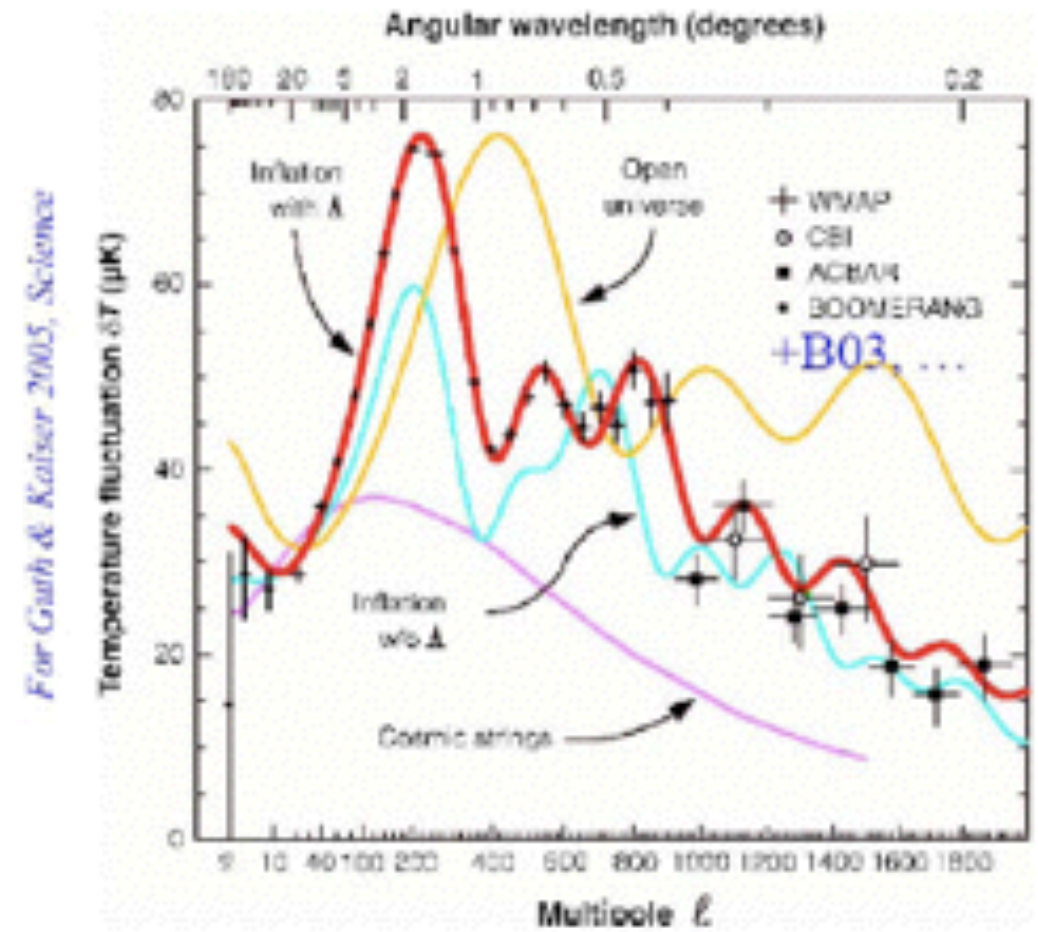
Shown at DM2002:



Shown at DM2004:



Shown at DM2006:



For Guth & Kaiser 2005, Science

THE COSMIC SYMPHONY

By Wayne Hu and Martin White

New observations of the cosmic microwave background radiation show that the early universe resounded with harmonious oscillations

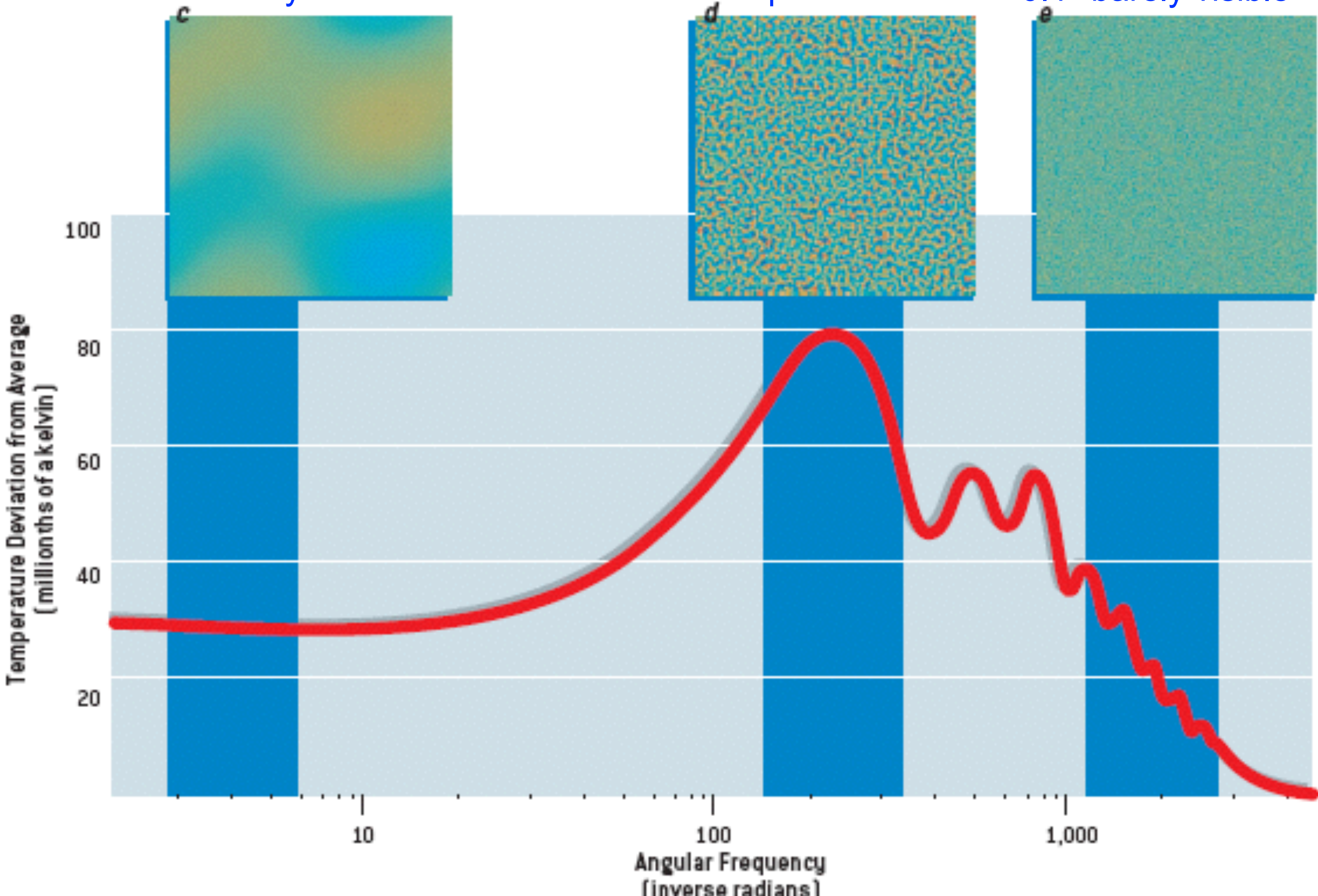
Scientific American February 2004

Angular Thermal Variations

30° barely visible

1° prominent

0.1° barely visible



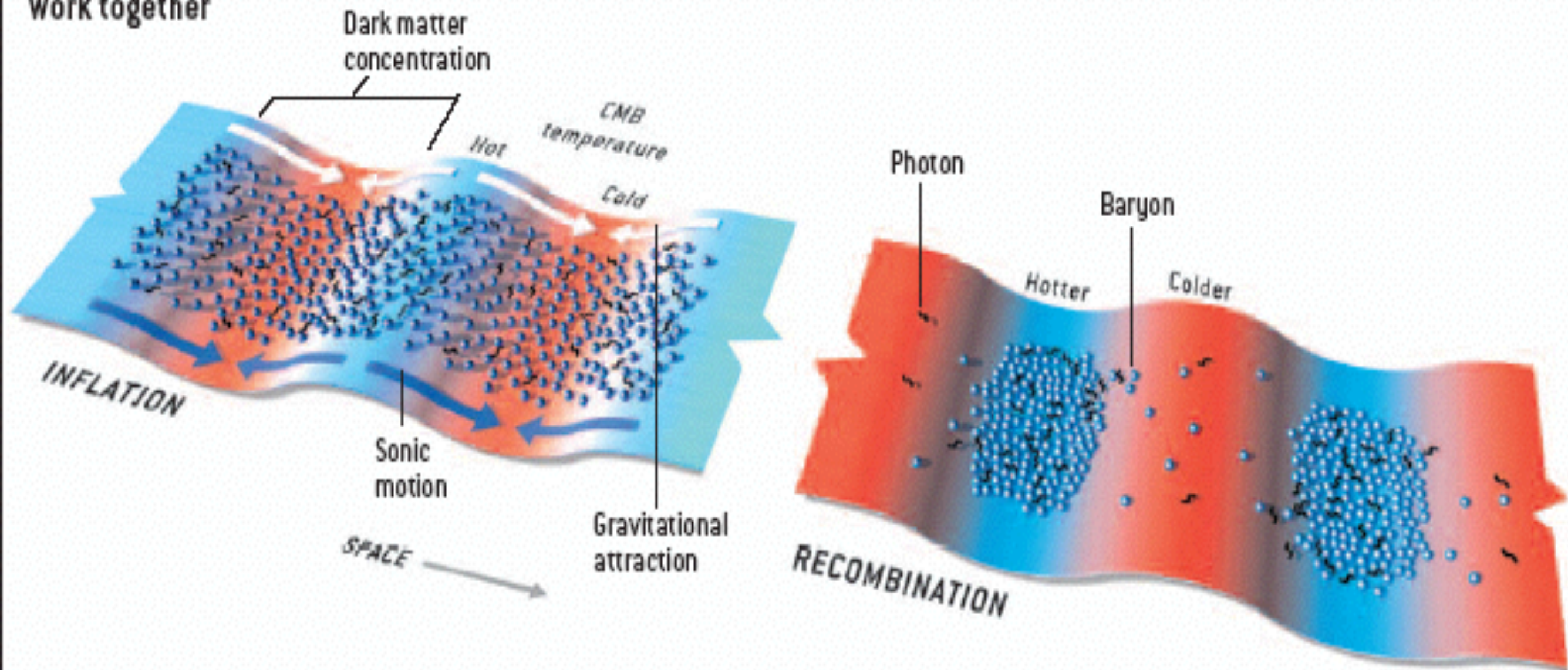
GRAVITATIONAL MODULATION

INFLUENCE OF DARK MATTER modulates the acoustic signals in the CMB. After inflation, denser regions of dark matter that have the same scale as the fundamental wave (represented as troughs in this potential-energy diagram) pull in baryons and photons by gravitational attraction. (The troughs are shown in

red because gravity also reduces the temperature of any escaping photons.) By the time of recombination, about 380,000 years later, gravity and sonic motion have worked together to raise the radiation temperature in the troughs (blue) and lower the temperature at the peaks (red).

FIRST PEAK

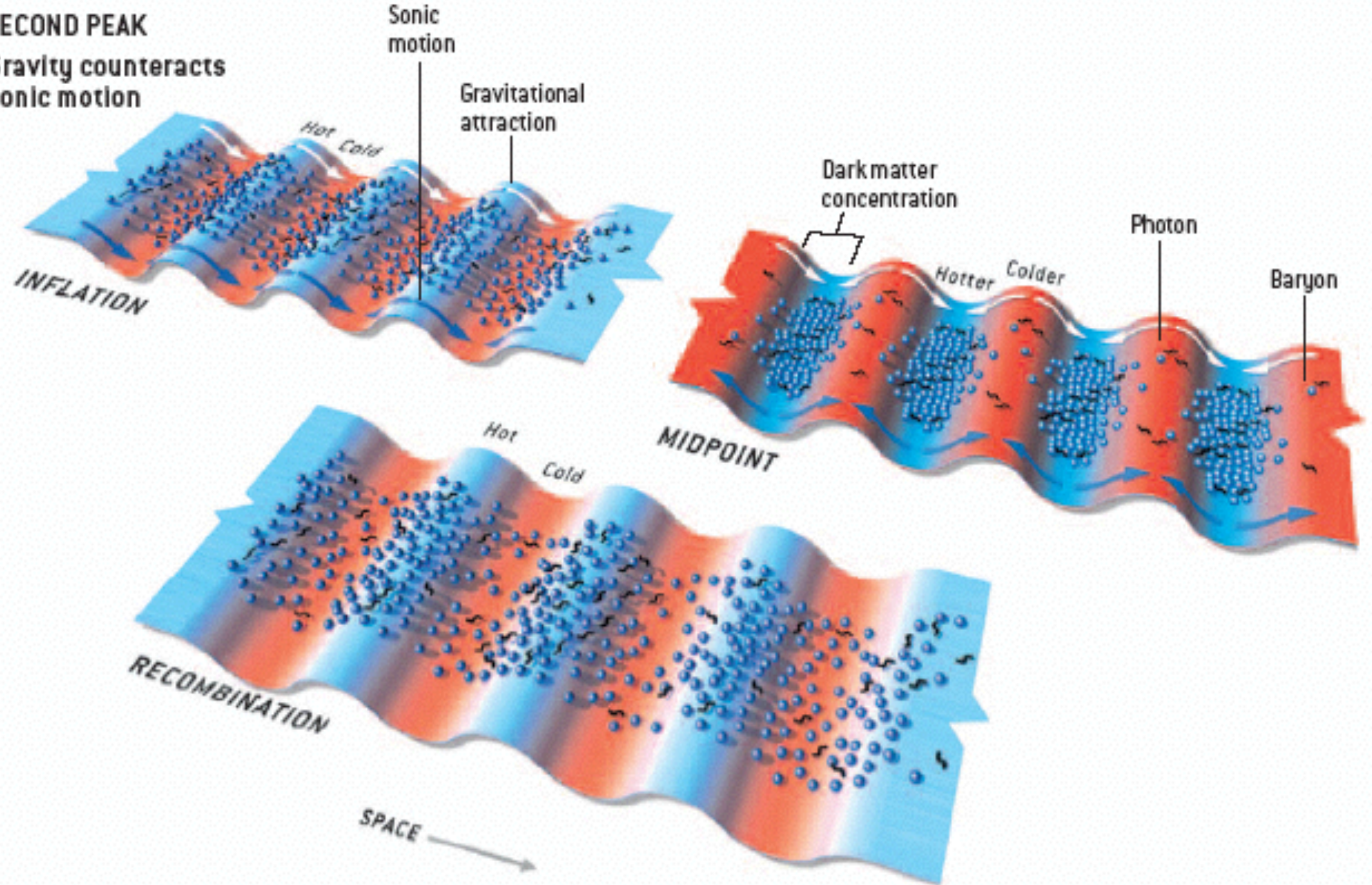
Gravity and sonic motion work together



AT SMALLER SCALES, gravity and acoustic pressure sometimes end up at odds. Dark matter clumps corresponding to a second-peak wave maximize radiation temperature in the troughs long before recombination. After this midpoint, gas pressure pushes

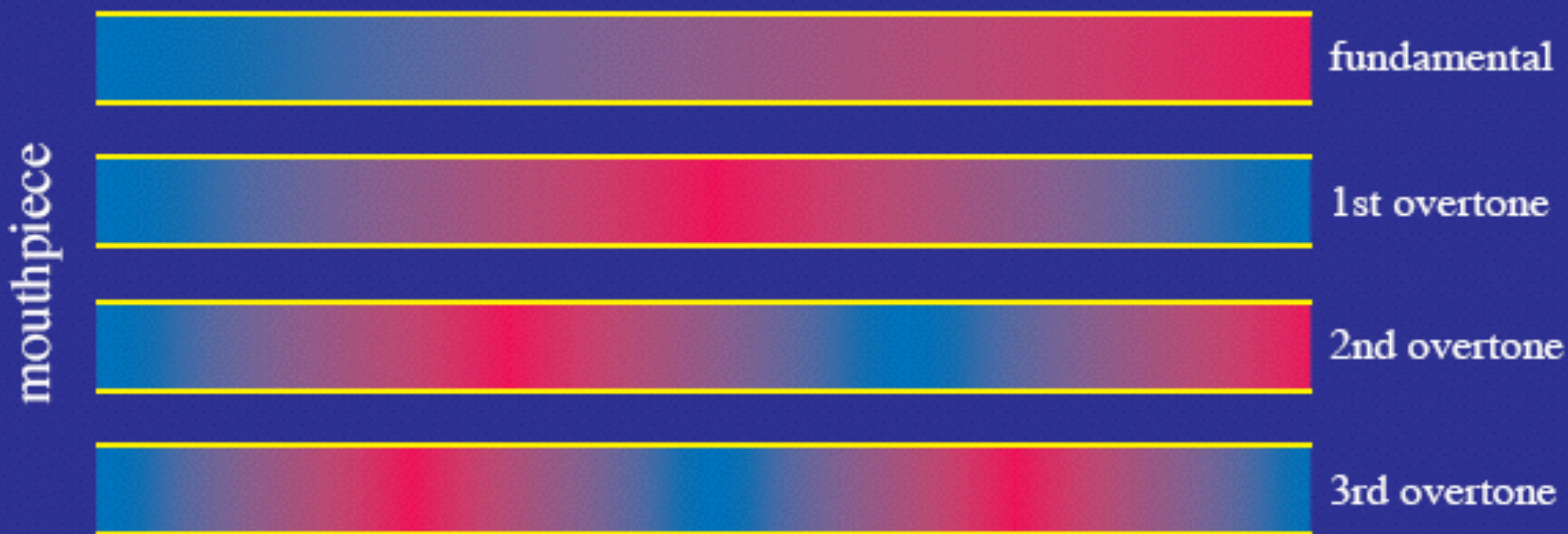
baryons and photons out of the troughs (*blue arrows*) while gravity tries to pull them back in (*white arrows*). This tug-of-war decreases the temperature differences, which explains why the second peak in the power spectrum is lower than the first.

SECOND PEAK
Gravity counteracts sonic motion



Piper at the Gates of Dawn

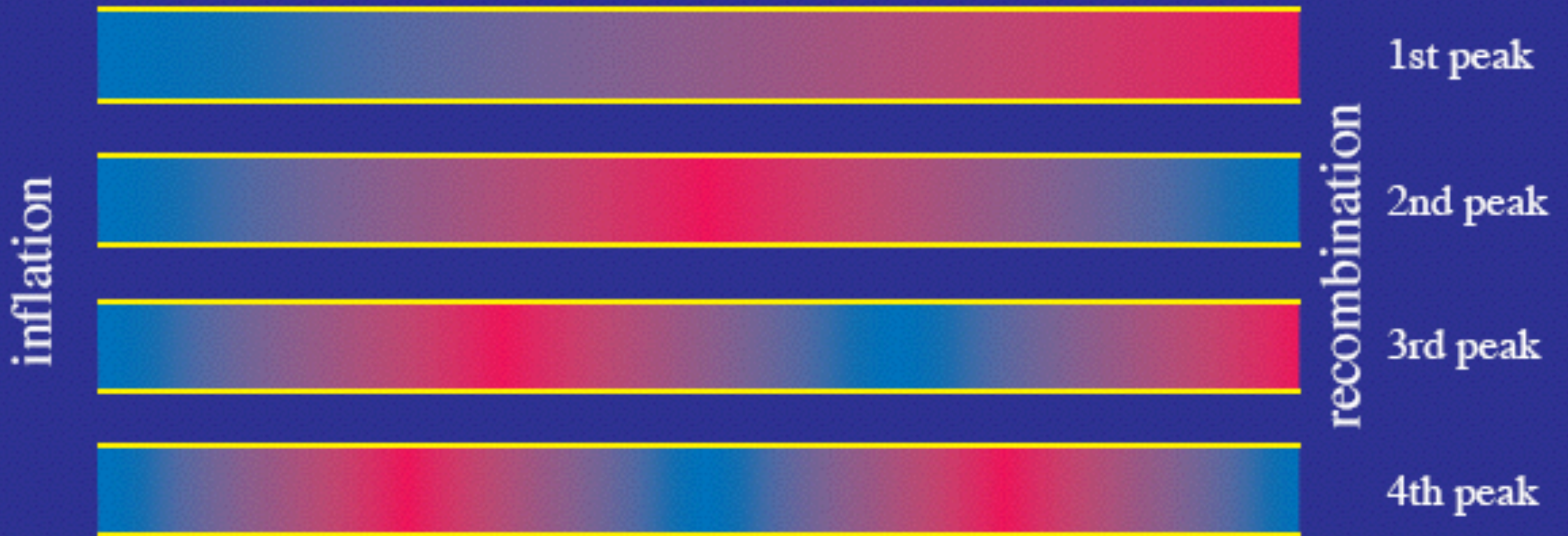
- Blow into a **flute** or an **open pipe**
- **Spectrum** of sound contains a **fundamental frequency** and **harmonic overtones**



This and the next several slides are from a talk by Wayne Hu; see <http://background.uchicago.edu/~whu/beginners/introduction.html>

Piper at the Gates of Dawn

- **Inflation** is the source of sound waves at the **beginning of time**
- Sound waves are frozen at **recombination**, yielding a **harmonic spectrum** of frequencies that reach **maximum displacement**



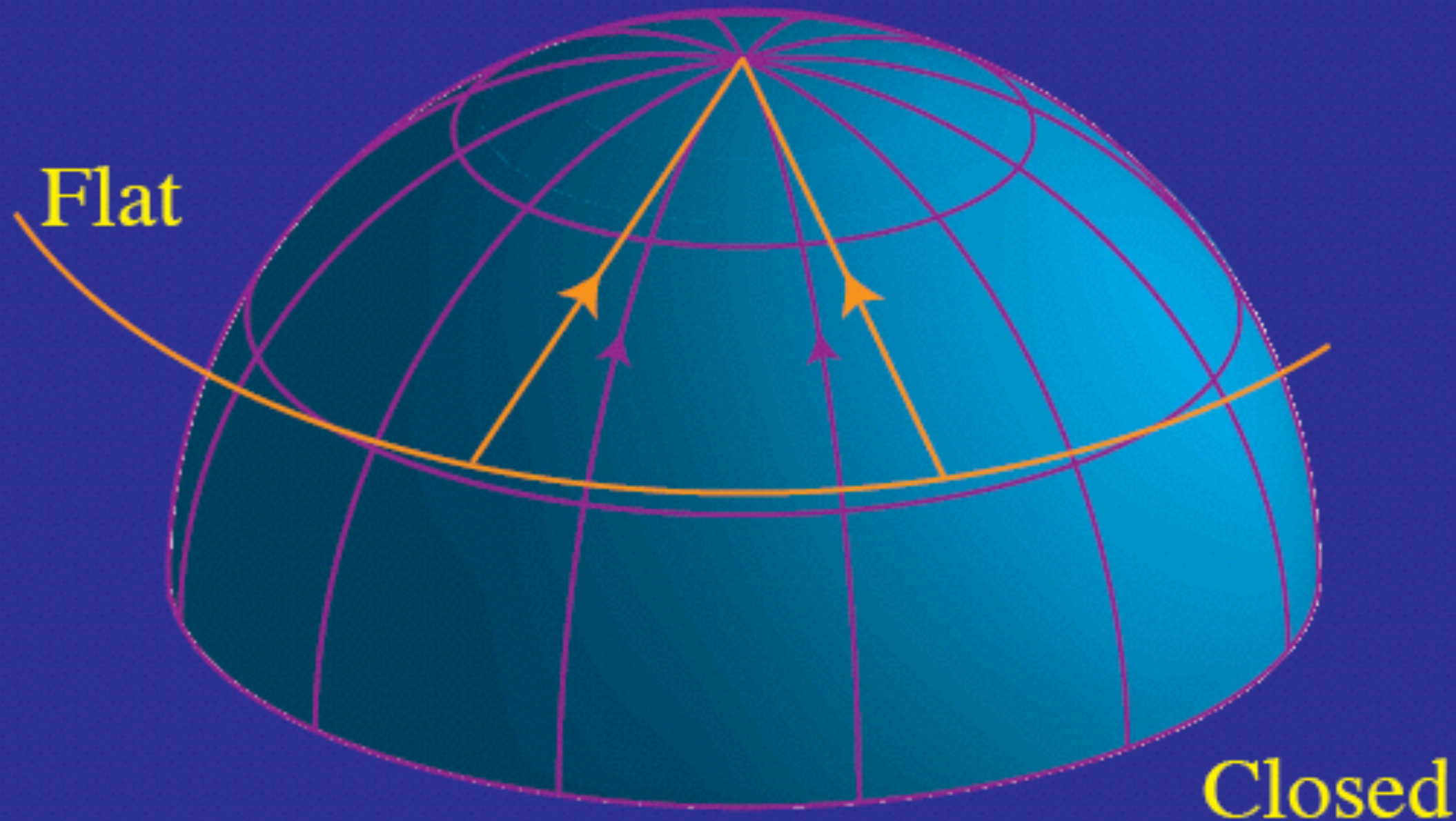
See also Annual Rev. Astron. and Astrophys. 2002
Cosmic Microwave Background Anisotropies
by **Wayne Hu** and **Scott Dodelson**

Harmonic Signature

- Much like a **musical instrument**, identify construction through the pattern of **overtones** on the **fundamental** frequency
- **Without inflation**, fluctuations must be generated at **intermediate times**
- Like **drilling holes** in the pipe and blowing in **random places**, **harmonic** structure of peaks **destroyed**
- **Observed** frequency **spectrum** consistent with **inflationary origin**
- Detailed examination of the **overtones**, reveals the **composition** of the universe
- But first...

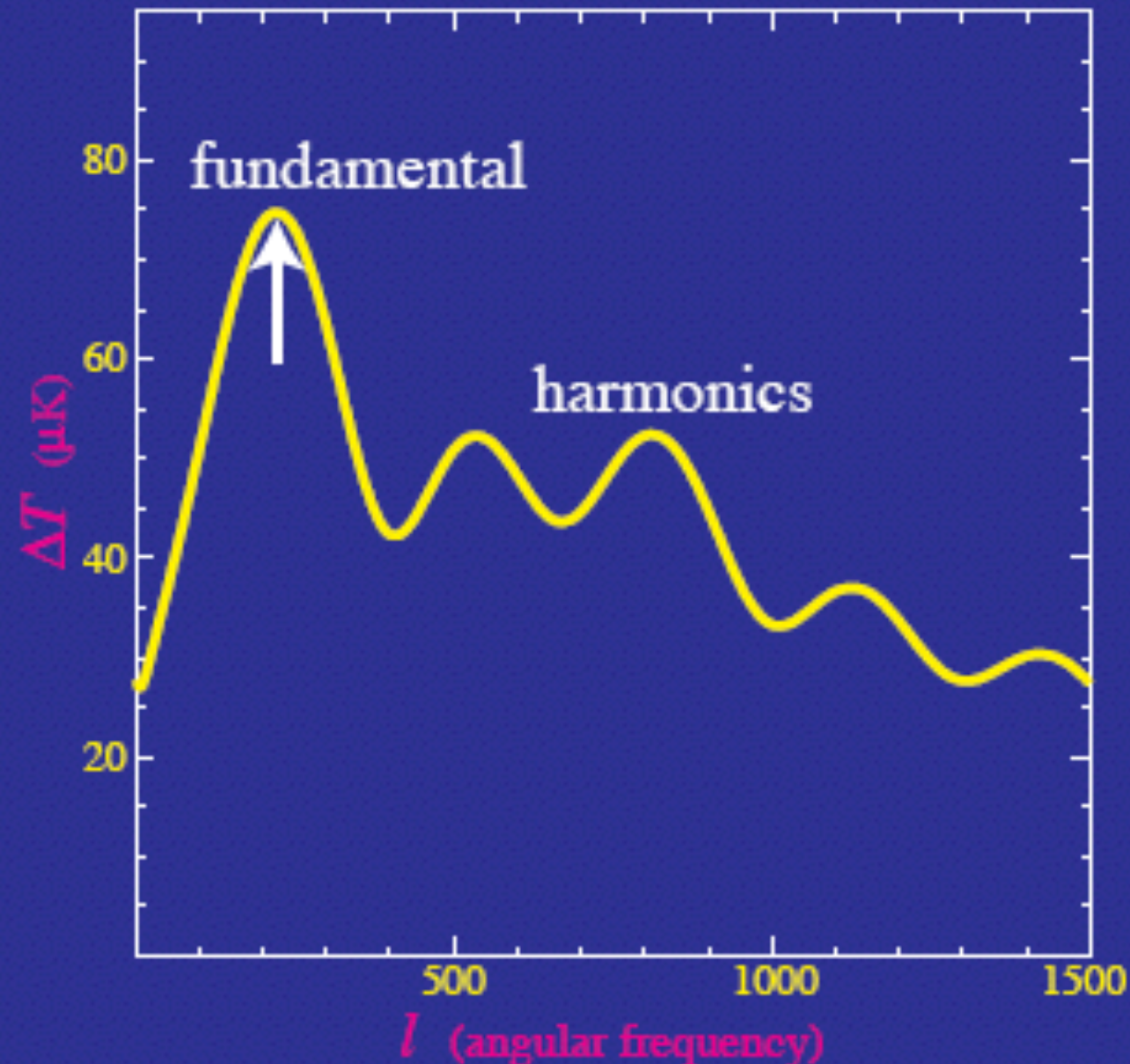
Fundamental: Weighing the Universe

- Measuring the **angular extent** of the **fundamental wavelength** (spot size) yields the **curvature** - universe is spatially **flat**
- Einstein says **matter-energy density** curves space: universe is at the **critical density**



Sound Spectrum

- Spectrum of sound shows harmonics at integer ratios of the fundamental
- Other models that generate structure causally at intermediate times would **not have** these harmonics



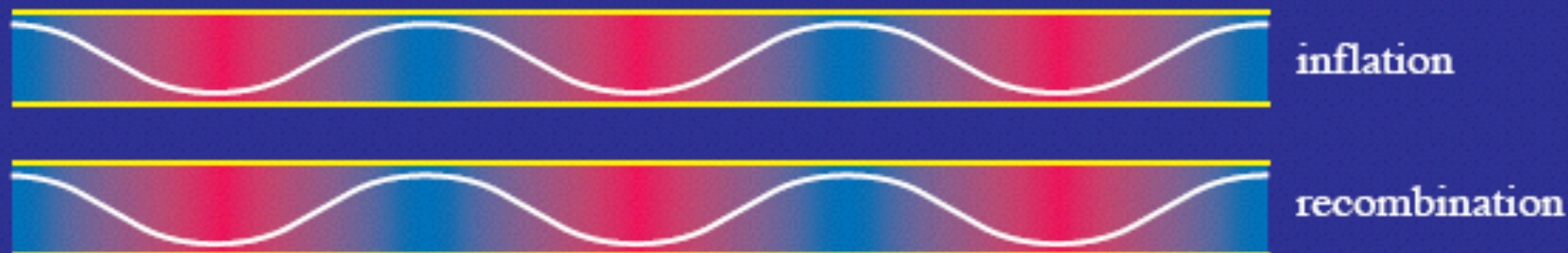
Harmonics: Ordinary Matter

- Competition between **gravity** and **pressure** depends on **phase** of oscillation
- At the **fundamental** (and **odd** frequency multiples) **gravity** **assists** sonic motion; at **second peak** (and **even** multiples) **gravity** **fights** sonic motion

Fundamental

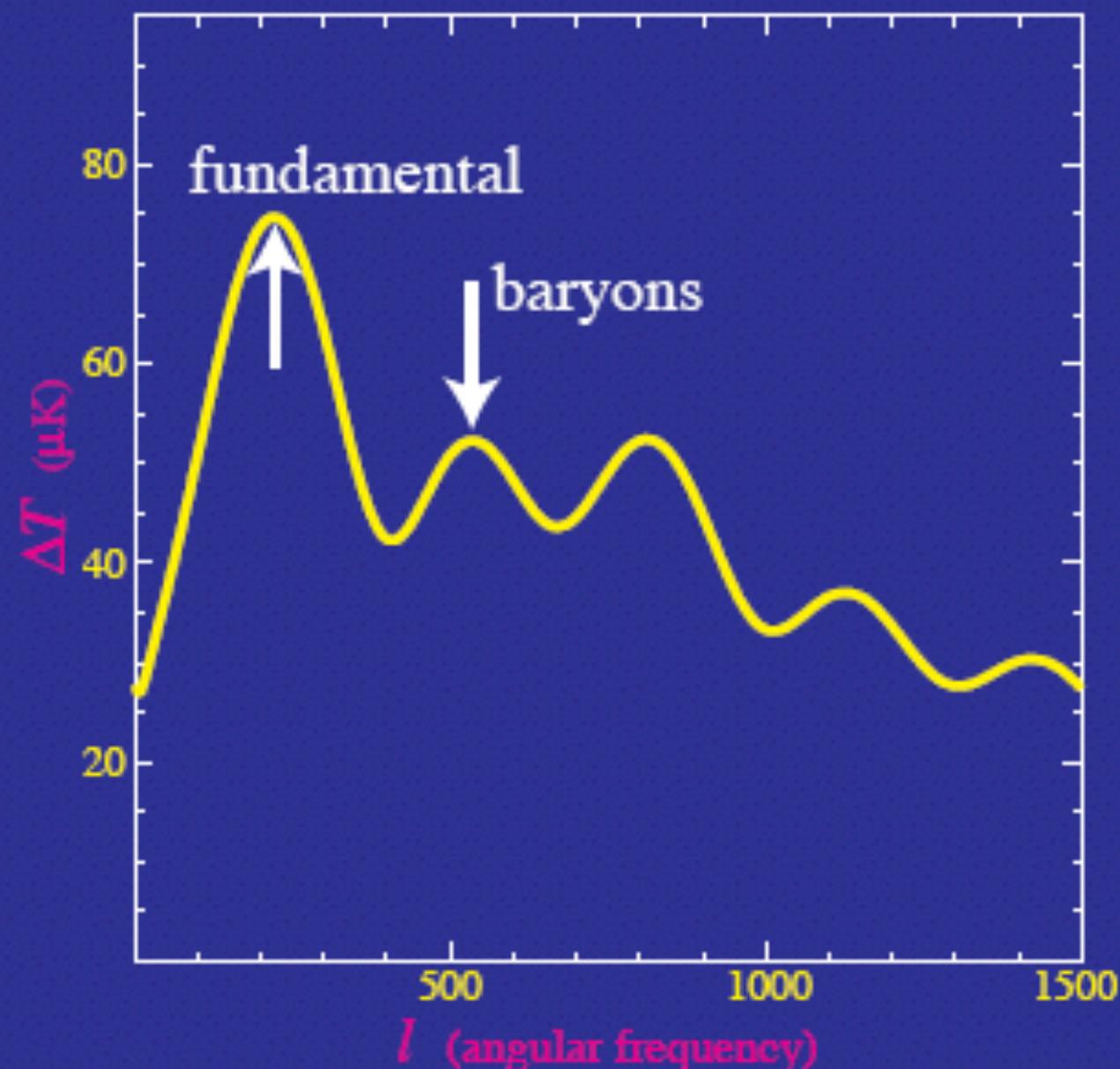


2nd Peak



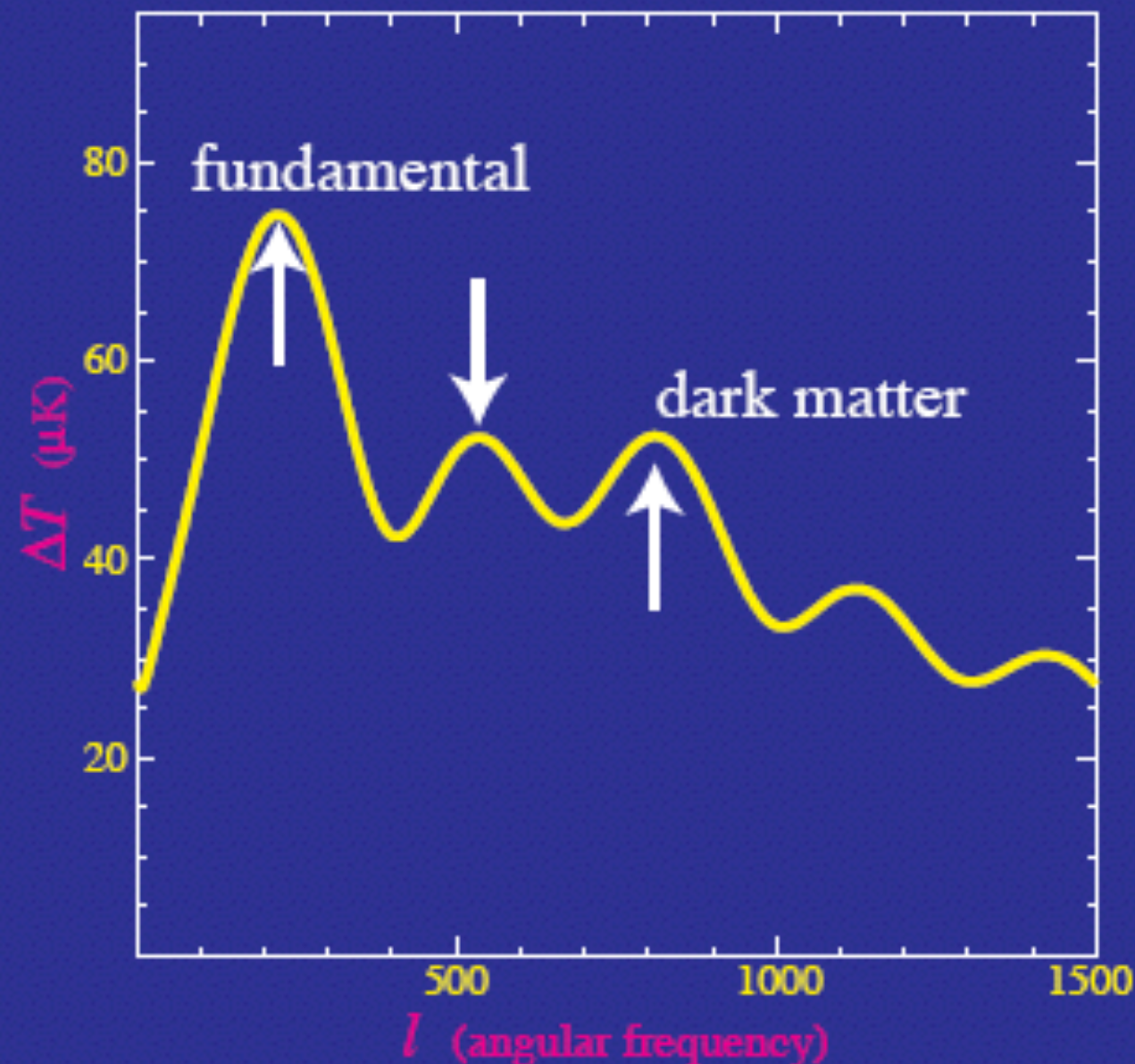
Ordinary Matter

- A **low second peak** indicates **baryon** or **ordinary matter** density **comparable** to **photon** density
- Ordinary matter consists of **$\sim 5\%$** of the critical density today



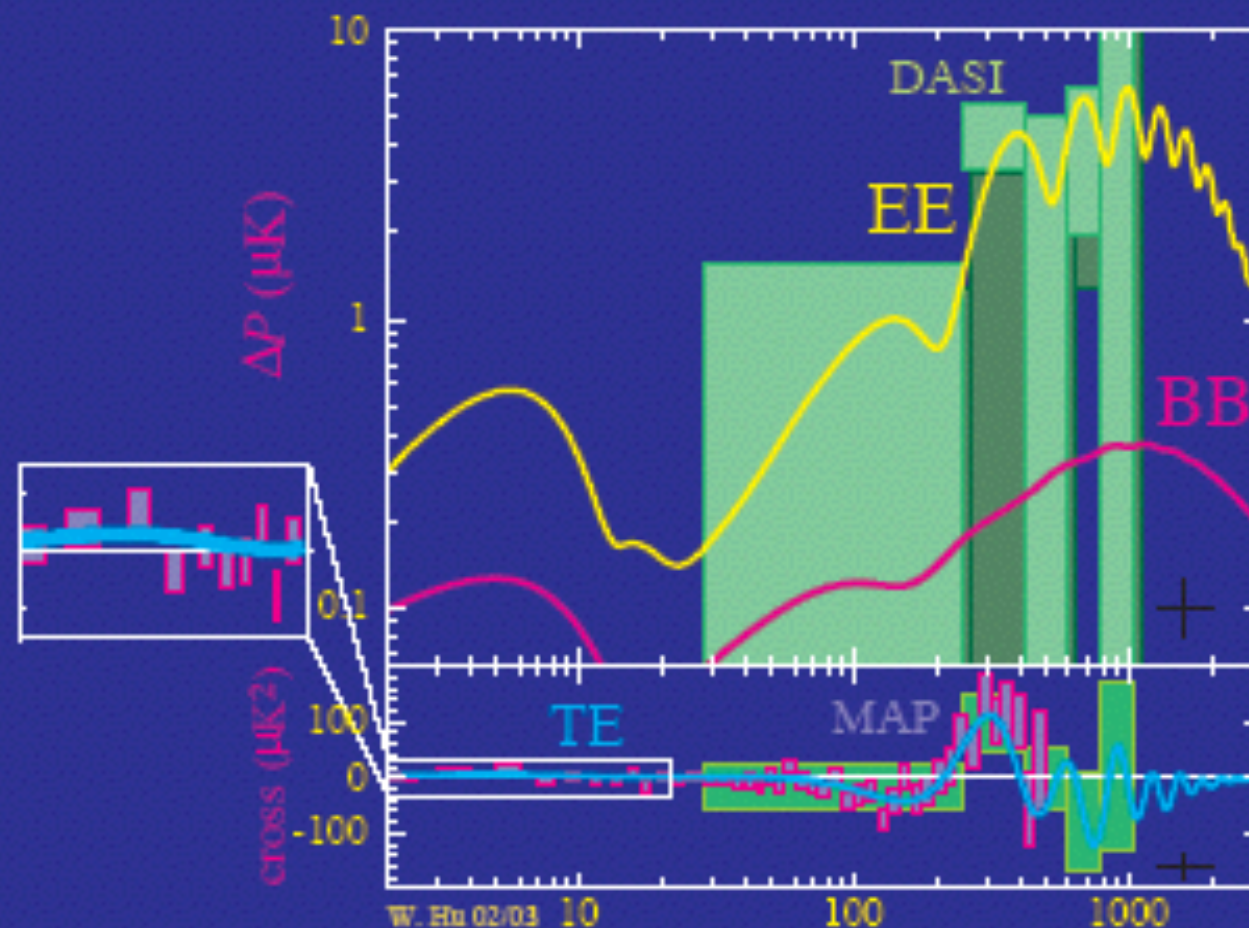
Dark Matter

- A third peak comparable to second peak indicates a dark matter density $\sim 5x$ that of ordinary matter
- Dark matter $\sim 25\%$ of the critical density



Predictive Power

- Model predicts the precise form of the damping of sound waves: observed ✓
- Model predicts that associated with the damping, the CMB becomes polarized: observed ✓
- Model predicts that temperature fluctuations correlated with local structure due to the dark energy: observed ✓



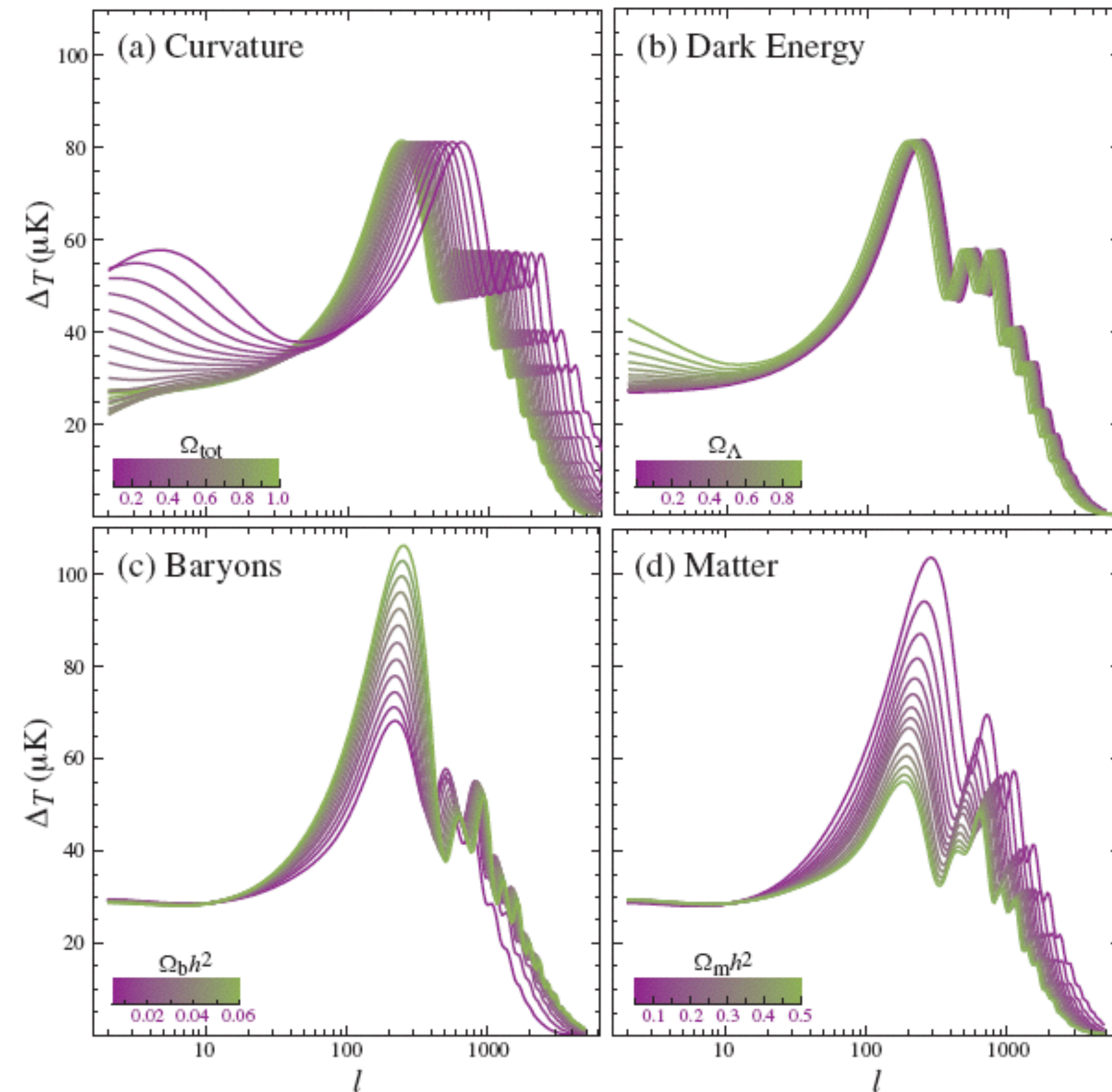


Plate 4: Sensitivity of the acoustic temperature spectrum to four fundamental cosmological parameters (a) the curvature as quantified by Ω_{tot} (b) the dark energy as quantified by the cosmological constant Ω_{Λ} ($w_{\Lambda} = -1$) (c) the physical baryon density $\Omega_b h^2$ (d) the physical matter density $\Omega_m h^2$, all varied around a fiducial model of $\Omega_{\text{tot}} = 1$, $\Omega_{\Lambda} = 0.65$, $\Omega_b h^2 = 0.02$, $\Omega_m h^2 = 0.147$, $n = 1$, $z_{\text{ri}} = 0$, $E_i = 0$.

Annu. Rev. Astron. and
Astrophys. 2002
Cosmic Microwave Background
Anisotropies by **Wayne Hu** and
Scott Dodelson

For animation of the effects of changes in cosmological parameters on the CMB angular power spectrum and the matter power spectrum, plus links to many CMB websites, see Max Tegmark's and Wayne Hu's websites:

<http://space.mit.edu/home/tegmark/movies.html>

<http://background.uchicago.edu/~whu/physics/physics.html>

WMAP 5-year data and papers are at <http://lambda.gsfc.nasa.gov/>

G. Hinshaw et al. ApJS, 180, 225 (2009)

Five-Year Wilkinson Microwave Anisotropy Probe (WMAP¹) Observations:
Data Processing, Sky Maps, & Basic Results

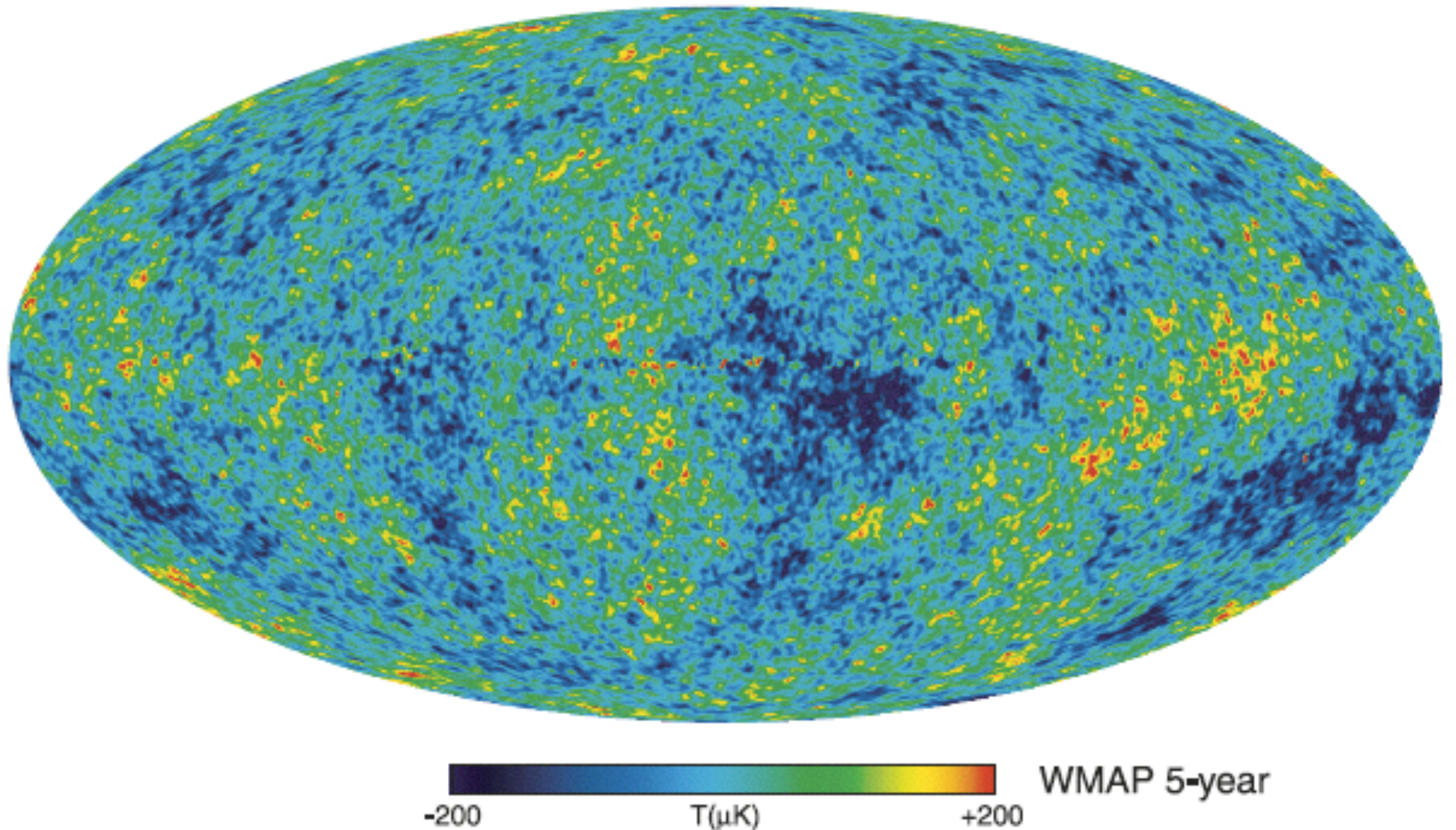


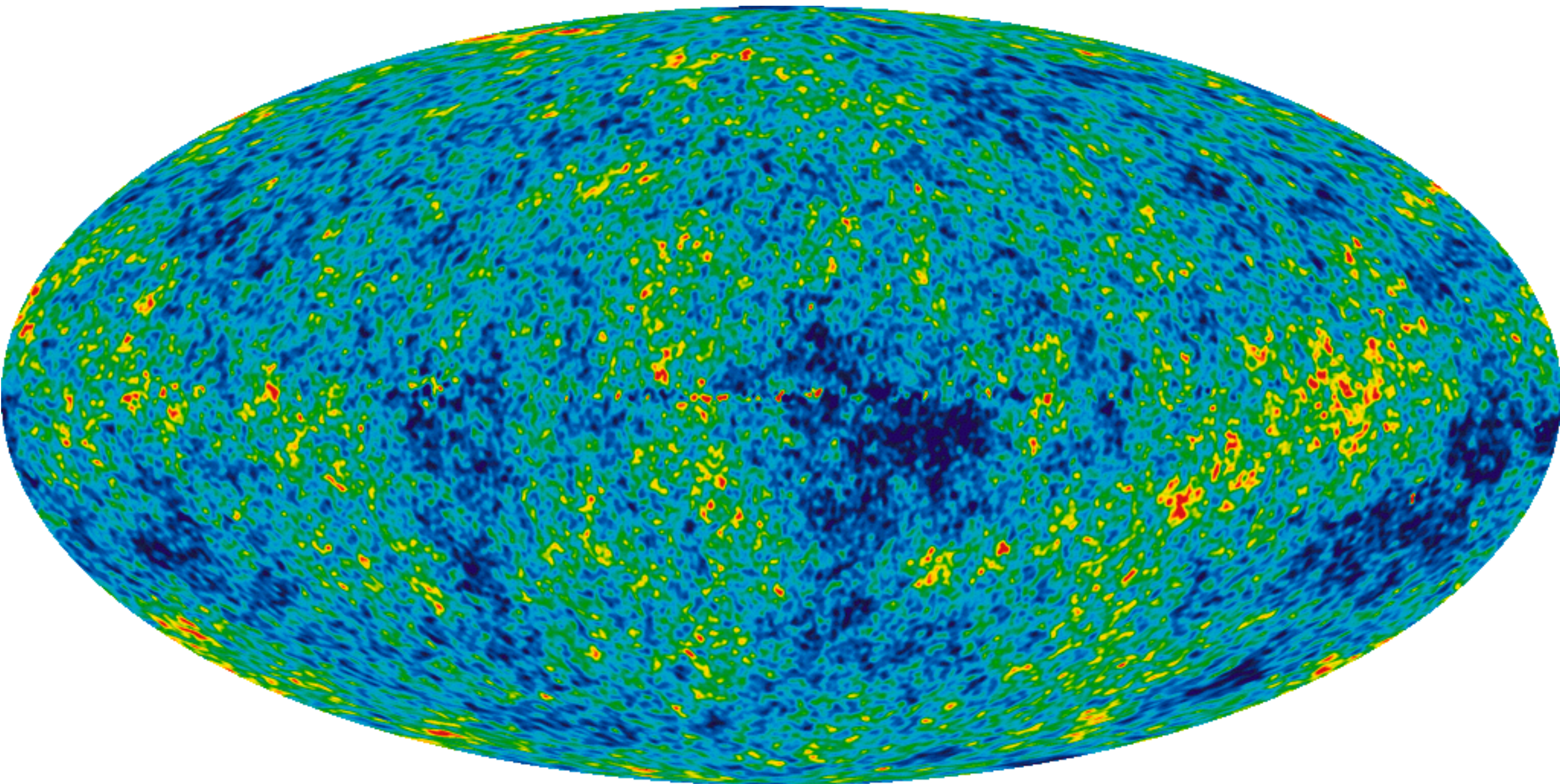
Fig. 12. The foreground-reduced Internal Linear Combination (ILC) map.

J. Dunkley, et.al. Five-Year Wilkinson Microwave Anisotropy Probe (WMAP) Observations: Likelihoods and Parameters from WMAP Data (2008)

Final paragraph of Conclusions:

Considering a range of extended models, we continue to find that **the standard Λ CDM model is consistently preferred by the data**. The improved measurement of the third peak now requires the existence of light relativistic species, assumed to be neutrinos, at high confidence. The standard scenario has three neutrino species, but the three-year WMAP data could not rule out models with none. **The CDM model also continues to succeed in fitting a substantial array of other observations**. Certain tensions between other observations and those of WMAP, such as the amplitude of matter fluctuations measured by weak lensing surveys and using the Ly- α forest, and the primordial lithium abundance, have either been resolved with improved understanding of systematics, or show promise of being explained by recent observations. With further WMAP observations we will better probe both the universe at a range of epochs, measuring fluctuation characteristics to probe the initial inflationary process, or other non-inflationary scenario, improving measurements of the composition of the universe at the recombination era, and characterizing the reionization process in the universe.

The WMAP 7-Year Internal Linear Combination Map is a weighted linear combination of the five WMAP frequency maps. The weights are computed using criteria which minimize the Galactic foreground contribution to the sky signal. The resultant map provides a low-contamination image of the CMB anisotropy.



<http://lambda.gsfc.nasa.gov/product/space/>

Seven-Year Wilkinson Microwave Anisotropy Probe (WMAP) Observations: Sky Maps, Systematic Errors, and Basic Results - N. Jarosik et al. - January 2010

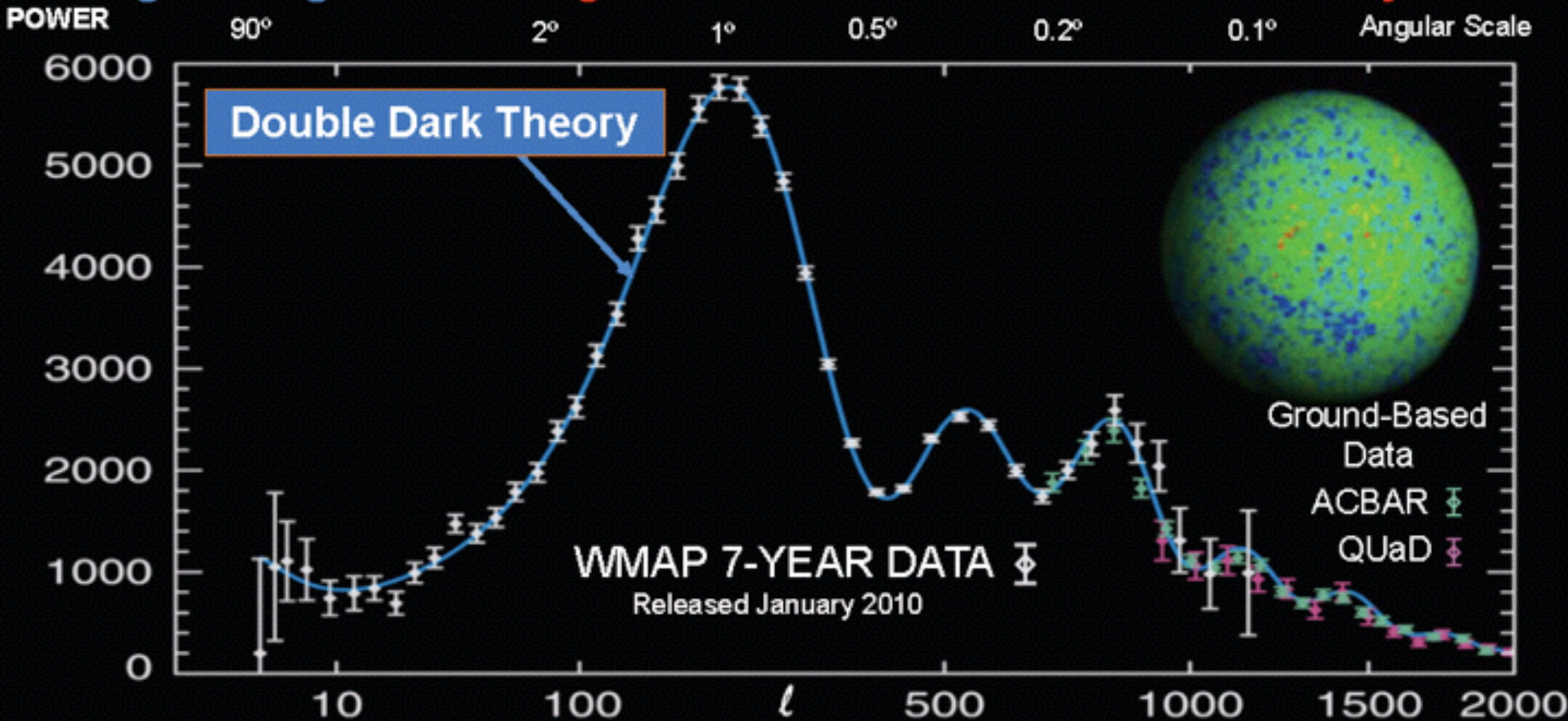
The seven year data set is well fit by a minimal six-parameter flat Λ CDM model. The parameters for this model, using the *WMAP* data in conjunction with baryon acoustic oscillation data from the Sloan Digital Sky Survey and priors on H_0 from Hubble Space Telescope observations, are: $\Omega_b h^2 = 0.02260 \pm 0.00053$, $\Omega_c h^2 = 0.1123 \pm 0.0035$, $\Omega_\Lambda = 0.728^{+0.015}_{-0.016}$, $n_s = 0.963 \pm 0.012$, $\tau = 0.087 \pm 0.014$ and $\sigma_8 = 0.809 \pm 0.024$ (68 % CL uncertainties).

The temperature power spectrum signal-to-noise ratio per multipole is greater than unity for multipoles $\ell \lesssim 919$, allowing a robust measurement of the third acoustic peak. This measurement results in improved constraints on the matter density, $\Omega_m h^2 = 0.1334^{+0.0056}_{-0.0055}$, and the epoch of matter-radiation equality, $z_{\text{eq}} = 3196^{+134}_{-133}$, using *WMAP* data alone.

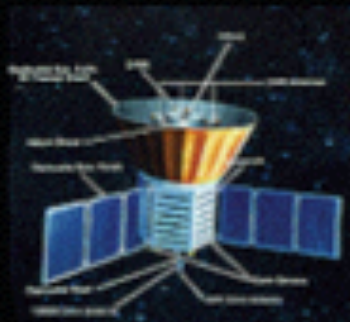
The new *WMAP* data, when combined with smaller angular scale microwave background anisotropy data, results in a 3σ detection of the abundance of primordial Helium, $Y_{\text{He}} = 0.326 \pm 0.075$. When combined with additional external data sets, the *WMAP* data also yield better determinations of the total mass of neutrinos, $\sum m_\nu = < 0.58$ eV (95% CL), and the effective number of neutrino species, $N_{\text{eff}} = 4.34^{+0.86}_{-0.88}$. The power-law index of the primordial power spectrum is now determined to be $n_s = 0.963 \pm 0.012$, excluding the Harrison-Zel'dovich-Peebles spectrum by $> 3\sigma$.

These new *WMAP* measurements provide important tests of Big Bang cosmology.

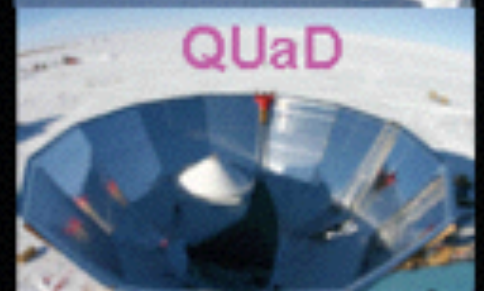
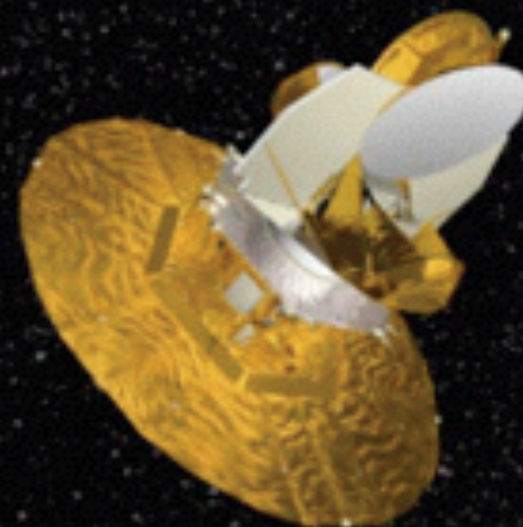
Big Bang Data Agrees with Double Dark Theory!



Cosmic Background Explorer
COBE
1992



Wilkinson Microwave Anisotropy Probe
WMAP
2003-



<http://lambda.gsfc.nasa.gov/product/space/>

Seven-Year Wilkinson Microwave Anisotropy Probe (WMAP) Observations:
Sky Maps, Systematic Errors, and Basic Results - N. Jarosik et al. - January 2010

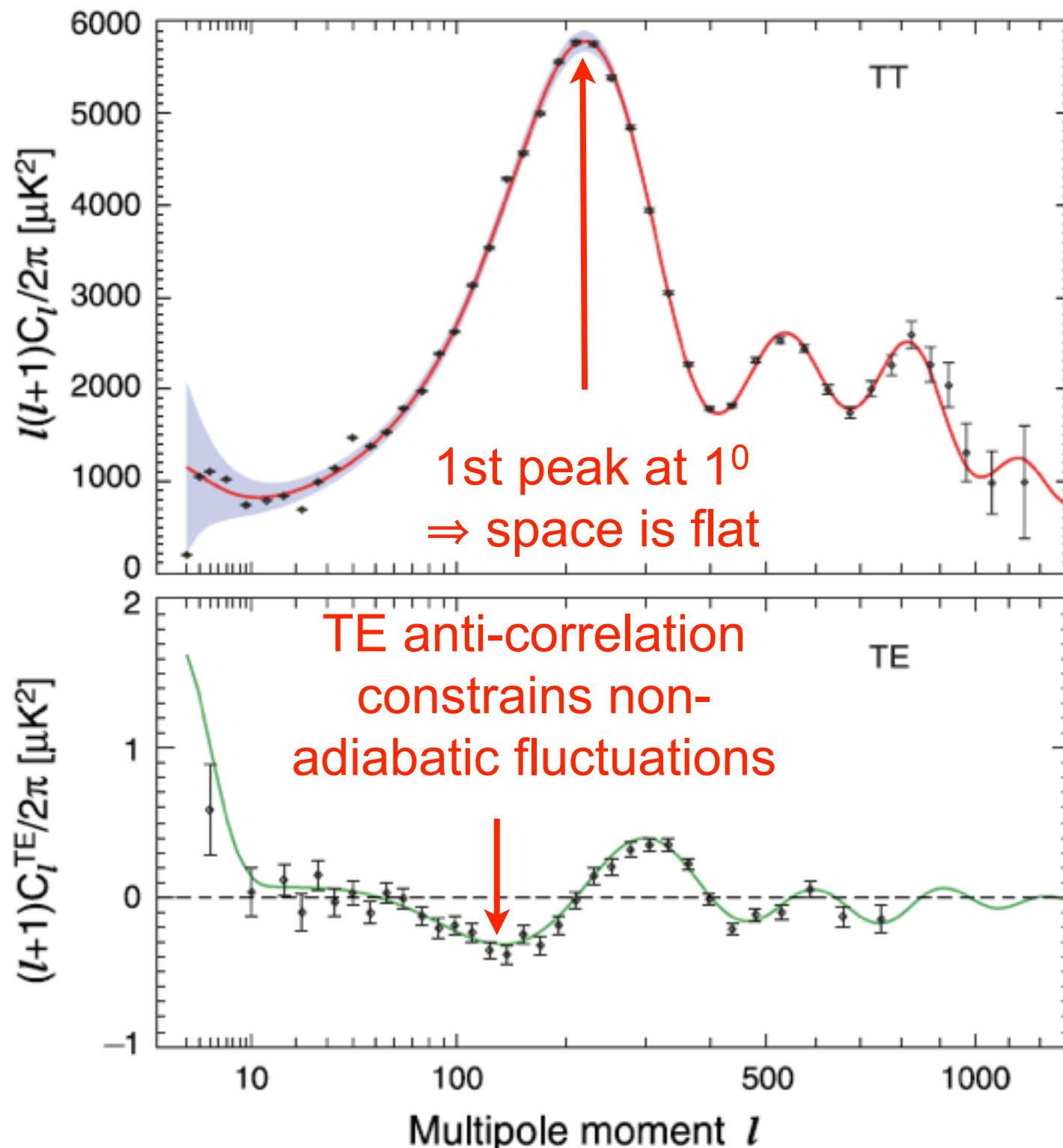


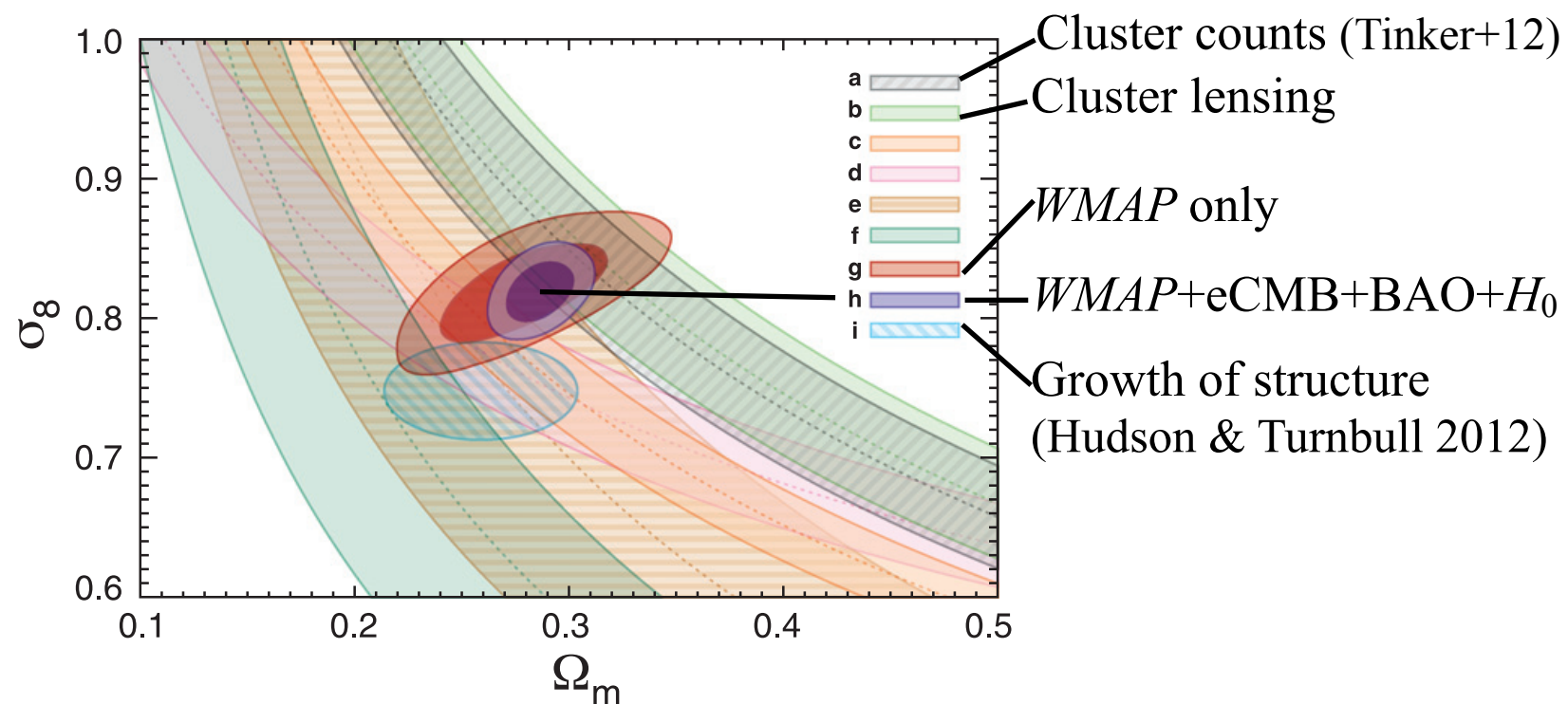
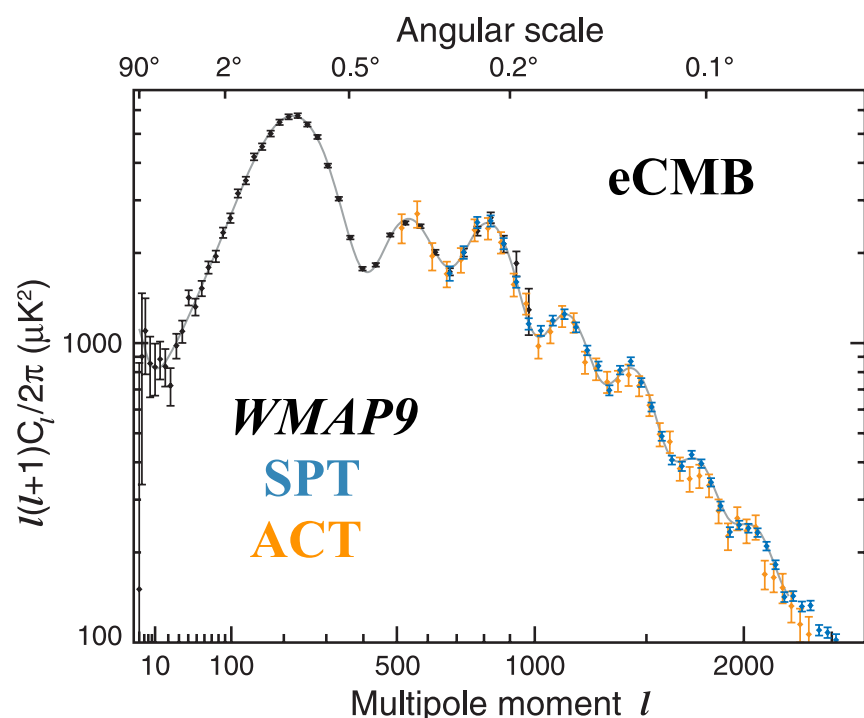
Fig. 9.— The temperature (TT) and temperature-polarization (TE) power spectra for the seven-year WMAP data set. The solid lines show the predicted spectrum for the best-fit flat Λ CDM model. The error bars on the data points represent measurement errors while the shaded region indicates the uncertainty in the model spectrum arising from cosmic variance.

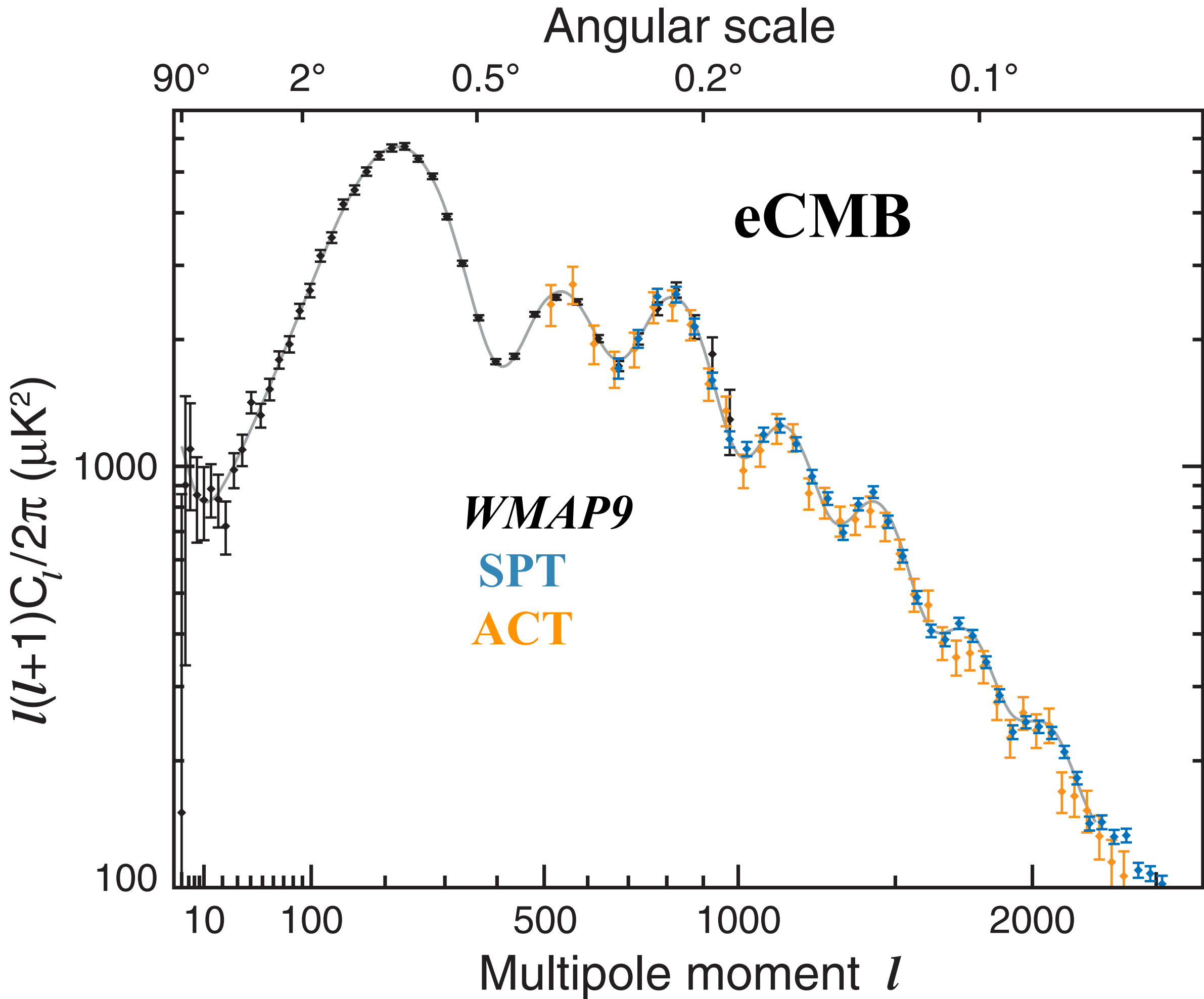
Successes: CMB, Expansion History, Large Scale Structure

NINE-YEAR WILKINSON MICROWAVE ANISOTROPY PROBE (WMAP) OBSERVATIONS: COSMOLOGICAL PARAMETER RESULTS - Hinshaw+13 - ApJS 208, 19

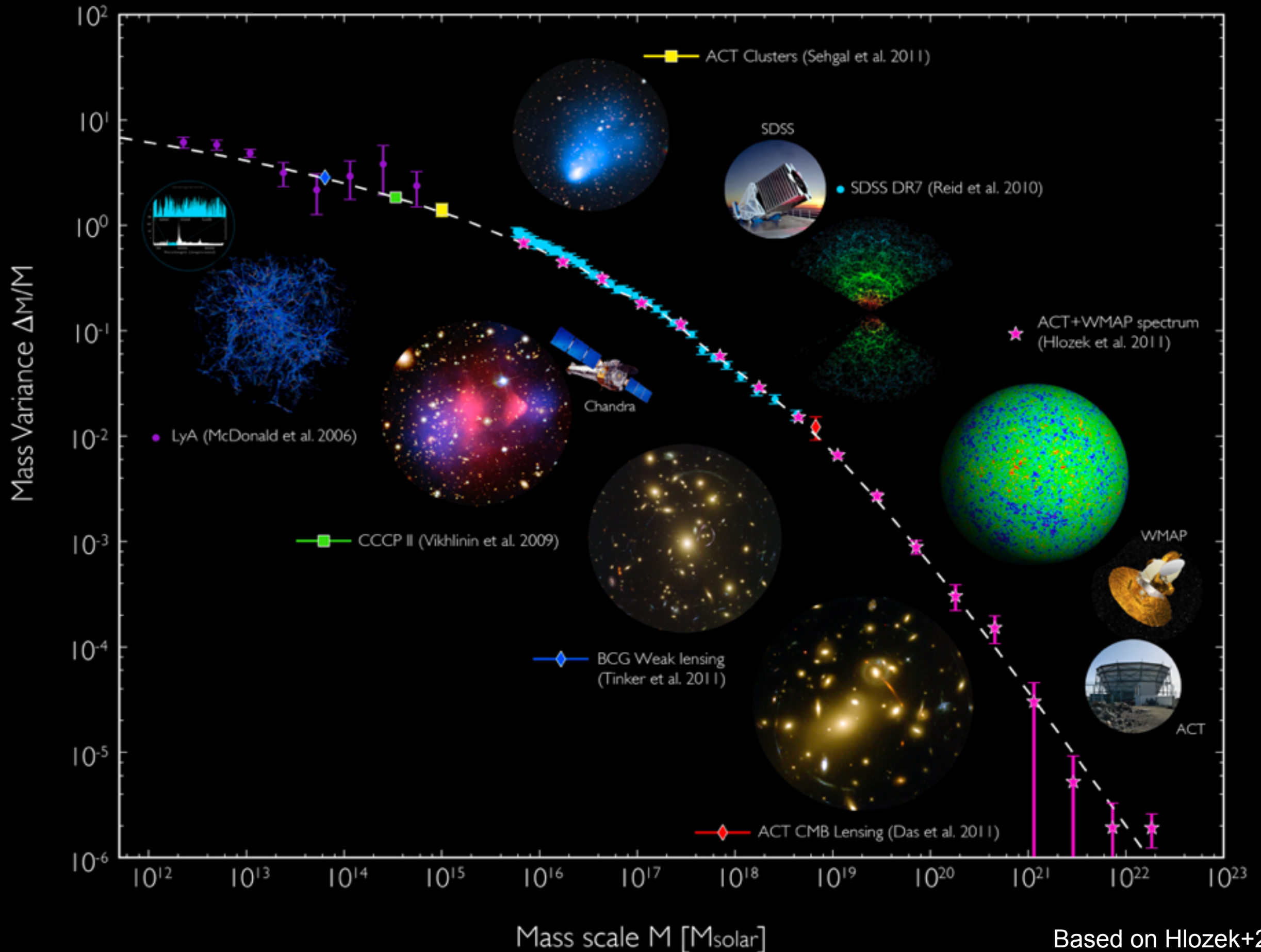
ABSTRACT: The *WMAP* data alone, and in combination, continue to be remarkably well fit by a six-parameter Λ CDM model. When *WMAP* data are combined with measurements of the high- ℓ cosmic microwave background anisotropy, the baryon acoustic oscillation scale, and the Hubble constant, the matter and energy densities, $\Omega_b h^2$, $\Omega_c h^2$, and Ω_Λ , are each determined to a precision of $\sim 1.5\%$. New limits on deviations from the six-parameter model are presented, for example: the fractional contribution of tensor modes is limited to $r < 0.13$ (95% CL); $\sum m_\nu < 0.44$ eV (95% CL); and the number of relativistic species is found to lie within $N_{\text{eff}} = 3.84 \pm 0.40$.

CONCLUSION: We have used the final, nine-year *WMAP* temperature and polarization data in conjunction with high- l CMB power spectrum data and a new H_0 measurement (Riess et al. 2011) to place stringent constraints on the six parameters of the minimal Λ CDM model, and on parameters beyond the minimal set. **The six-parameter model continues to describe all the data remarkably well, and we find no convincing evidence for deviations from this model: the geometry of the observable universe is flat and dark energy is consistent with a cosmological constant.** The amplitude of matter fluctuations derived from *WMAP* data alone, assuming the minimal model, $\sigma_8 = 0.821 \pm 0.023$ (68% CL), is consistent with all the existing data on matter fluctuations, including cluster abundances, peculiar velocities, and gravitational lensing. The combined (*WMAP*+eCMB+BAO+ H_0) data set gives $\sigma_8 = 0.820^{+0.013}_{-0.014}$ (68% CL).



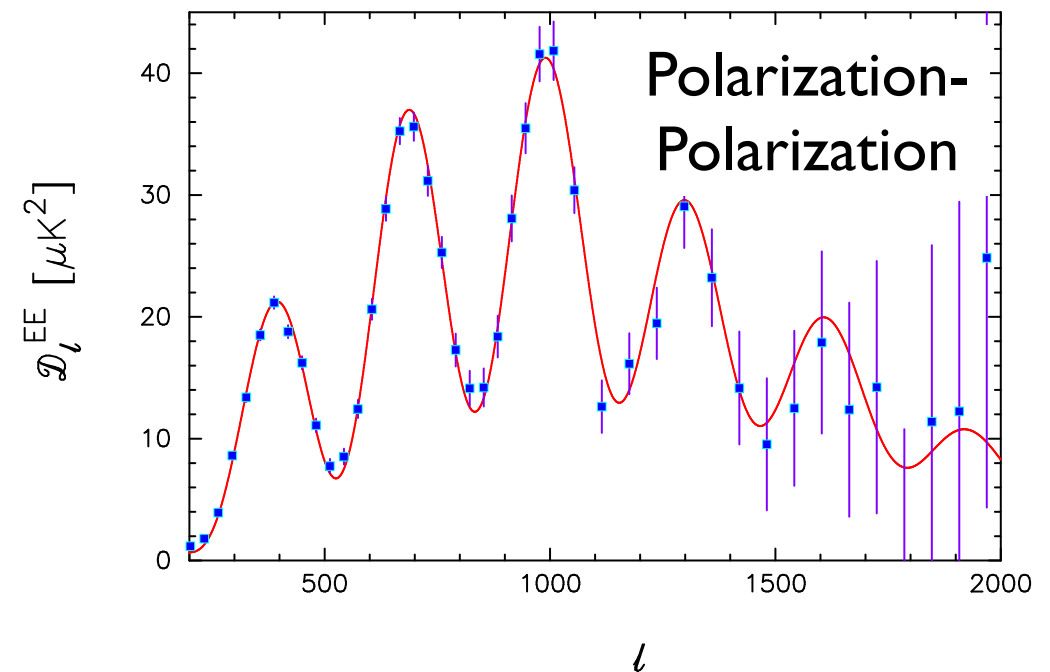
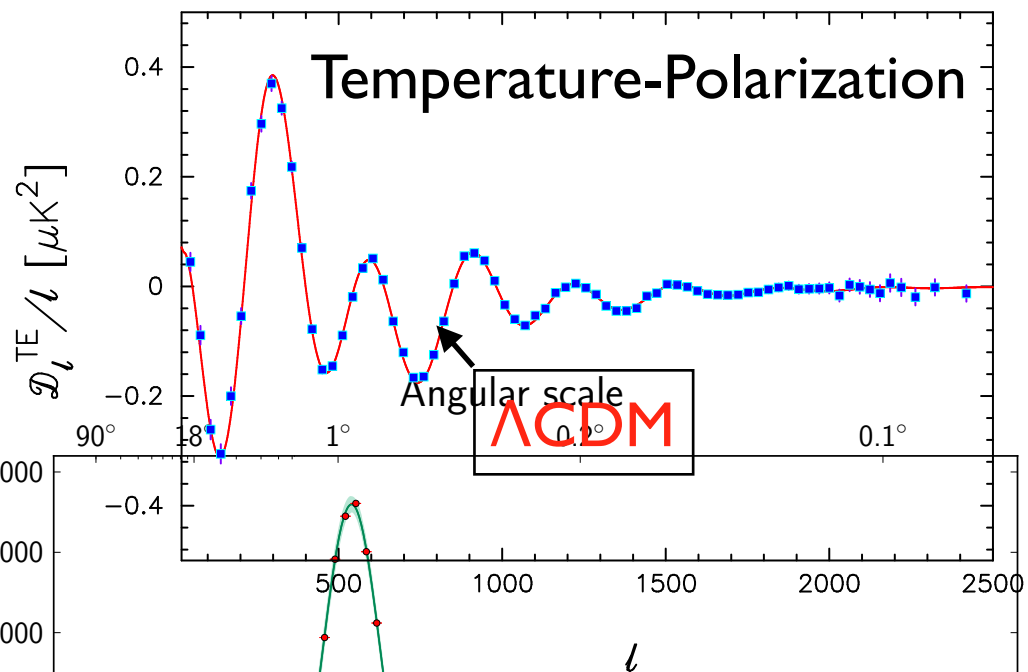
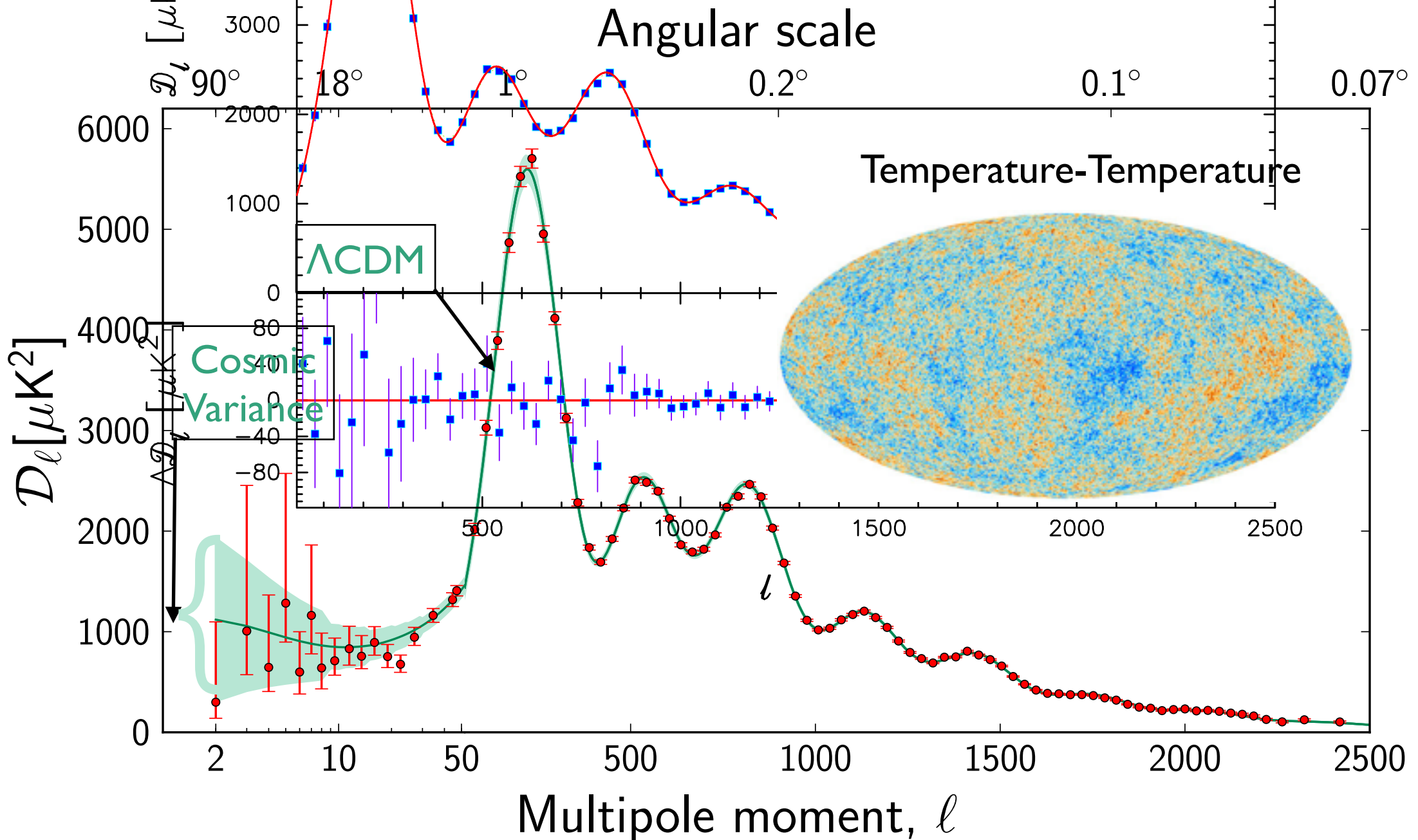
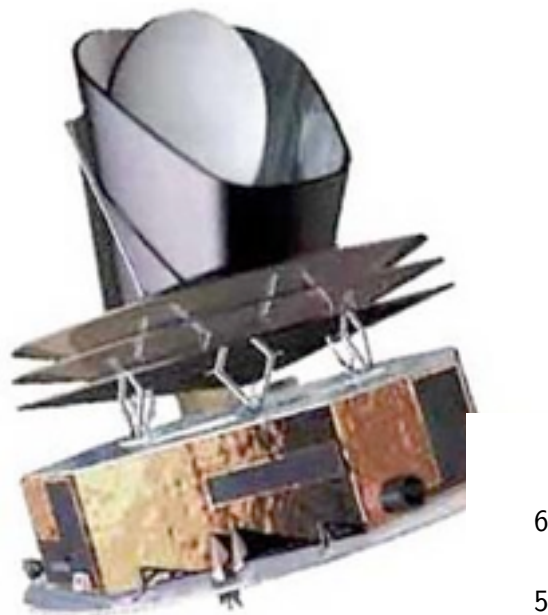


Matter Distribution **Agrees with Λ CDM!**



European
Space
Agency
PLANCK
Satellite
Data

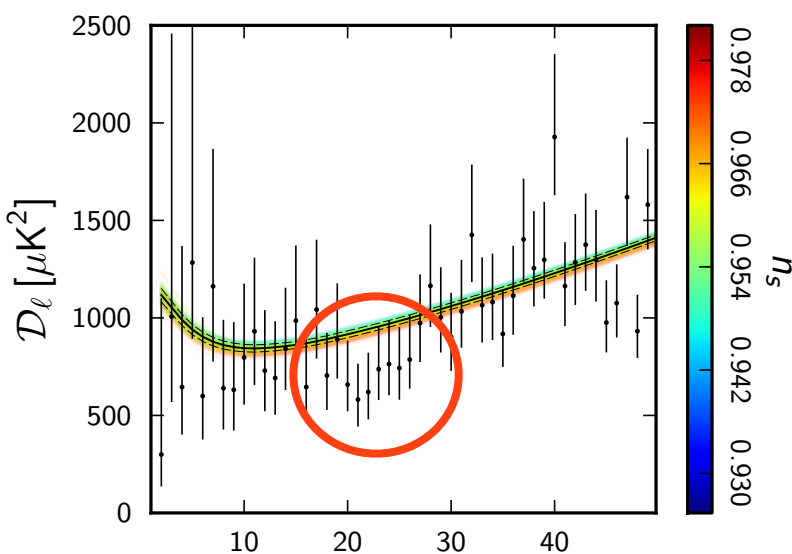
Released
March 21,
2013



Successes: CMB, Expansion History, Large Scale Structure

Planck 2013 results. XVI. Cosmological parameters

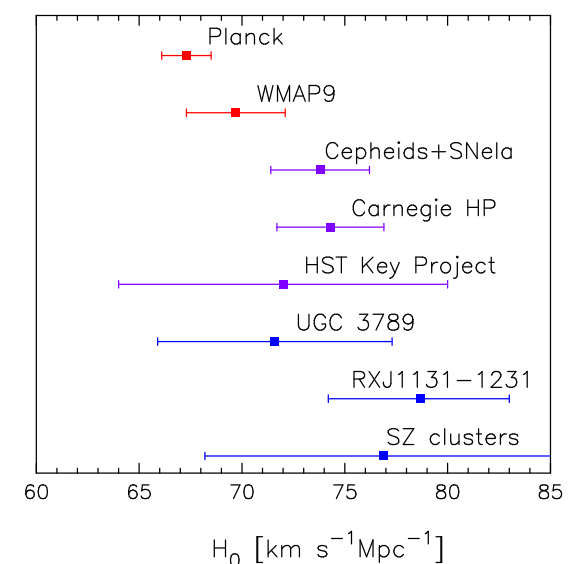
ABSTRACT: We find that the *Planck* spectra at high multipoles ($\ell > 40$) are extremely well described by the standard spatially-flat six-parameter Λ CDM cosmology with a power-law spectrum of adiabatic scalar perturbations. Within the context of this cosmology, the *Planck* data determine the cosmological parameters to high precision: the physical densities of baryons and cold dark matter, and the scalar spectral index are estimated to be $\Omega_b h^2 = 0.02205 \pm 0.00028$, $\Omega_c h^2 = 0.1199 \pm 0.0027$, and $n_s = 0.9603 \pm 0.0073$, respectively (68% errors). For this cosmology, we find a low value of the Hubble constant, $H_0 = 67.3 \pm 1.2$ km/s/Mpc, and a high value of the matter density parameter, $\Omega_m = 0.315 \pm 0.017$. These values are in tension with recent direct measurements of H_0 and the magnitude-redshift relation for Type Ia supernovae, but are in excellent agreement with geometrical constraints from baryon acoustic oscillation (BAO) surveys. We present selected results from a large grid of cosmological models, using a range of additional astrophysical data sets in addition to *Planck* and high-resolution CMB data. **None of these models are favoured over the standard six-parameter Λ CDM cosmology.** Using BAO and CMB data, we find $N_{\text{eff}} = 3.30 \pm 0.27$ for the effective number of relativistic degrees of freedom, and an **upper limit of 0.23 eV for the sum of neutrino masses.** We find no evidence for dynamical dark energy; using BAO and CMB data, the dark energy equation of state parameter is constrained to be $w = 1.13^{+0.13}_{-0.10}$. Despite the success of the six-parameter Λ CDM model in describing the *Planck* data at high multipoles, we note that this cosmology does not provide a good fit to the temperature power spectrum at low multipoles. The unusual shape of the spectrum in the multipole range $20 < \ell < 40$ was seen previously in the *WMAP* data and is a real feature of the primordial CMB anisotropies. The poor fit to the spectrum at low multipoles is not of decisive significance, but is an “anomaly” in an otherwise self-consistent analysis of the *Planck* temperature data.



The main Planck anomaly is the low amplitudes at $\ell \approx 21-27$

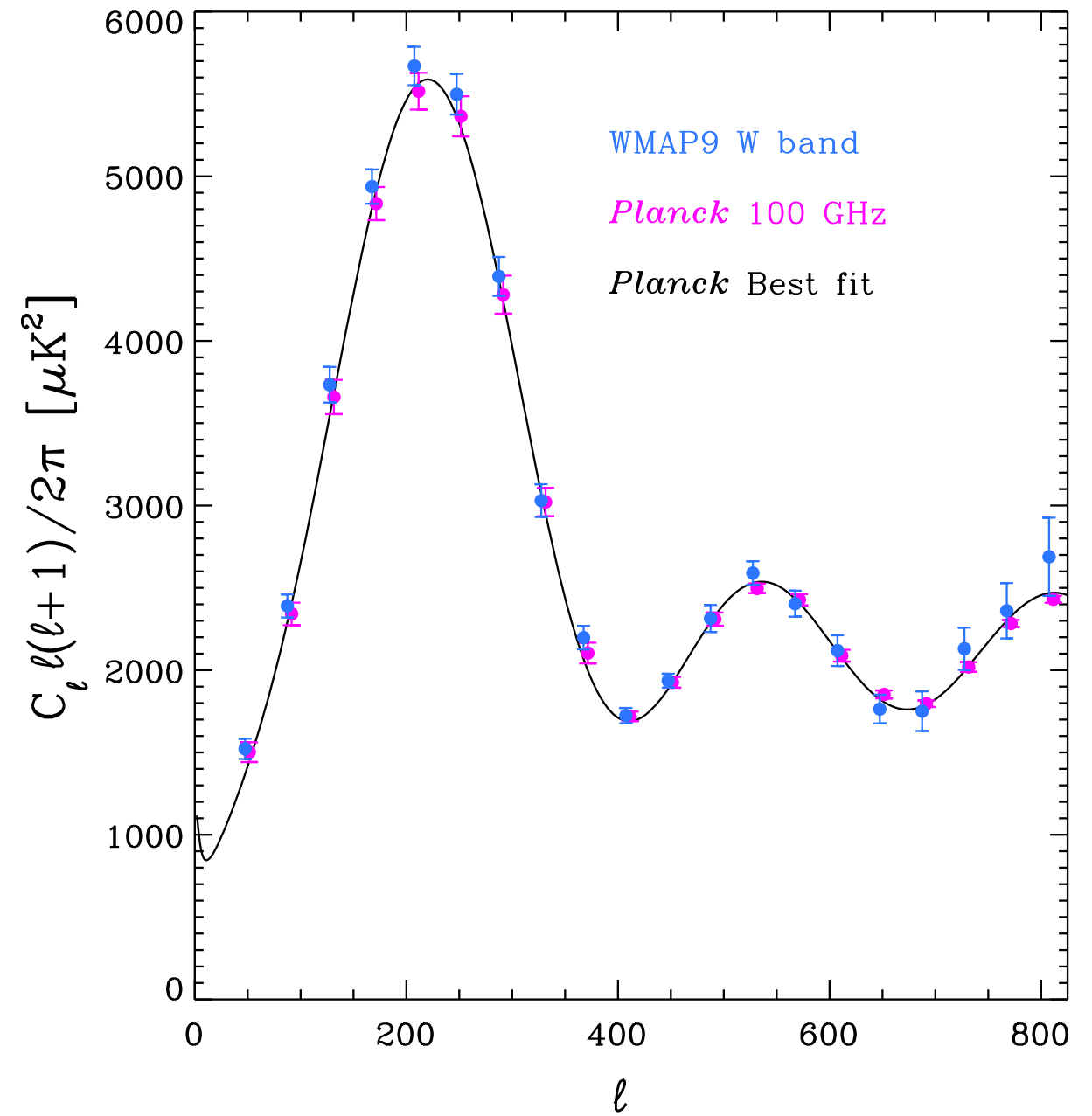
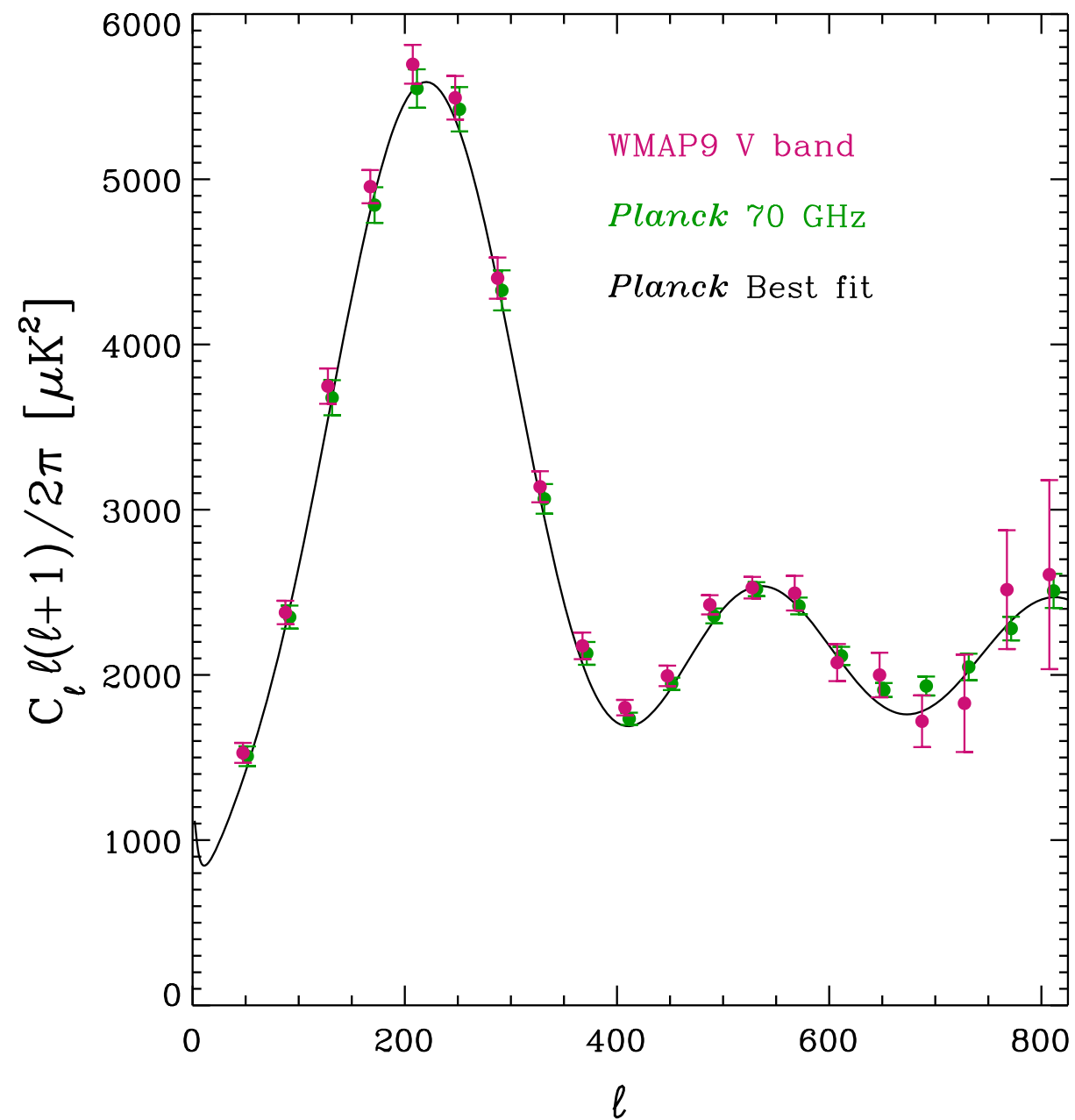
Planck errors are small and Planck's values for H_0 and Ω_m are somewhat different from WMAP's

See also Efstathiou
 H_0 revisited
arXiv:1311.3461



But: WMAP9 vs. Planck, Planck Clusters vs. CMB?

There is a systematic offset between WMAP9 and Planck!



These plots are from a Planck paper in prep. (Kris Gorski, private communication, 2/16/14)

But: WMAP9 vs. Planck, Planck Clusters vs. CMB?

COSMOLOGICAL PARAMETERS - OBSERVATIONS AND SIMULATIONS

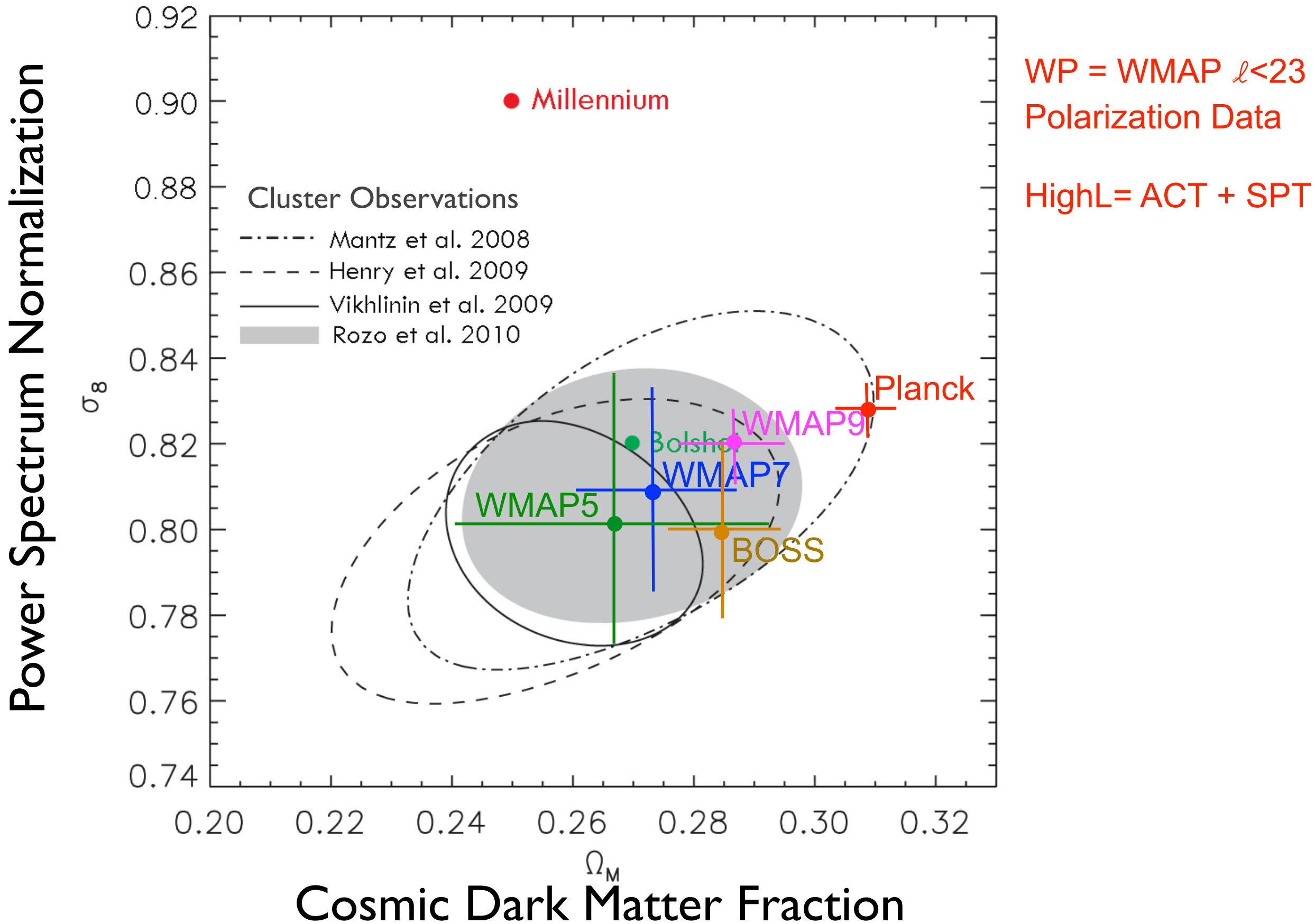
Parameter	<i>WMAP9*</i>	<i>Bolshoi</i>	<i>Planck+WP+highL+BAO**</i>	<i>Bolshoi-Planck***</i>	<i>Millennium</i>
Ω_Λ	0.7135 ± 0.0096	0.73	0.692 ± 0.010	0.6929	0.75
Ω_m	0.2865 ± 0.0088	0.27		0.3071	0.25
σ_8	0.820 ± 0.014	0.82	0.826 ± 0.012	0.8225	0.90
H_0	69.32 ± 0.80	70.0	67.80 ± 0.77	67.77	73.0
n_s	0.9608 ± 0.0080	0.95	0.9608 ± 0.0054	0.96	1.00
t_0 (Gyr)	13.772 ± 0.059	13.86	13.798 ± 0.037	13.814	13.573

*WMAP9 is WMAP+eCMB+BAO+ H_0 from Table 17 of Bennett et al. 2013, ApJS 208, 20

**The 4th column is the 68% limits for *Planck+WP+highL+BAO* from Table 5 of of the Planck Collaboration: Cosmological parameters paper, Planck 2013 results. XVI. Cosmological parameters

***Bolshoi-Planck parameters were used for the Bolshoi-Planck and MultiDark-Planck simulations

Determination of σ_8 and Ω_M from CMB+ WMAP9+SN+Clusters Planck+WP+HighL+BAO



But: Planck Clusters vs. CMB?

Planck 2013 results. XX. Cosmology from Sunyaev–Zeldovich cluster counts - arXiv:1303.5080

Assuming a bias between the X-ray determined mass and the true mass of 20%, motivated by comparison of the observed mass scaling relations to those from a set of numerical simulations, we find that ... $\sigma_8 = 0.77 \pm 0.02$ and $\Omega_m = 0.29 \pm 0.02$. The values of the cosmological parameters are degenerate with the mass bias, and it is found that the larger values of σ_8 and Ω_m preferred by the Planck's measurements of the primary CMB anisotropies can be accommodated by a mass bias of about 45%. Alternatively, consistency with the primary CMB constraints can be achieved by inclusion of processes that suppress power on small scales, such as a component of massive neutrinos.

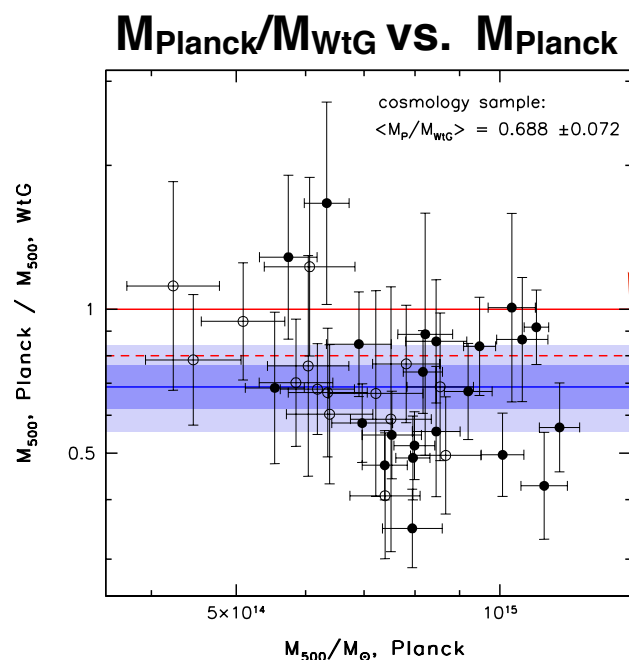
This has led to papers proposing $\Sigma m_\nu > 0.23$ eV such as Hamann & Hasenkamp JCAP 2013

Relative cluster masses can be determined accurately cluster-by-cluster using X-rays as was done by Vikhlinin+09, Mantz+10, and Planck paper XX, but the absolute masses should be calibrated using gravitational lensing, say Rozo+13,14 and van der Linden+14. The Arnaud+07,10 X-ray cluster masses used in Planck paper XX are the lowest of all. Using gravitational lensing mass calibration raises the cluster masses and thus predicts fewer expected clusters. This lessens the tension between the CMB and cluster observations.

Closing the loop: self-consistent ... scaling relations for clusters of Galaxies - Rozo+14 MNRAS

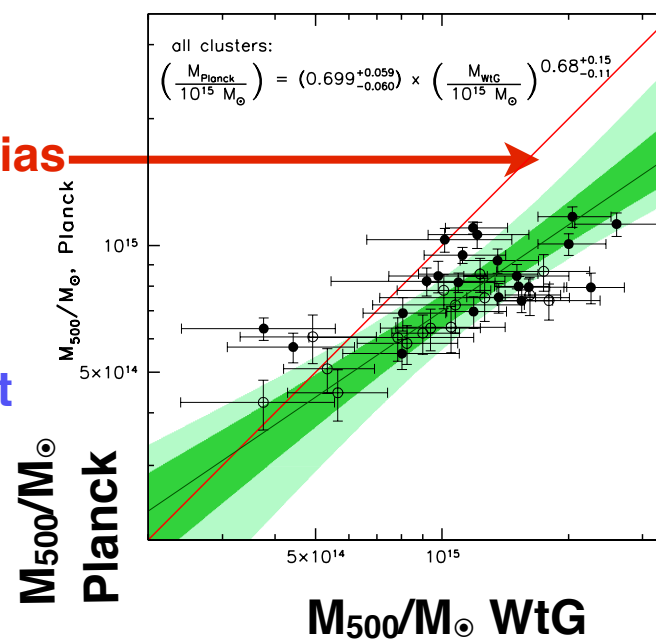
Robust weak-lensing mass calibration of Planck galaxy cluster masses - von der Linden+14

The ratio of cluster masses measured by Planck and by Weighing the Giants (WtG).



No Bias

Best Fit



MPlanck VS. MWtG

Best Fit

This decreases the tension between clusters and CMB and the motivation for $\Sigma m_\nu > 0.23$ eV.

Astro/Phys 224

Spring 2014

Origin and Evolution of the Universe

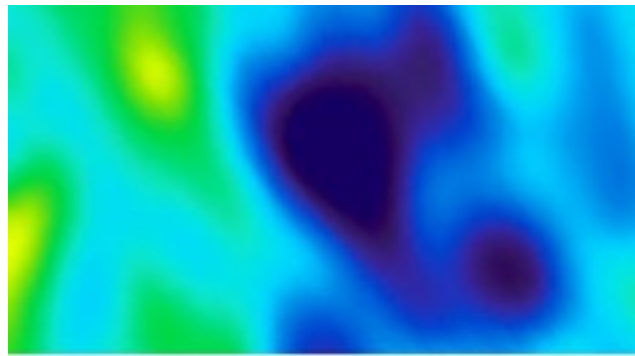
Week 5

Structure Formation

Joel Primack

University of California, Santa Cruz

Late Cosmological Epochs



380 kyr $z \sim 1000$

recombination
last scattering



dark ages



~ 100 Myr $z \sim 30$

first stars

~ 480 Myr $z \sim 10$

"reionization"



galaxy formation

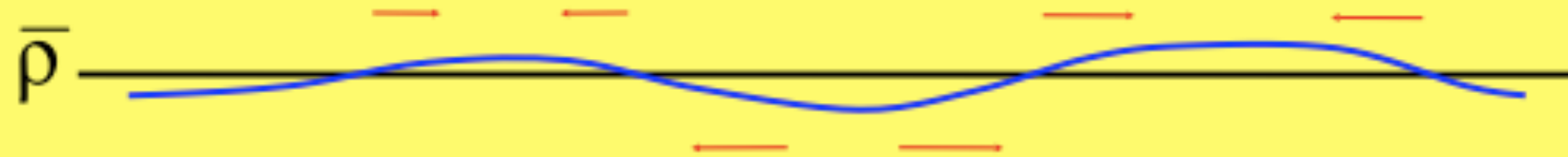


13.7 Gyr $z=0$

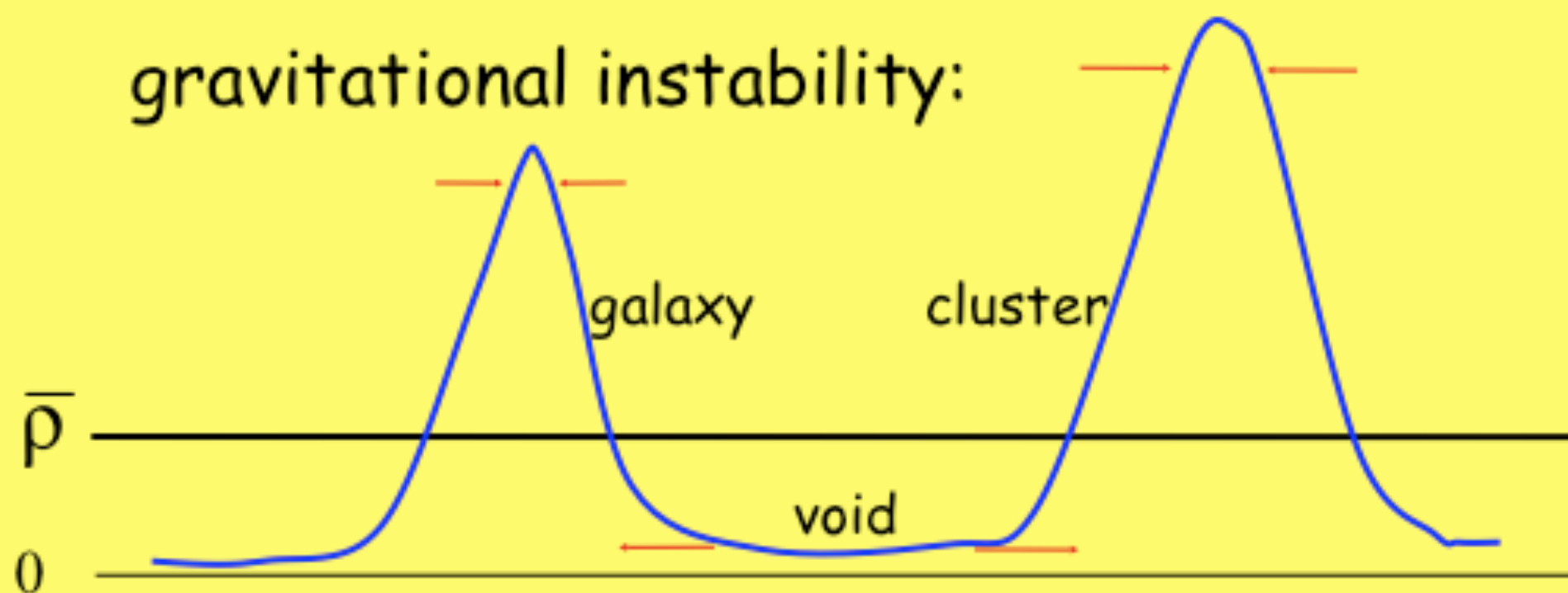
today

Gravitational instability

small-amplitude fluctuations:



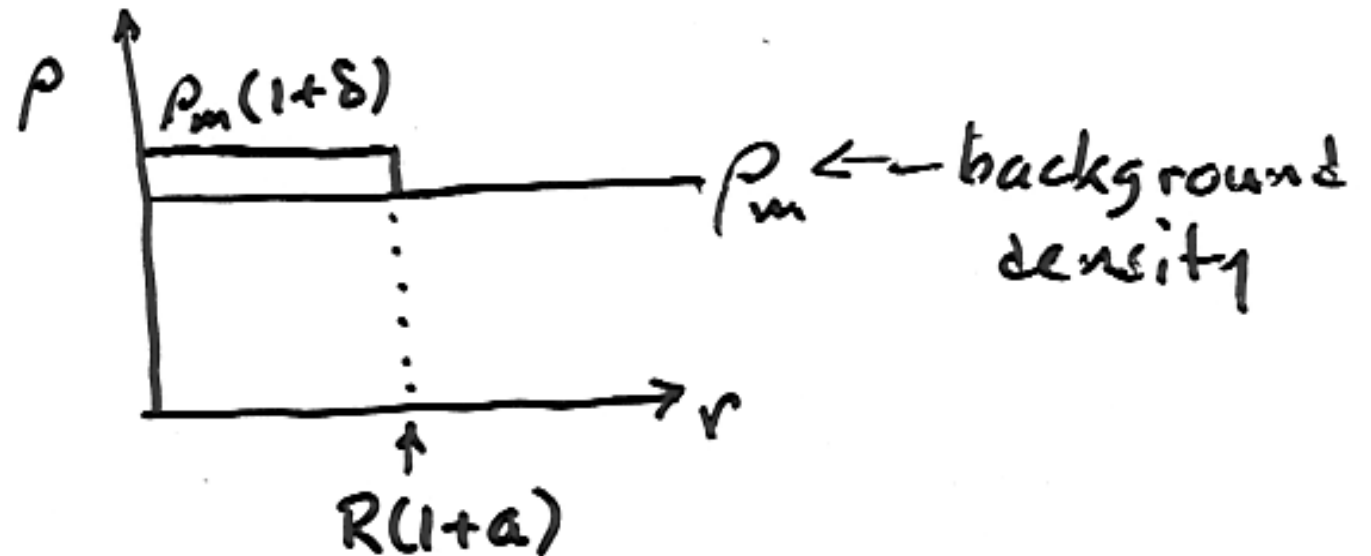
gravitational instability:



FLUCTUATIONS: LINEAR THEORY

Recall: $E(ii) - E(00) \Rightarrow \frac{2\ddot{a}}{a} = -\frac{8\pi}{3}G\rho - 8\pi Gp + \frac{2}{3}\Lambda$ (here $a = R, \Lambda=0$)

"TOP HAT MODEL"



MASS CONS. \Rightarrow

$$\rho_m (1+\delta) R^3 (1+a)^3 = \text{const.} \Rightarrow$$

$$\delta = -3a$$

GRAVITY: $\ddot{R} = -\frac{4\pi G}{3}(\rho + 3p)R$

$$\ddot{\delta} + 2\frac{\dot{R}}{R}\dot{\delta} = 4\pi G\rho_m\delta$$

RAD ERA $\dot{R}/R = \frac{1}{2}t^{-1}$,
 MATTER ERA $= \frac{2}{3}t^{-1}$,

APPLIED BOTH TO FLUCT. + BCG. \Rightarrow

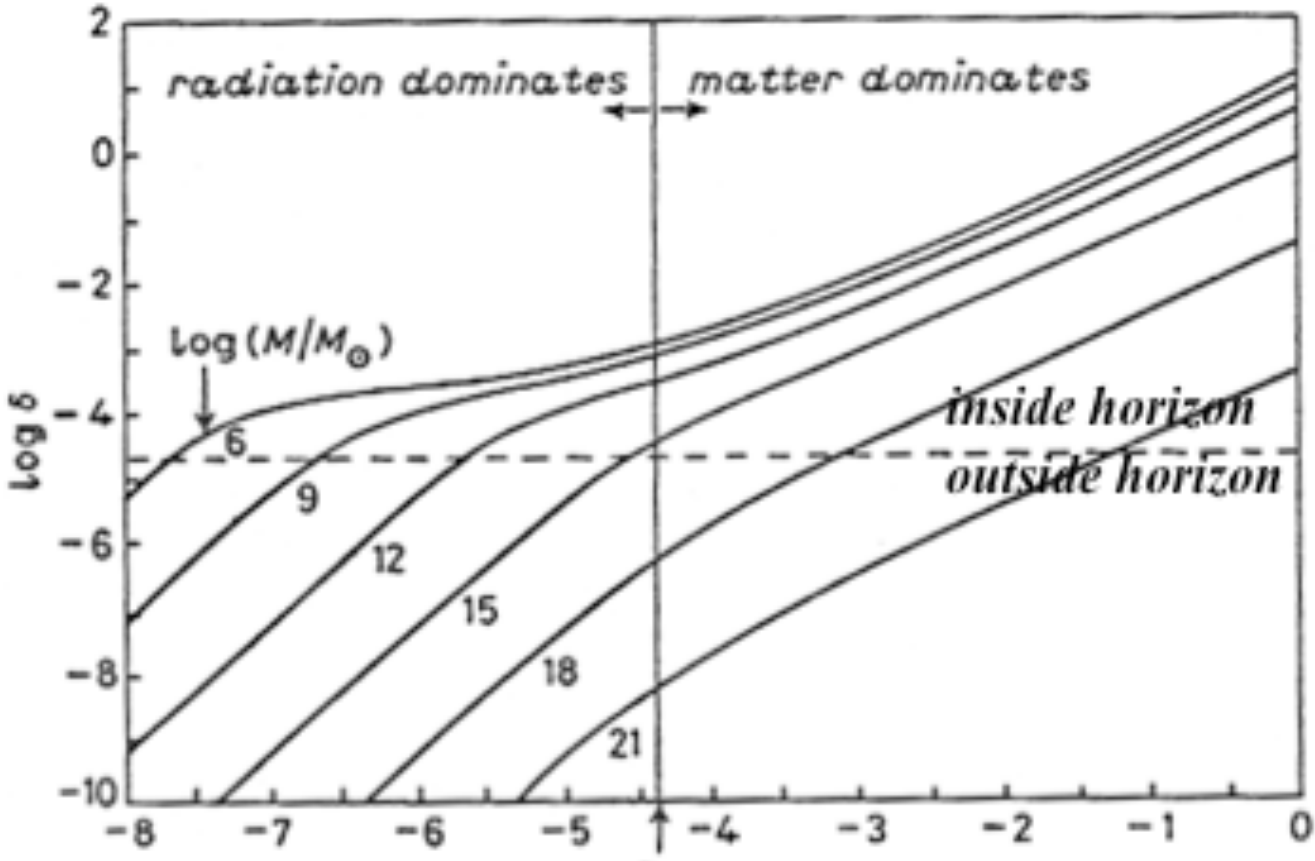
Try $\delta = t^\alpha$

$$\delta = At + Bt^{-1} = \underline{AR^2} + BR^{-2}$$

$$\delta = At^{2/3} + Bt^{-1} = \underline{AR} + BR^{-3/2}$$

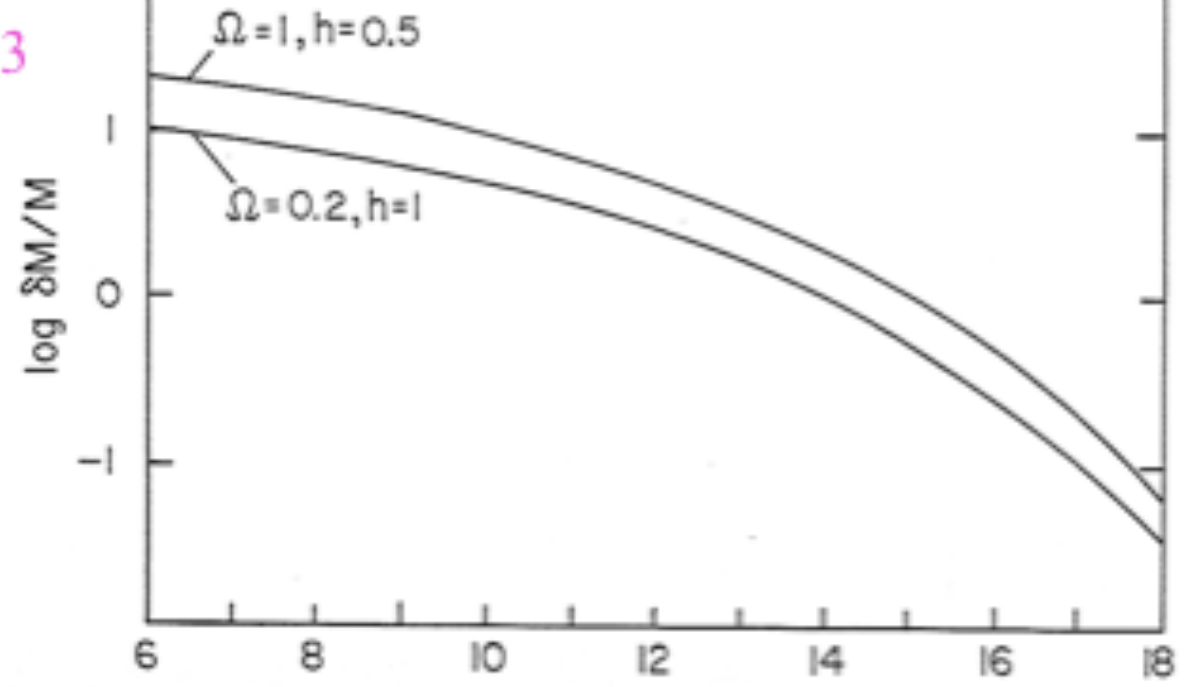
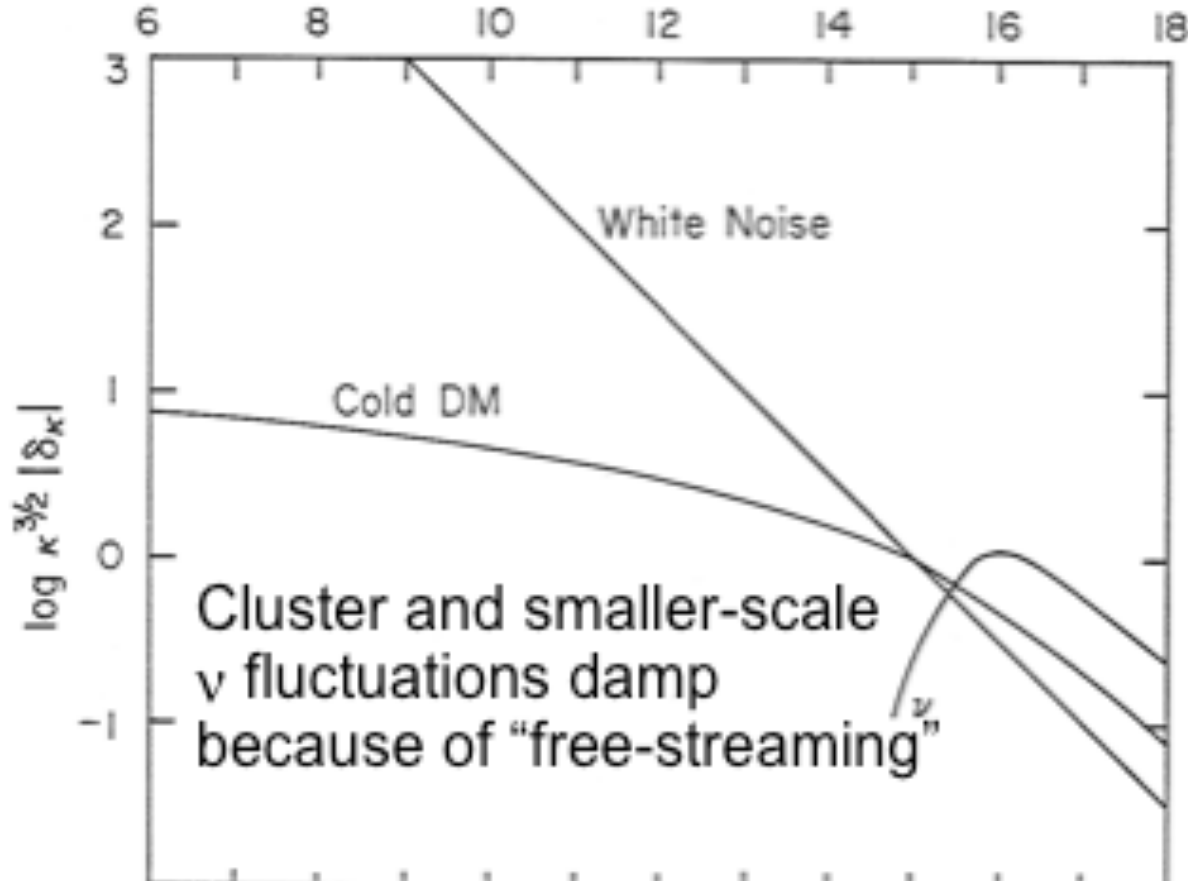
GROWING MODE

CDM Structure Formation: Linear Theory



Primack & Blumenthal 1983

Matter fluctuations that enter the horizon during the radiation dominated era, with masses less than about $10^{15} M_{\odot}$, grow only $\propto \log a$, because they are not in the gravitationally dominant component. But matter fluctuations that enter the horizon in the matter-dominated era grow $\propto a$. This explains the characteristic shape of the CDM fluctuation spectrum, with $\delta(k) \propto k^{-n/2-2} \log k$ for $k \gg k_{eq}$.



Blumenthal, Faber, Primack, & Rees 1984

The Initial Fluctuations

At Inflation: Gaussian, adiabatic

Fourier transform:

$$\delta(\vec{x}) = \sum_{\vec{k}} \delta_{\vec{k}} e^{i\vec{k}\cdot\vec{x}}$$

Power Spectrum:

$$P(k) \equiv \langle |\tilde{\delta}(\vec{k})|^2 \rangle \propto k^n$$

rms perturbation:

$$\delta_{rms} = \langle \delta^2 \rangle^{1/2} \propto \int_{k=0}^{k_{max}} P_k d^3k \propto M^{-(n+3)/6}$$

Correlation function:

$$\xi(r) \equiv \langle \delta(\vec{x})\delta(\vec{x} + \vec{r}) \rangle \propto \int |\tilde{\delta}(\vec{k})|^2 e^{-i\vec{k}\cdot\vec{r}} d^3k \propto r^{-(n+3)}$$

$$dP = [1 + \xi(r)] n dV$$

Gravitational Instability: Dark Matter

Small fluctuations: $\delta, v, \varphi(x, t)$ comoving coordinates

$$r = a(t)x \text{ etc.}$$

Continuity:

$$\dot{\delta} + \nabla \cdot v + \nabla \cdot (v\delta) = 0$$

$$H \equiv \dot{a}/a, \quad \Omega(t)$$

Euler:

$$\dot{v} + 2Hv + (v \cdot \nabla)v = -\nabla\varphi$$

matter era

Poisson:

$$\nabla^2\varphi = (3/2)H^2\Omega\delta$$

Linear approximation:

$$\ddot{\delta} + 2H\dot{\delta} = (3/2)H^2\Omega\delta$$

growing mode:

$$\delta \propto D(t) = t^{2/3} \xrightarrow{\Omega_m \rightarrow 0} t^0$$

$$\delta = -\nabla \cdot v / [Hf(\Omega)]$$

$$f(\Omega) \equiv \dot{D}/(HD) \approx \Omega^{0.6}$$

irrotational, potential flow:

$$\nabla \times v = 0 \quad v = -\nabla\varphi_v$$

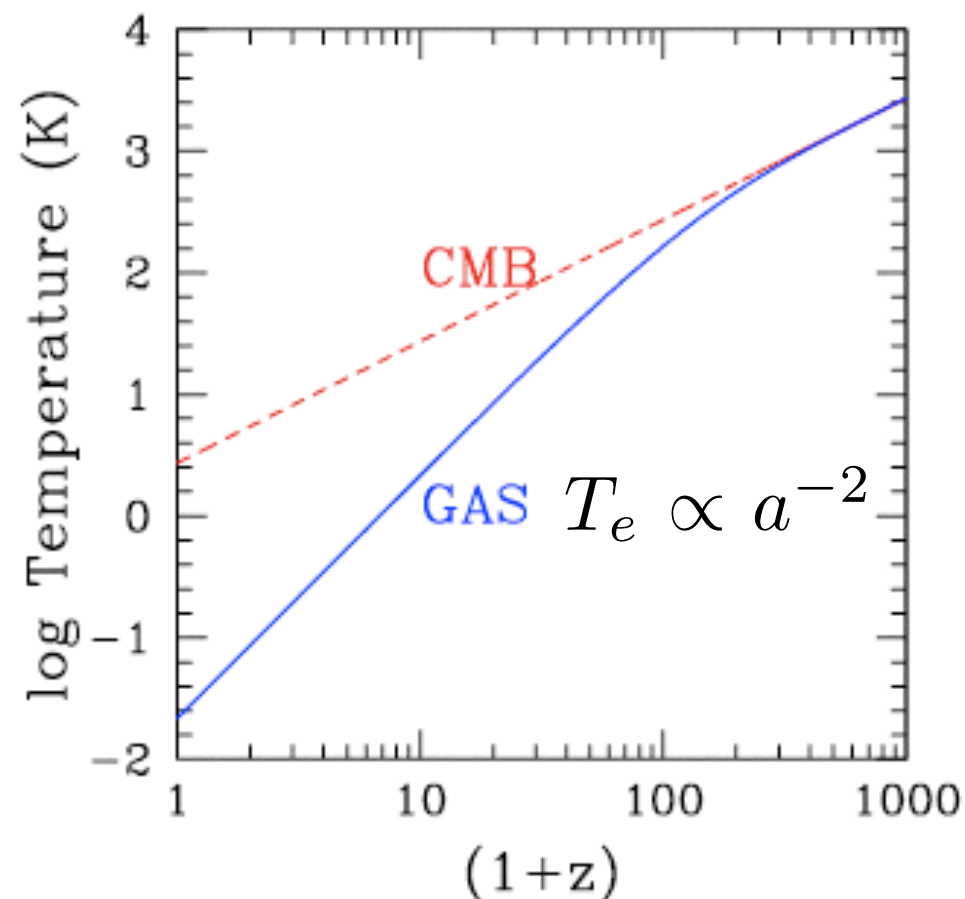
Thus far, we have considered only the evolution of fluctuations in the dark matter. But of course we have to consider also the ordinary matter, known in cosmology as “baryons” (implicitly including the electrons). See Madau’s lectures “The Astrophysics of Early Galaxy Formation” (<http://arxiv.org/abs/0706.0123v1>) for a summary. We have already seen that the baryons are primarily in the form of atoms after $z \sim 1000$, with a residual ionization fraction of a few $\times 10^{-4}$. They become fully reionized by $z \sim 6$, but they were not reionized at $z \sim 20$ since the COBE satellite found that “Compton parameter” $y \leq 1.5 \times 10^{-5}$, where

$$y = \int_0^z \frac{k_B T_e}{m_e c^2} \frac{d\tau_e}{dz} dz \quad \text{with} \quad (n_e \sigma_T c dt) = d\tau_e, \quad \sigma_T = (8\pi/3)(e^2/mc^2)^2$$

This implies that $\langle x_e T_e \rangle [(1+z)^{3/2} - 1] < 4 \times 10^7 \text{ K}$. Thus, for example, a universe that was reionized and reheated at $z = 20$ to $(x_e, T_e) = (1, > 4 \times 10^5 \text{ K})$ would violate the COBE y -limit.

The figure at right shows the evolution of the radiation (dashed line, labeled **CMB**) and matter (solid line, labeled **GAS**) temperatures after recombination, in the absence of any reheating mechanism.

(From Madau’s lectures, at physics.ucsc.edu/~joel/Phys224.)



The linear evolution of sub-horizon density perturbations in the dark matter-baryon fluid is governed in the matter-dominated era by two second-order differential equations:

$$\ddot{\delta}_{\text{dm}} + 2H\dot{\delta}_{\text{dm}} = \frac{3}{2}H^2\Omega_m^z (f_{\text{dm}}\delta_{\text{dm}} + f_b\delta_b) \quad (1)$$

for the dark matter, and

$$\ddot{\delta}_b + 2H\dot{\delta}_b = \frac{3}{2}H^2\Omega_m^z (f_{\text{dm}}\delta_{\text{dm}} + f_b\delta_b) - \frac{c_s^2}{a^2}k^2\delta_b$$

for the baryons, where $\delta_{\text{dm}}(\mathbf{k})$ and $\delta_b(\mathbf{k})$ are the Fourier components of the density fluctuations in the dark matter and baryons,† f_{dm} and f_b are the corresponding mass fractions, c_s is the gas sound speed, k is the (comoving) wavenumber, and the derivatives are taken with respect to cosmic time. Here

$$\Omega_m^z \equiv 8\pi G\rho(t)/3H^2 = \Omega_m(1+z)^3/[\Omega_m(1+z)^3 + \Omega_\Lambda] \quad (2)$$

is the time-dependent matter density parameter, and $\rho(t)$ is the total background matter density. Because there is ~ 5 times more dark matter than baryons, it is the former that defines the pattern of gravitational wells in which structure formation occurs. In the case where $f_b \approx 0$ and the universe is static ($H = 0$), equation (1) above becomes

† For each fluid component ($i = b, \text{dm}$) the real space fluctuation in the density field,

$\delta_i(\mathbf{x}) \equiv \delta\rho_i(\mathbf{x})/\rho_i$, can be written as a sum over Fourier modes,

$\delta_i(\mathbf{x}) = \int d^3\mathbf{k} (2\pi)^{-3} \delta_i(\mathbf{k}) \exp i\mathbf{k}\cdot\mathbf{x}$.

$$\ddot{\delta}_{\text{dm}} = 4\pi G\rho\delta_{\text{dm}} \equiv \frac{\delta_{\text{dm}}}{t_{\text{dyn}}^2},$$

where t_{dyn} denotes the dynamical timescale. This equation has the solution

$$\delta_{\text{dm}} = A_1 \exp(t/t_{\text{dyn}}) + A_2 \exp(-t/t_{\text{dyn}}).$$

After a few dynamical times, only the exponentially growing term is significant: gravity tends to make small density fluctuations in a static pressureless medium grow exponentially with time. Sir James Jeans (1902) was the first to discuss this.

The additional term $\propto H\dot{\delta}_{\text{dm}}$ present in an expanding universe can be thought as a “**Hubble friction**” term that acts to slow down the growth of density perturbations. Equation (1) admits the general solution for the growing mode:

$$\delta_{\text{dm}}(a) = \frac{5\Omega_m}{2} H_0^2 H \int_0^a \frac{da'}{(\dot{a}')^3}, \quad (3)$$

so that an Einstein-de Sitter universe gives the familiar scaling $\delta_{\text{dm}}(a) = a$ with coefficient unity. The right-hand side of equation (3) is called the linear growth factor $D(a) = D_+(a)$. Different values of Ω_m, Ω_Λ lead to different linear growth factors.

Growing modes actually decrease in density, but not as fast as the average universe. Note how, in contrast to the exponential growth found in the static case, the growth of perturbations even in the case of an Einstein-de Sitter ($\Omega_m = 1$) universe is just algebraic rather than exponential. This was discovered by the Russian physicist Lifshitz (1946).

Since cosmological curvature is at most marginally important at the present epoch, it was negligible during the radiation-dominated era and at least the beginning of the matter-dominated era. But for $k = -1$, i.e. $\Omega < 1$, the growth of δ slows for $(R/R_o) \gtrsim \Omega_o$, as gravity becomes less important and the universe begins to expand freely. To discuss this case, it is convenient to introduce the variable

$$x \equiv \Omega^{-1}(t) - 1 = (\Omega_o^{-1} - 1)R(t)/R_o. \quad (2.55)$$

(Note that $\Omega(t) \rightarrow 1$ at early times.) The general solution in the matter-dominated era is then (Peebles, 1980, §11)

$$\delta = \tilde{A}D_1(t) + \tilde{B}D_2(t), \quad (2.56)$$

where the growing solution is

$$D_1 = 1 + \frac{3}{x} + \frac{3(1+x)^{1/2}}{x^{3/2}} \ln \left[(1+x)^{1/2} - x^{1/2} \right] \quad (2.57)$$

and the decaying solution is

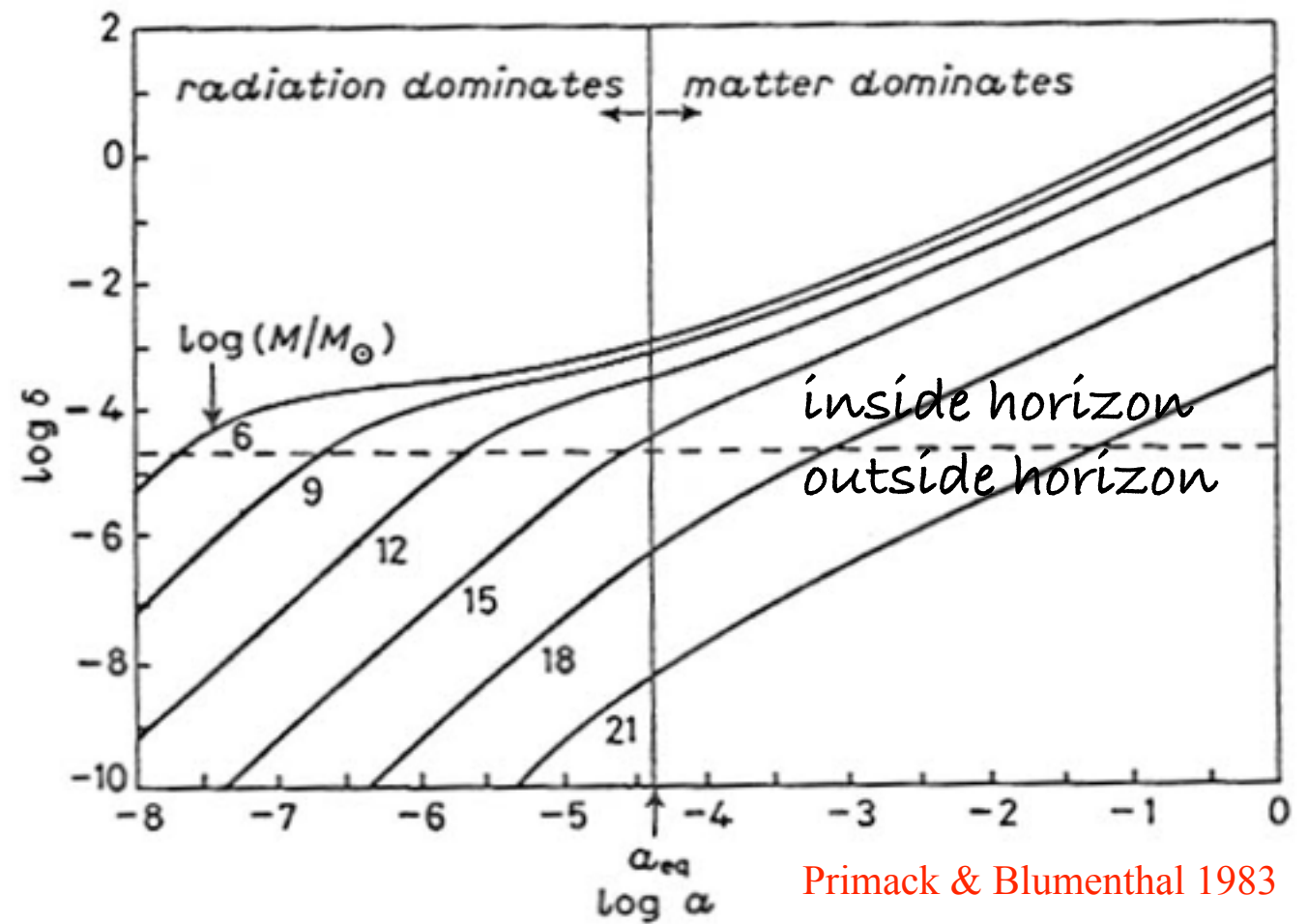
$$D_2 = (1+x)^{1/2}/x^{3/2}. \quad (2.58)$$

These agree with the Einstein-de Sitter results (2.53) at early times ($t \ll t_o, x \ll 1$). For late times ($t \gg t_o, x \gg 1$) the solutions approach

$$D_1 = 1, D_2 = x^{-1}; \quad (2.59)$$

in this limit the universe is expanding freely and the amplitude of fluctuations stops growing.

The consequence is that dark matter fluctuations grow proportionally to the scale factor $a(t)$ when matter is the dominant component of the universe, but only logarithmically when radiation is dominant. Thus there is not much difference in the amplitudes of fluctuations of mass $M < 10^{15} M_{\text{sun}}$, which enter the horizon before $z_{\text{mr}} \sim 4 \times 10^3$, while there is a stronger dependence on M for fluctuations with $M > 10^{15} M_{\text{sun}}$.



There is a similar suppression of the growth of matter fluctuations once the gravitationally dominant component of the universe is the dark energy, for example a cosmological constant. Lahav, Lilje, Primack, & Rees (1991) showed that the growth factor in this case is well approximated by

$$\delta_{\text{dm}}(a) = D(a) \simeq \frac{5\Omega_m^z}{2(1+z)} \left[(\Omega_m^z)^{4/7} - \frac{(\Omega_m^z)^2}{140} + \frac{209}{140}\Omega_m^z + \frac{1}{70} \right]^{-1}.$$

Here Ω_m^z is again given by $\Omega_m^z \equiv 8\pi G\rho(t)/3H^2 = \Omega_m(1+z)^3/[\Omega_m(1+z)^3 + \Omega_\Lambda]$

The Linear Transfer Function $T(k)$

The observed uniformity of the CMB guarantees that density fluctuations must have been quite small at decoupling, implying that the evolution of the density contrast can be studied at $z \lesssim z_{\text{dec}}$ using linear theory, and each mode $\delta(k)$ evolves independently. The inflationary model predicts a scale-invariant primordial power spectrum of density fluctuations $P(k) \equiv \langle |\delta(k)|^2 \rangle \propto k^n$, with $n = 1$ (the so-called Harrison-Zel'dovich spectrum). It is the index n that governs the balance between large and small-scale power. In the case of a Gaussian random field with zero mean, the power spectrum contains the complete statistical information about the density inhomogeneity. It is often more convenient to use the dimensionless quantity $\Delta_k^2 \equiv [k^3 P(k)/2\pi^2]$, which is the power per logarithmic interval in wavenumber k . In the matter-dominated epoch, this quantity retains its initial primordial shape ($\Delta_k^2 \propto k^{n+3}$) only on very large scales. Small wavelength modes enter the horizon earlier on and their growth is suppressed more severely during the radiation-dominated epoch: on small scales the amplitude of Δ_k^2 is essentially suppressed by four powers of k (from k^{n+3} to k^{n-1}). If $n = 1$, then small scales will have nearly the same power except for a weak, logarithmic dependence. Departures from the initially scale-free form are described by the transfer function $T(k)$, defined such that $T(0) = 1$:

$$P(k, z) = Ak^n \left[\frac{D(z)}{D(0)} \right]^2 T^2(k),$$

where A is the normalization.

An approximate fitting function for $T(k)$ in a Λ CDM universe is (Bardeen et al. 1986)

$$T_k = \frac{\ln(1 + 2.34q)}{2.34q} [1 + 3.89q + (16.1q)^2 + (5.46q)^3 + (6.71q)^4]^{-1/4},$$

where (Sugayama 1995)

$$q \equiv \frac{k/\text{Mpc}^{-1}}{\Omega_m h^2 \exp(-\Omega_b - \Omega_b/\Omega_m)}.$$

For accurate work, for example for starting high-resolution N-body simulations, it is best to use instead of fitting functions the numerical output of highly accurate integration of the Boltzmann equations, for example from CMBFast, which is available at <http://lambda.gsfc.nasa.gov/toolbox/> which points to http://lambda.gsfc.nasa.gov/toolbox/tb_cmbfast_ov.cfm

W e l c o m e to the CMBFAST Website!

This is the most extensively used code for computing cosmic microwave background anisotropy, polarization and matter power spectra. The code has been tested over a wide range of cosmological parameters. We are continuously testing and updating the code based on suggestions from the cosmological community. Do not hesitate to contact us if you have any questions or suggestions.

U. Seljak & M. Zaldarriaga

CMB Toolbox Overview

We provide links to a number of useful tools for CMB and Astronomy in general.

CMB Tools

- [CMB Simulations](#) - High-resolution, full-sky microwave temperature simulations including secondary anisotropies.
- [Contributed Software](#) is an archive at a LAMBDA partner site for tools built by members of the community.
- [CMBFast](#) - A tool that computes spectra for the cosmic background for a given set of CMB parameters. LAMBDA provides a [web-based interface](#) for this tool. Seljak and Zaldarriaga
- [CAMB](#) - Code for Anisotropies in the Microwave Background that computes spectra for a set of CMB parameters. LAMBDA provides a [web-based interface](#) for this tool. Lewis and Challinor
- [CMBEASY](#) - A C++ package, initially based on CMBFAST, now featuring a parameter likelihood package as well. Doran
- [CMBview](#) - A Mac OS X program for viewing HEALPix-format CMB data on an OpenGL-rendered sphere. Portsmouth
- [COMBAT](#) - A set of computational tools for CMB analysis. Borrill et al.
- [CosmoMC](#) - A Markov-Chain Monte-Carlo engine for exploring cosmological parameter space. Lewis and Bridle
- [CosmoNet](#) - Accelerated cosmological parameter estimation using Neural Networks.
- [GLESP](#) - Gauss-Legendre sky pixelization package. Doroshkevich, et al.
- [GSM](#) - Predicted all-sky maps at any frequency from 10 MHz to 100 GHz. de Oliveira-Costa.
- [HEALPix](#) - A spherical sky pixelization scheme. The Wilkinson Microwave Anisotropy Probe (WMAP) data skymap products are supplied in this form. Górski et al.
- [IGLOO](#) - A sky pixelization package. Crittenden and Turok
- [MADCAP](#) - Microwave Anisotropy Data Computational Analysis Package. Borrill et al.
- [PICO](#) - Integrates with CAMB and/or CosmoMC for cosmological parameter estimation using machine learning. Wandelt and Fendt
- [RADPACK](#) - Radical Compression Analysis Package. Knox
- [RECFAST](#) - Software to calculate the recombination history of the Universe. Seager, Sasselov, and Scott
- [SkyViewer](#) - A LAMBDA-developed OpenGL-based program to display HEALPix-based skymaps stored in FITS format files. Phillips
- [SpiCE](#) - Spatially Inhomogenous Correlation Estimator. Szapudi et al.
- [WMAPViewer](#) - A LAMBDA-developed web-based CMB map viewing tool using a technology similar to that found on maps.google.com. Phillips
- [WOMBAT](#) - Microwave foreground emission tools. Gawiser, Finkbeiner, Jaff et al.

Likelihood Software

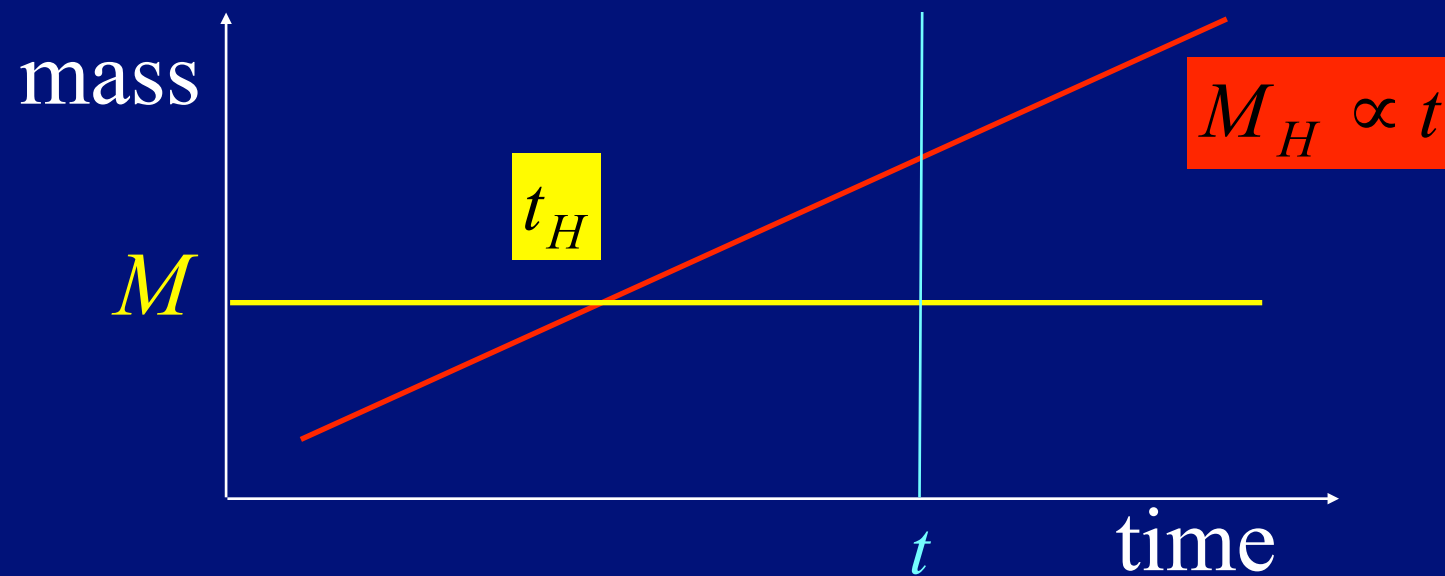
- [SDSS LRG DR7 Likelihood Software](#) - A software package that computes likelihoods for Luminous Red Galaxies (LRG) data from the seventh release of the Sloan Digital Sky Survey (SDSS).
- [WMAP Likelihood Software](#) - A software library used by the WMAP team to compute Fisher and Master matrices and to compute the likelihoods of various models. This is the same software found on the [WMAP products list](#); more information may be found [here](#).

Other Tools

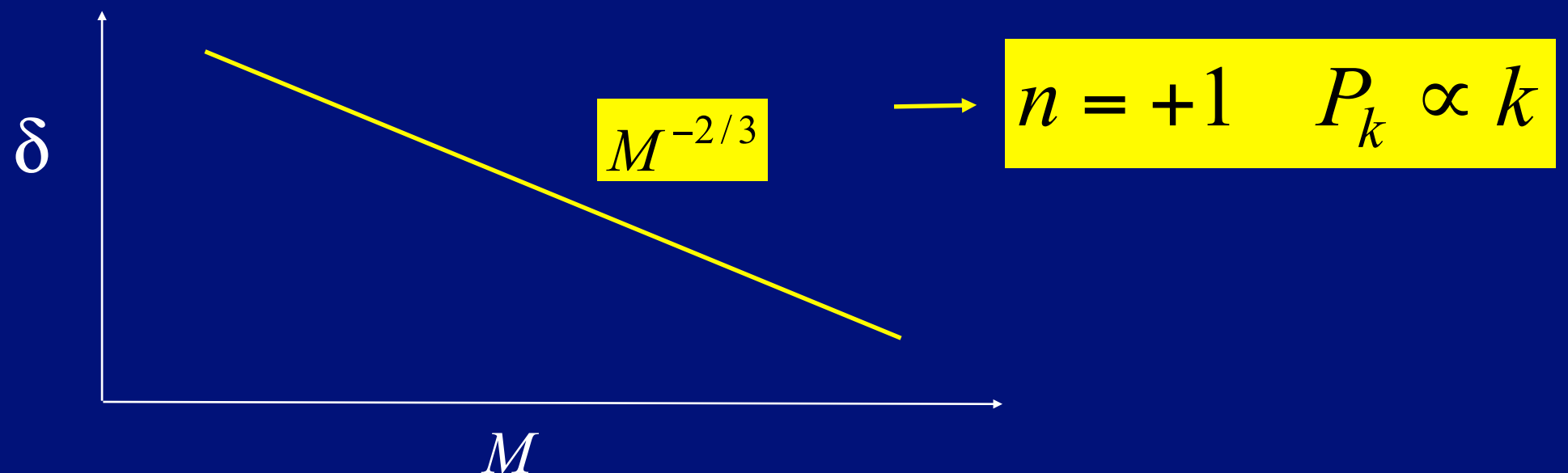
- [WMAP Effective Frequency Calculator](#) - A tool that calculates the effective frequencies of the five WMAP frequency bands.
- [CFITSIO](#) - A library of C and Fortran routines for reading and writing data in the FITS format.
- [IDL Astro](#) - The IDL Astronomy Users Library.
- [Conversion Utilities](#) - A small collection of astronomical conversion utilities.
- [Calculators](#) - A list of links to calculators.

This collection of tools can only be extended and improved with your input! Please feel free to send us [suggestions and comments](#).

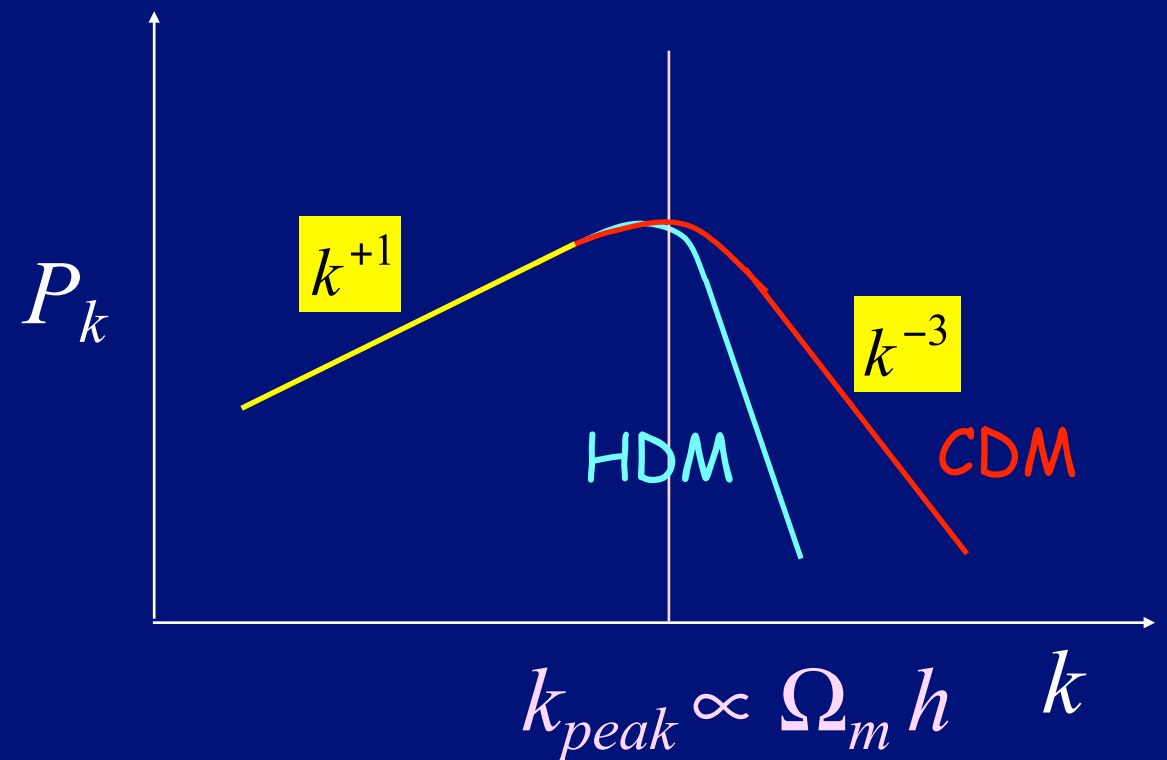
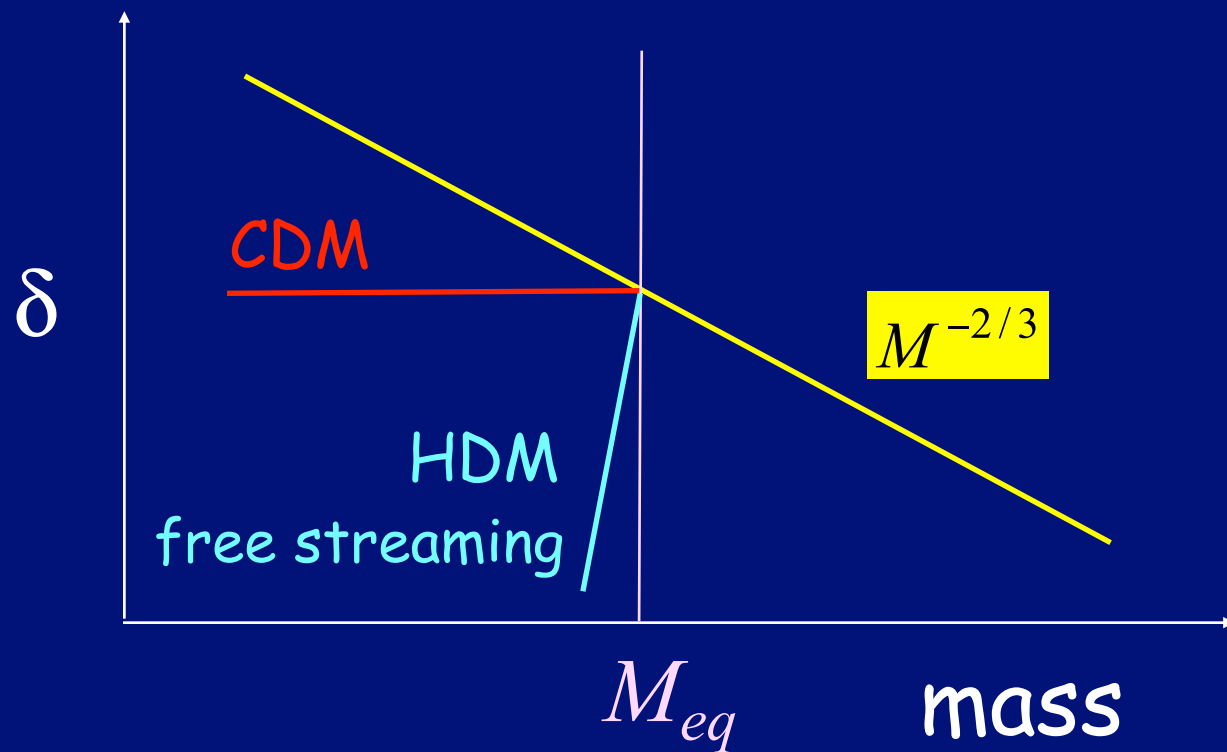
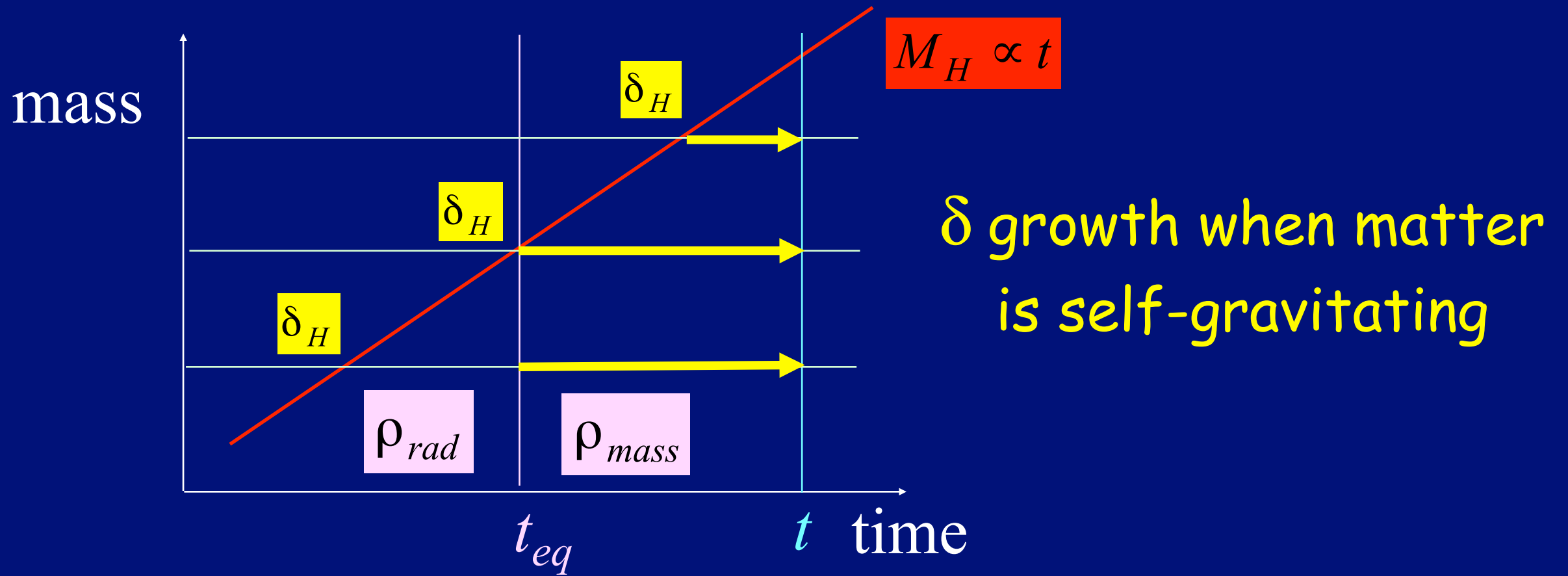
Scale-Invariant Spectrum (Harrison-Zel'dovich)



$$\delta(M, t) = \delta_H \left(\frac{t}{t_H(M)} \right)^{2/3} \propto M^{-2/3} t^{2/3}$$

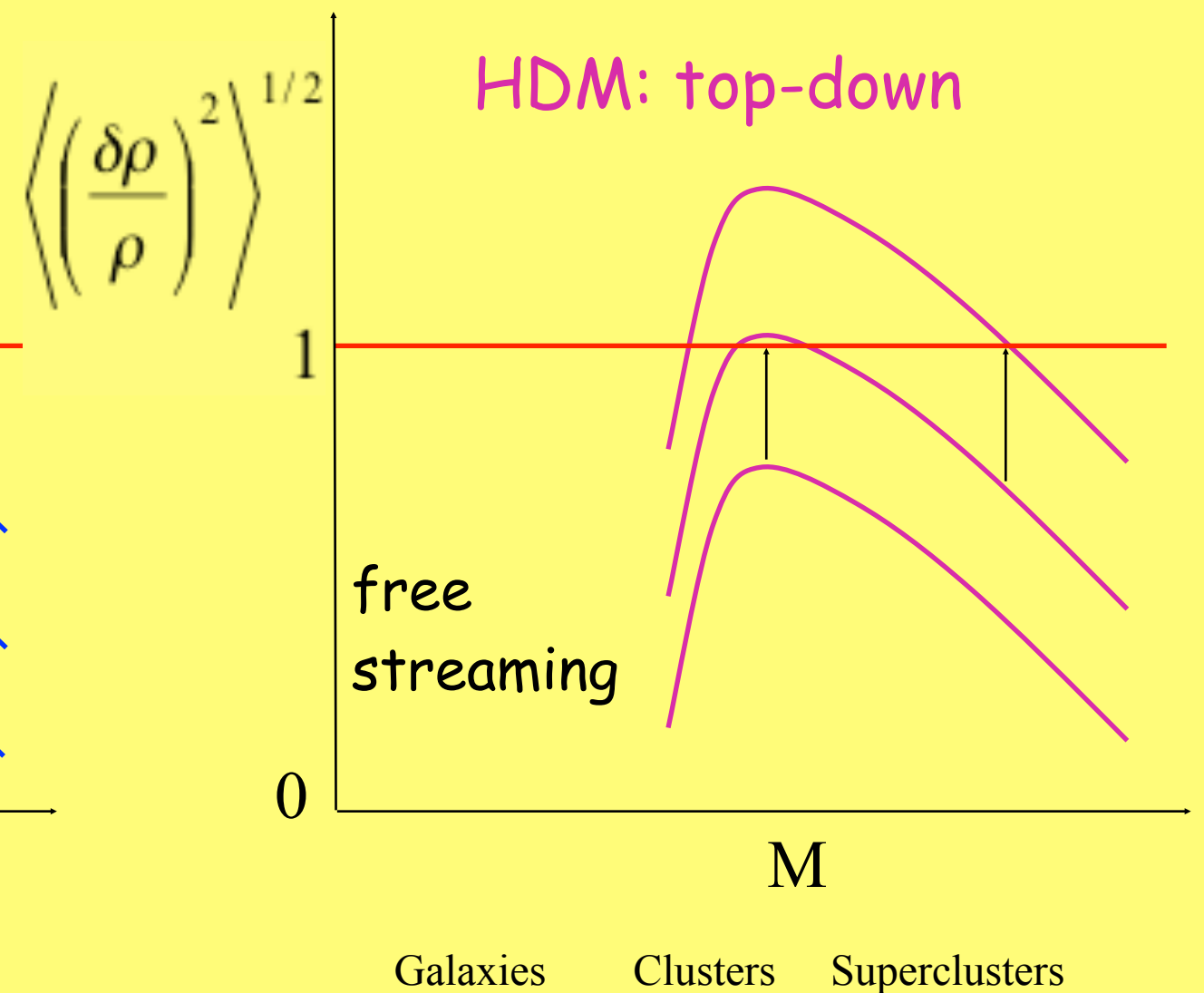
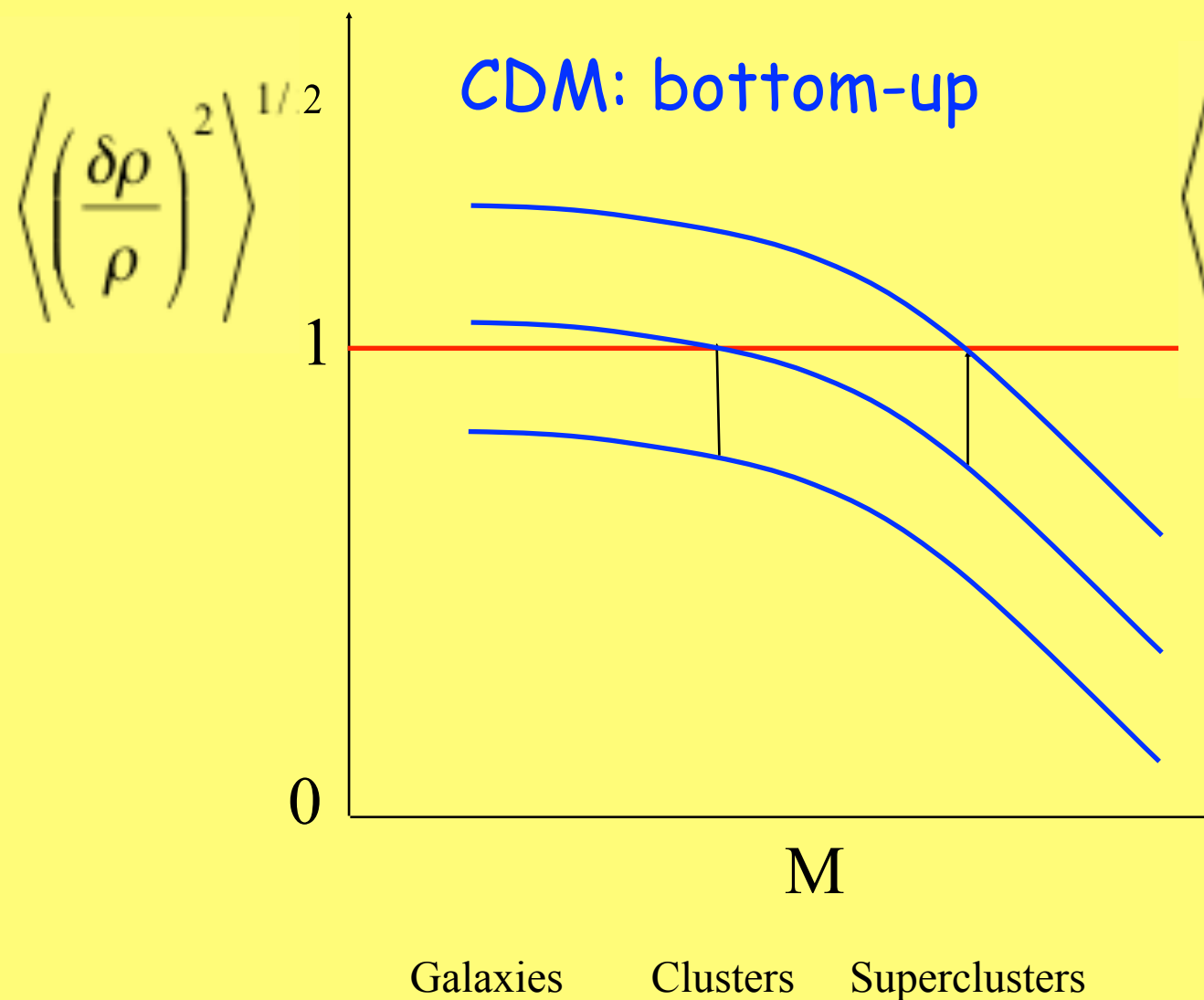


CDM Power Spectrum



Formation of Large-Scale Structure

Fluctuation growth in the linear regime: $\delta \ll 1 \longrightarrow \delta \propto t^{2/3}$
 rms fluctuation at mass scale M : $\delta \propto M^{-\alpha} \quad 0 < \alpha \leq 2/3$



Structure forms earliest in Open, next in Benchmark, latest in EdS model.

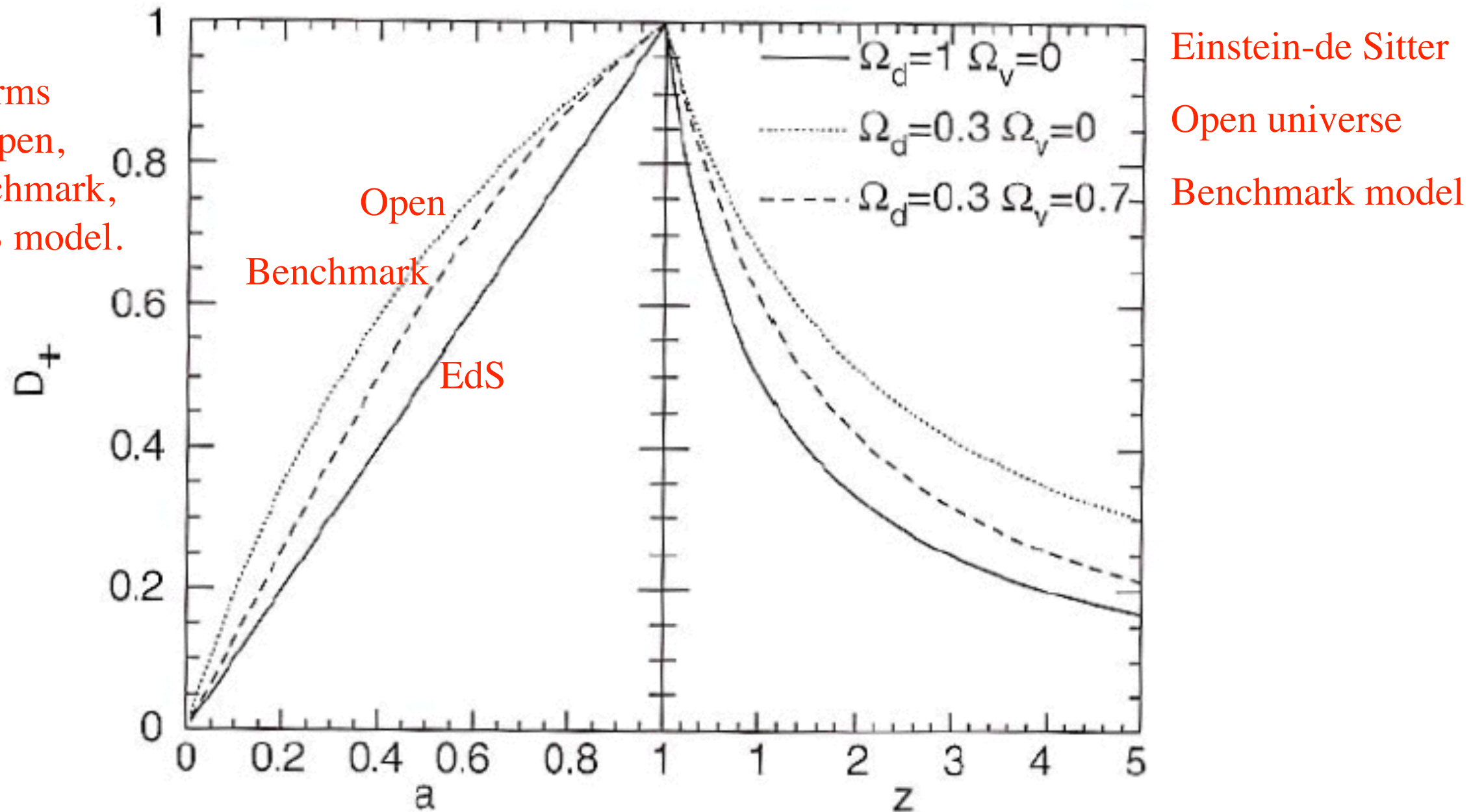


Fig. 7.3. Growth factor D_+ for three different cosmological models, as a function of the scale factor a (left panel) and of redshift (right panel). It is clearly visible how quickly D_+ decreases with increasing redshift in the EdS model, in comparison to the models of lower density

From Peter Schneider, *Extragalactic Astronomy and Cosmology* (Springer, 2006)

Linear Growth Rate Function $D(a)$

For completeness, here we present some approximations used in the text. For the family of flat cosmologies ($\Omega_m + \Omega_\Lambda = 1$) an accurate approximation for the value of the virial overdensity Δ_{vir} is given by the analytic formula (Bryan & Norman 1998):

$$\Delta_{\text{vir}} = (18\pi^2 + 82x - 39x^2)/\Omega(z), \quad (\text{A1})$$

where $\Omega(z) \equiv \rho_m(z)/\rho_{\text{crit}}$ and $x \equiv \Omega(z) - 1$.

The linear growth-rate function $\delta(a)$, used in eqs. (14-15) and also in $\sigma_8(a)$ is defined as

$$\delta(a) = D(a)/D(1), \quad (\text{A2})$$

where $a = 1/(1+z)$ is the expansion parameter and $D(a)$ is:

$$D(a) = \frac{5}{2} \left(\frac{\Omega_{m,0}}{\Omega_{\Lambda,0}} \right)^{1/3} \frac{\sqrt{1+x^3}}{x^{3/2}} \int_0^x \frac{x^{3/2} dx}{[1+x^3]^{3/2}}, \quad (\text{A3})$$

$$x \equiv \left(\frac{\Omega_{\Lambda,0}}{\Omega_{m,0}} \right)^{1/3} a, \quad (\text{A4})$$

where $\Omega_{m,0}$ and $\Omega_{\Lambda,0}$ are density contributions of matter and cosmological constant at $z = 0$. For $\Omega_m > 0.1$ the growth rate factor $D(a)$ can be accurately approximated by the following expressions (Lahav et al. 1991; Carroll et al. 1992):

$$D(a) = \frac{(5/2)a\Omega_m}{\Omega_m^{4/7} - \Omega_\Lambda + (1 + \Omega_m/2)(1 + \Omega_\Lambda/70)}, \quad (\text{A5})$$

$$\Omega_m(a) = \Omega_{m,0}/(1+x^3), \quad (\text{A6})$$

$$\Omega_\Lambda(a) = 1 - \Omega_m(a) \quad (\text{A7})$$

For $\Omega_{m,0} = 0.27$ the error of these approximation is less than 7×10^{-4} .

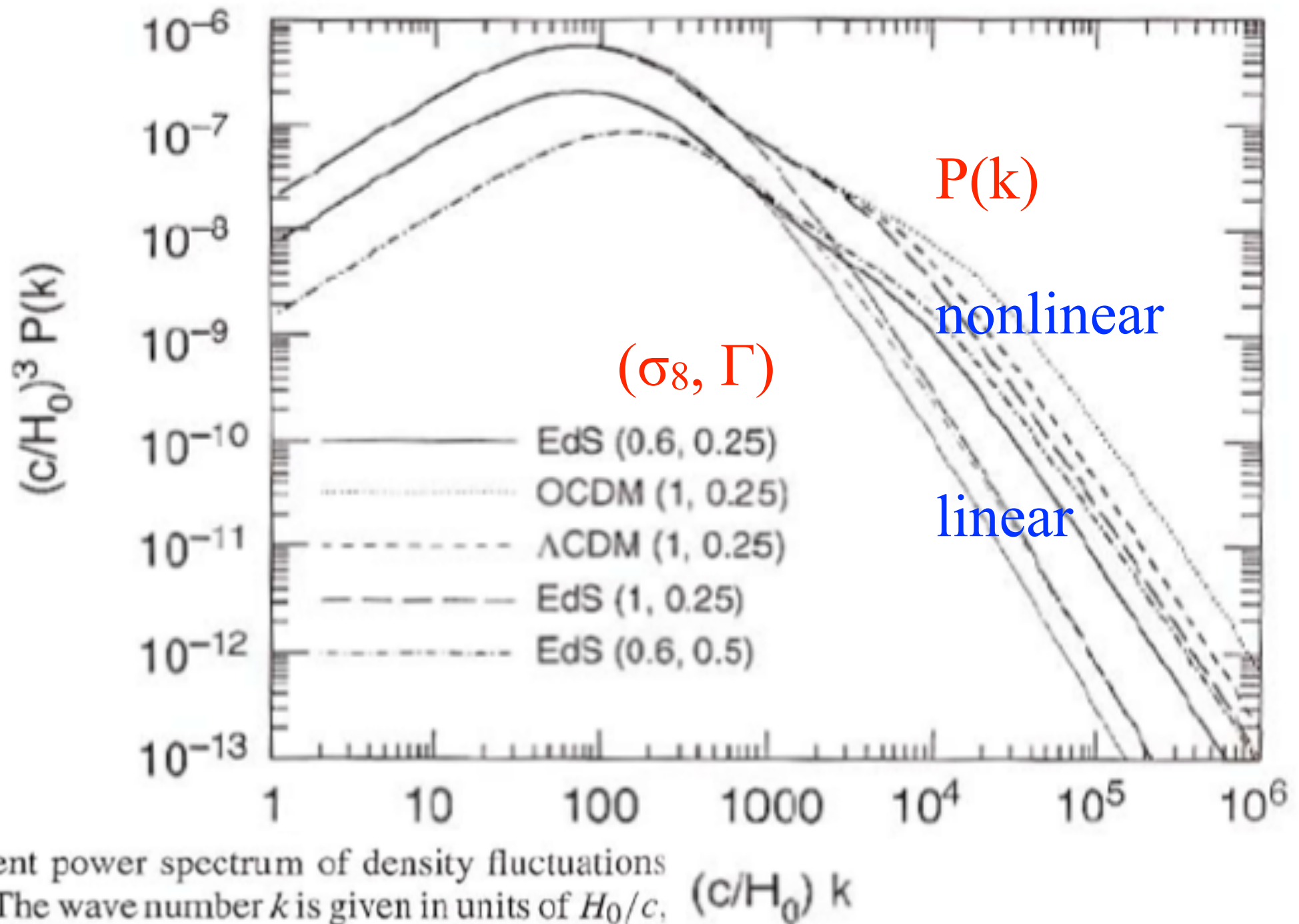


Fig. 7.6. The current power spectrum of density fluctuations for CDM models. The wave number k is given in units of H_0/c , and $(H_0/c)^3 P(k)$ is dimensionless. The various curves have different cosmological parameters: EdS: $\Omega_m = 1$, $\Omega_\Lambda = 0$; OCDM: $\Omega_m = 0.3$, $\Omega_\Lambda = 0$; Λ CDM: $\Omega_m = 0.3$, $\Omega_\Lambda = 0.7$. The values in parentheses specify (σ_8, Γ) , where σ_8 is the normalization of the power spectrum (which will be discussed below), and where Γ is the shape parameter. The thin curves correspond to the power spectrum $P_0(k)$ linearly extrapolated to the present day, and the bold curves take the non-linear evolution into account

From Peter Schneider,
*Extragalactic Astronomy and
 Cosmology* (Springer, 2006)

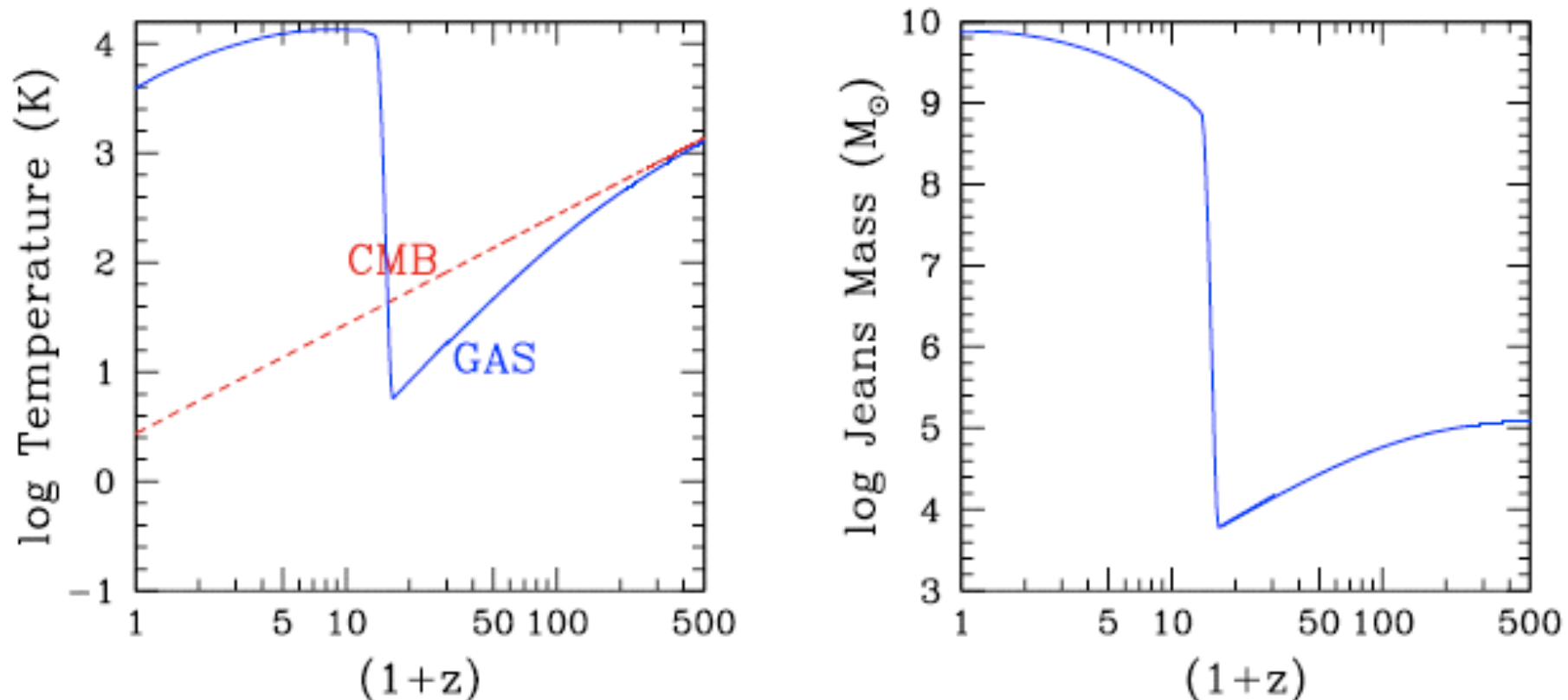
On large scales (k small), the gravity of the dark matter dominates. But on small scales, pressure dominates and growth of baryonic fluctuations is prevented. Gravity and pressure are equal at the Jeans scale

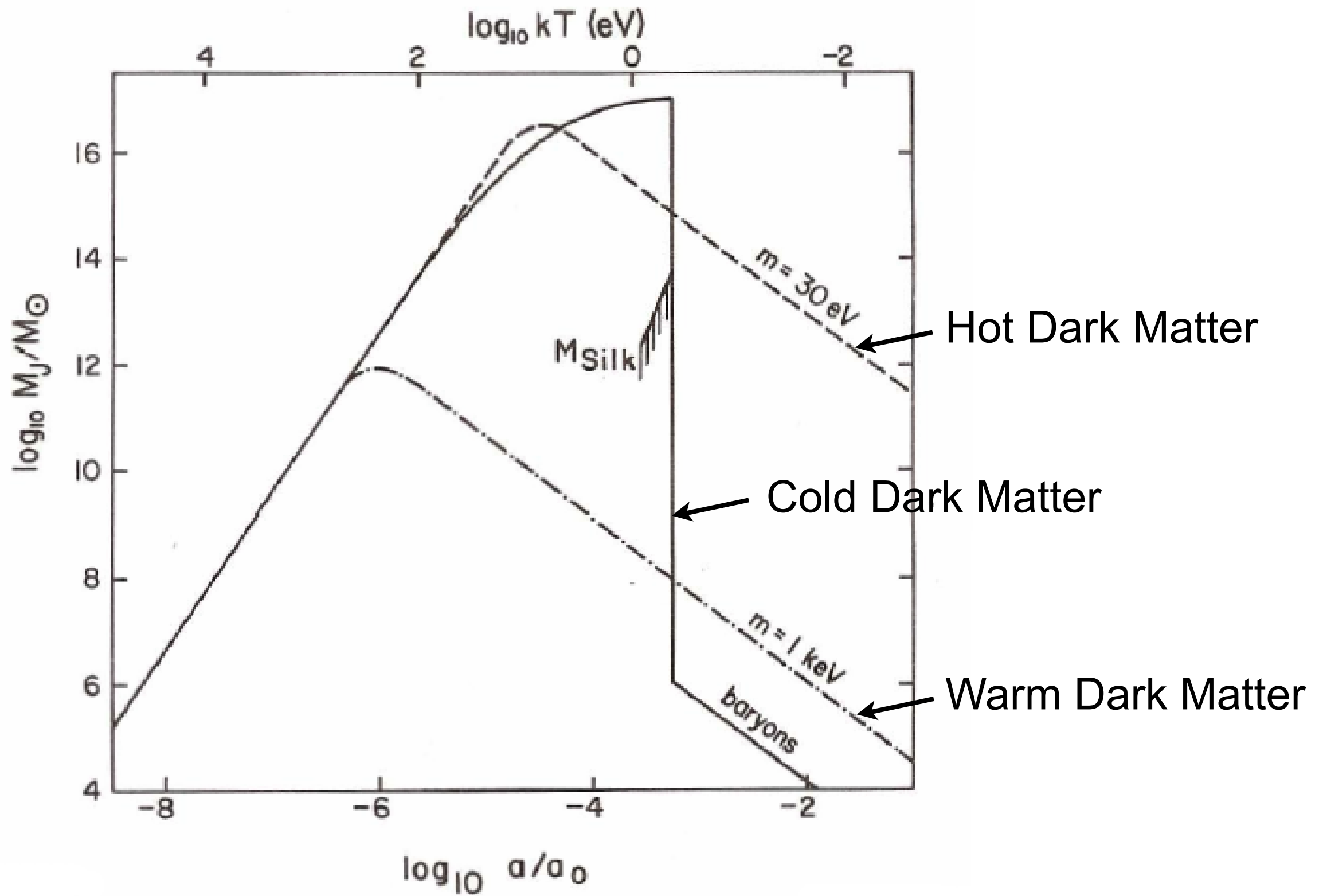
$$k_J = \frac{a}{c_s} \sqrt{4\pi G \rho}.$$

The Jeans mass is the dark matter + baryon mass enclosed within a sphere of radius $\pi a/k_J$,

$$M_J = \frac{4\pi}{3} \rho \left(\frac{\pi a}{k_J} \right)^3 = \frac{4\pi}{3} \rho \left(\frac{5\pi k_B T_e}{12G\rho m_p \mu} \right)^{3/2} \approx 8.8 \times 10^4 M_\odot \left(\frac{a T_e}{\mu} \right)^{3/2},$$

where μ is the mean molecular weight. The evolution of M_J is shown below, assuming that reionization occurs at $z=15$:

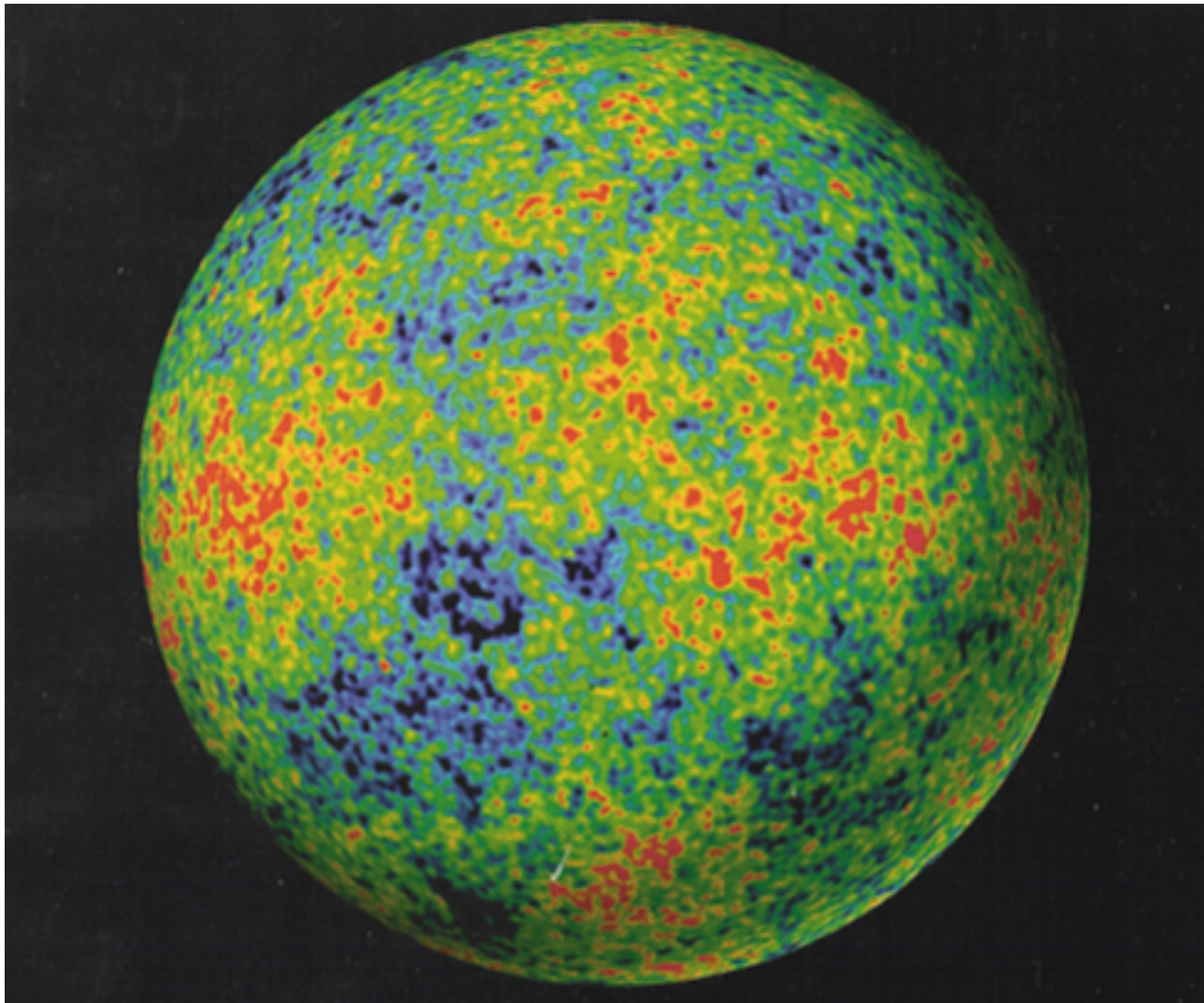




Jeans-type analysis for HDM, WDM, and CDM

GRAVITY – The Ultimate Capitalist Principle

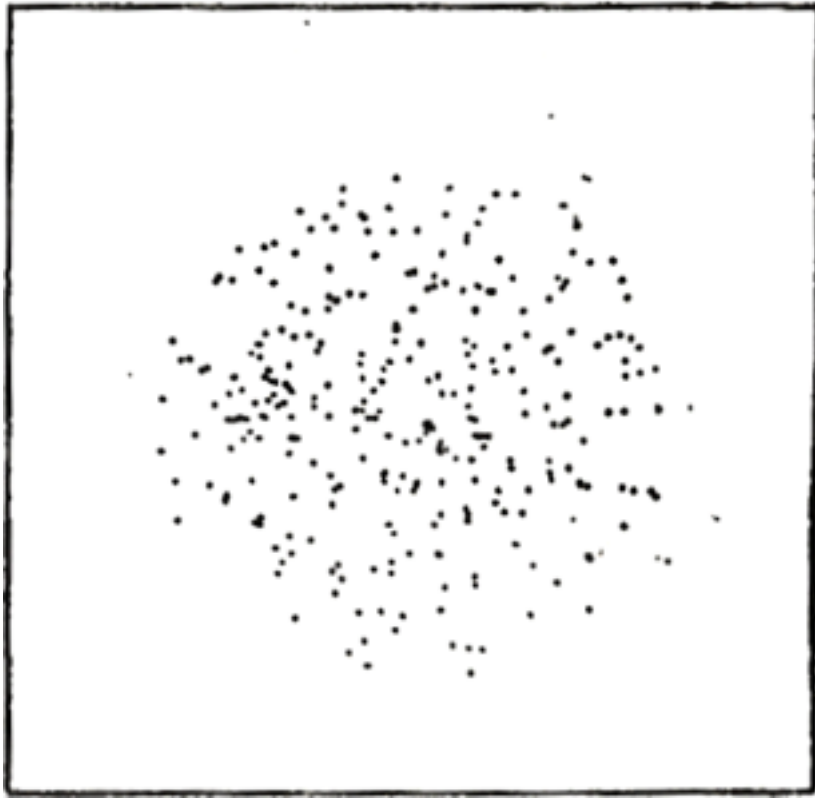
Astronomers say that a region of the universe with more matter is “richer.” Gravity magnifies differences—if one region is slightly denser than average, it will expand slightly more slowly and grow relatively denser than its surroundings, while regions with less than average density will become increasingly less dense. The rich always get richer, and the poor poorer.



The early universe expands *almost* perfectly uniformly. But there are small differences in density from place to place (about 30 parts per million). Because of gravity, denser regions expand more slowly, less dense regions more rapidly. Thus gravity amplifies the contrast between them, until...

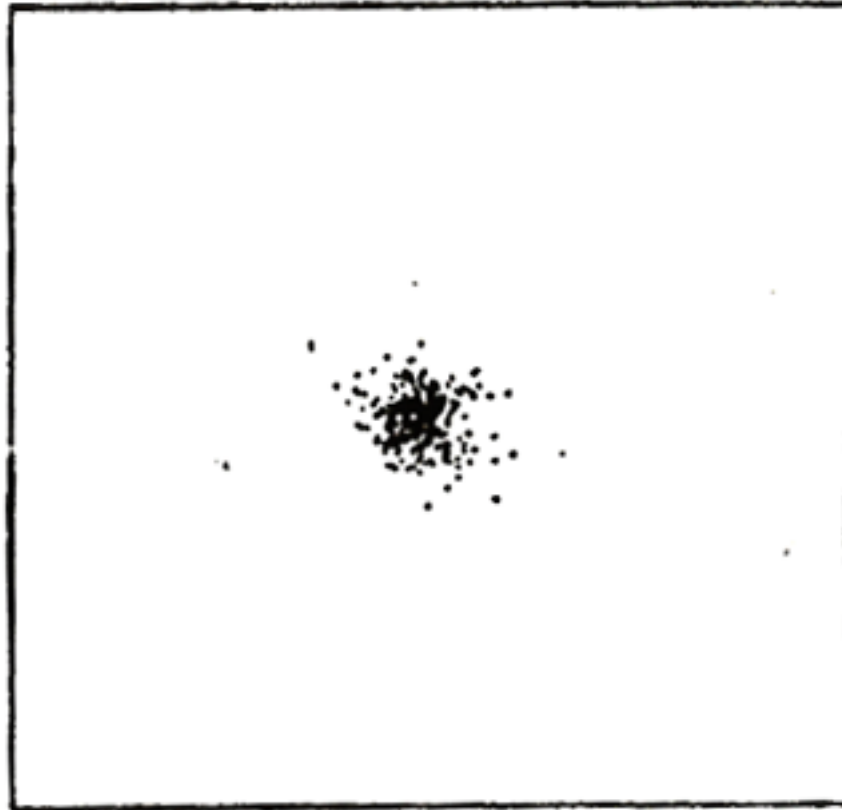
Temperature map at 380,000 years after the Big Bang. **Blue** (cooler) regions are slightly denser. From NASA's **WMAP** satellite, 2003.

Structure Formation by Gravitational Collapse



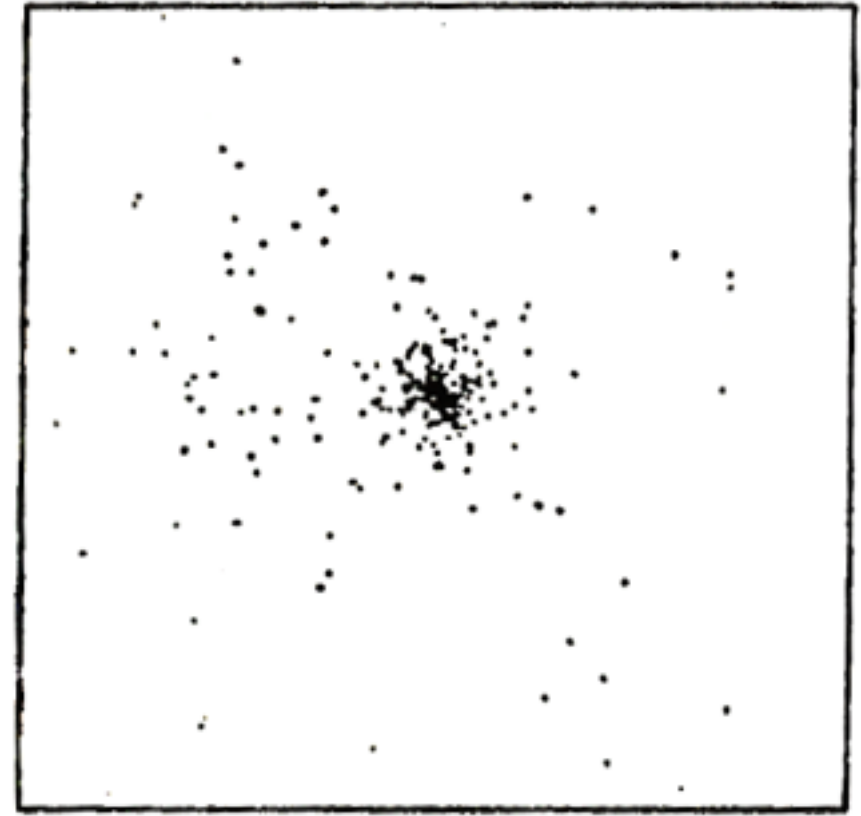
When any region becomes about twice as dense as typical regions its size, it reaches a maximum radius, *stops expanding,*

Simulation of top-hat collapse:
P.J.E. Peebles 1970, ApJ, 75, 13.

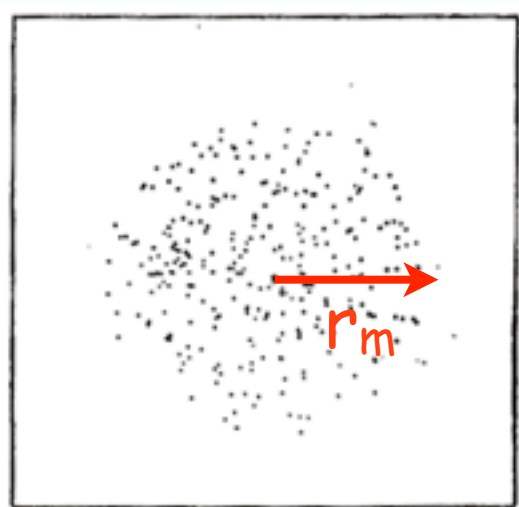


and starts falling together. The forces between the subregions generate velocities which *prevent* the material from *all falling toward the center.*

Used in my 1984 summer school lectures “Dark matter, Galaxies, and Large Scale Structure,” <http://tinyurl.com/3bjknb3>

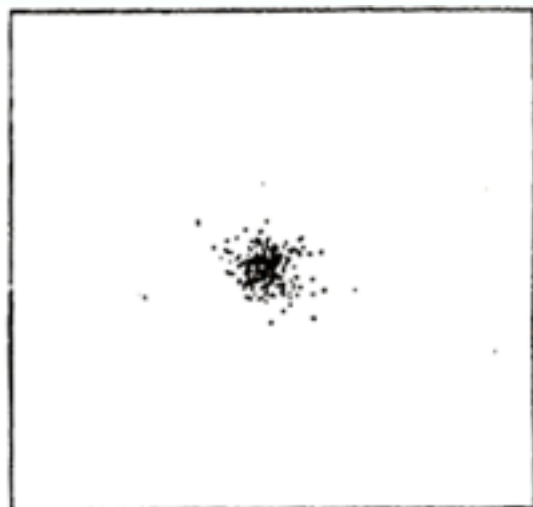


Through Violent Relaxation the dark matter quickly reaches a *stable configuration* that’s about half the maximum radius but denser in the center.

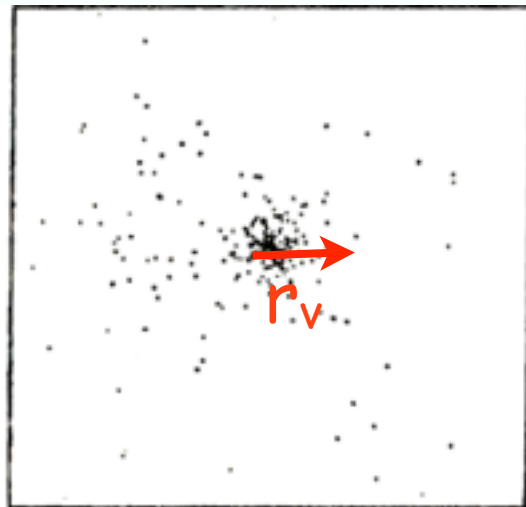


TOP HAT

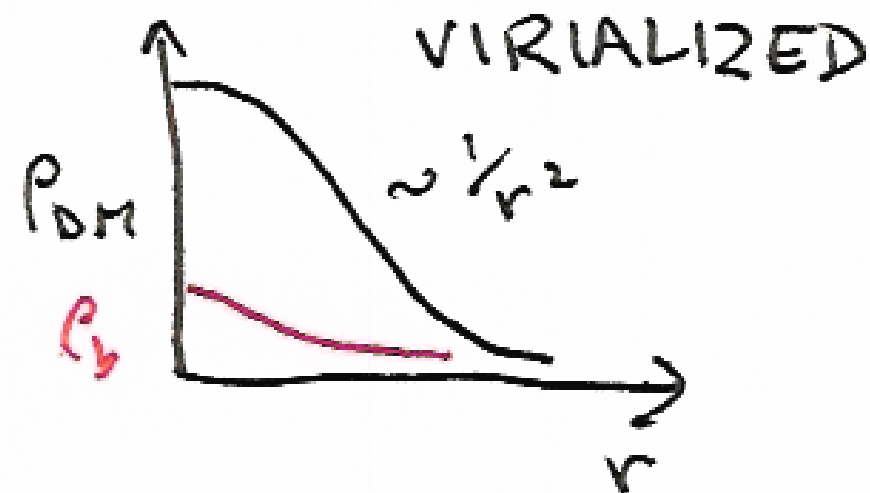
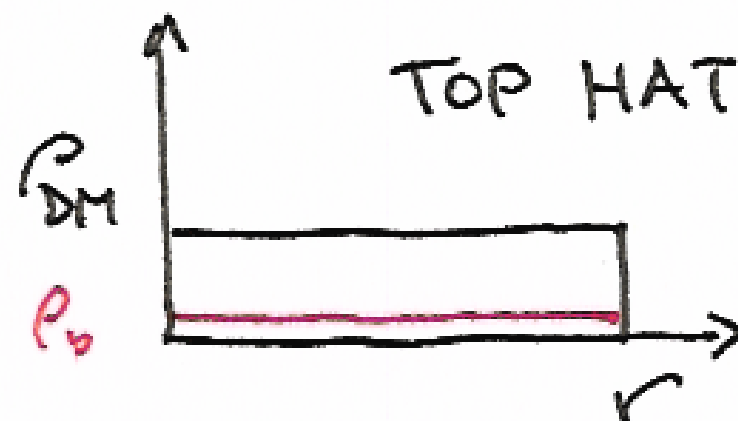
Max Expansion



VIOLENT
RELAXATION



VIRIALIZED



Virial Theorem: $\langle K \rangle = -\frac{1}{2} \langle W \rangle$

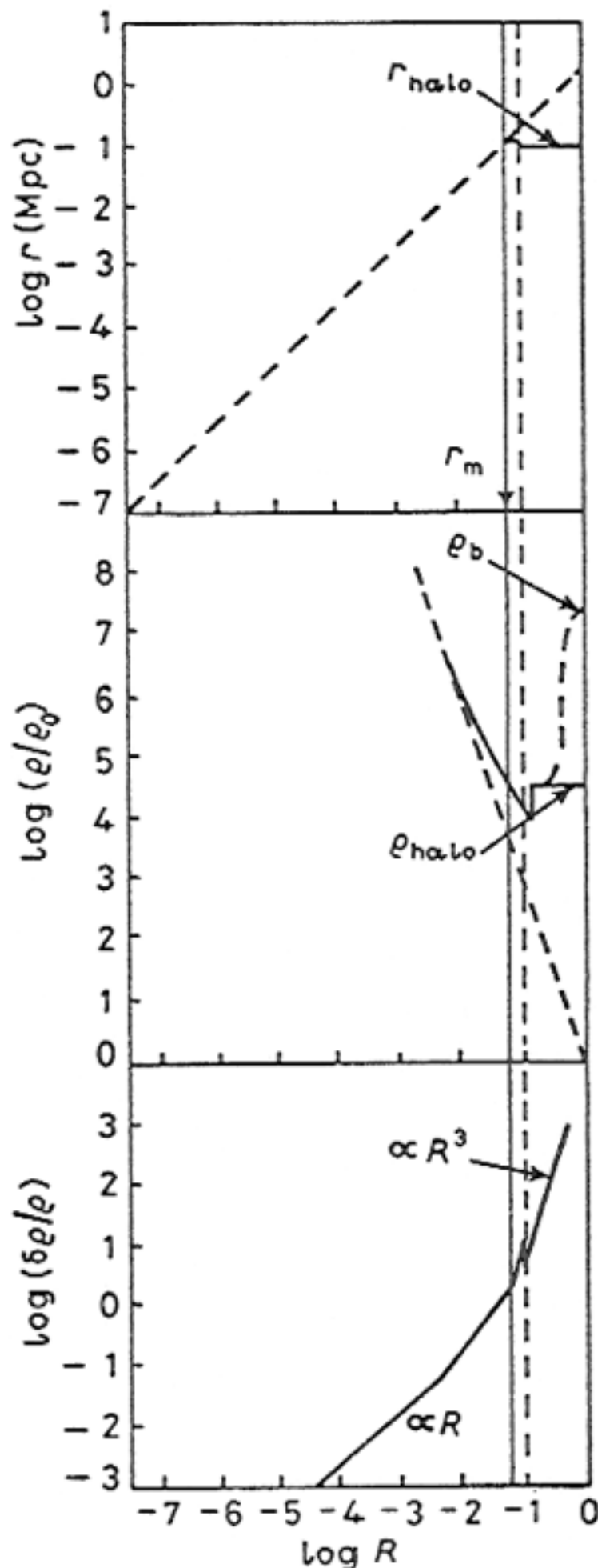
$W_m = \frac{C}{r_m}$, so after virialization

$$\frac{C}{r_m} = E = W + K = \frac{1}{2} \langle W \rangle = \frac{C}{2r_v}$$

$$\Rightarrow r_v = \frac{1}{2} r_m, \quad \rho_v = 8 \rho_m \approx 50 \bar{\rho}(t_m)$$

$$\langle v^2 \rangle \approx \frac{GM}{r_v}$$

Growth and Collapse of Fluctuations



Schematic sketches of radius, density, and density contrast of an overdense fluctuation. It initially expands with the Hubble expansion, reaches a maximum radius (solid vertical line), and undergoes violent relaxation during collapse (dashed vertical line), which results in the dissipationless matter forming a stable halo.

Meanwhile the ordinary matter ρ_b continues to dissipate kinetic energy and contract, thereby becoming more tightly bound, until dissipation is halted by star or disk formation, explaining the origin of galactic spheroids and disks.

(This was the simplified discussion of [BFPR84](#); the figure is from my 1984 lectures at the Varenna school. Now we take into account halo growth by accretion, and the usual assumption is that large stellar spheroids form mostly as a result of galaxy mergers [Toomre 1977](#). Now we think that the most intermediate mass stellar spheroids form because of disk instability.)